A COMPARATIVE STUDY OF AISC360 AND EC3 PROVISIONS FOR MEMBER STABILITY

A THESIS SUBMITTED TO
THE GRADUATE SCHOOL OF NATURAL AND APPLIED SCIENCES
OF
MIDDLE EAST TECHNICAL UNIVERSITY

BY

ÖMER KEVRAN

IN PARTIAL FULFILLMENT OF THE REQUIREMENTS
FOR
THE DEGREE OF MASTER OF SCIENCE
IN
CIVIL ENGINEERING

APRIL 2016

Approval of the thesis:

A COMPARATIVE STUDY OF AISC360 AND EC3 PROVISIONS FOR MEMBER STABILITY

submitted by **ÖMER KEVRAN** in partial fulfillment of the requirements for the degree of **Master of Science in Civil Engineering Department, Middle East Technical University** by,

Prof. Dr. Gülbin Dural Ünver
Dean, Graduate School of **Natural and Applied Sciences** _____

Prof. Dr. İsmail Özgür Yaman
Head of Department, **Civil Engineering** _____

Prof. Dr. Cem Topkaya
Supervisor, **Civil Engineering Dept., METU** _____

Examining Committee Members:

Prof. Dr. Mehmet Utku
Civil Engineering Dept., METU _____

Prof. Prof. Dr. Cem Topkaya
Civil Engineering Dept., METU _____

Assoc. Prof. Dr. Afşin Sarıtaş
Civil Engineering Dept., METU _____

Assoc. Prof. Dr. Eray Baran
Civil Engineering Dept., METU _____

Asst. Prof. Dr. Burcu Güldür
Civil Engineering Dept., HACETTEPE UNIVERSITY _____

Date: **21.04.2016**

I hereby declare that all information in this document has been obtained and presented in accordance with academic rules and ethical conduct. I also declare that, as required by these rules and conduct, I have fully cited and referenced all material and results that are not original to this work.

Name, Last Name : Ömer Kevran

Signature :

ABSTRACT

A COMPARATIVE STUDY OF AISC360 AND EC3 PROVISIONS FOR MEMBER STABILITY

Kevran, Ömer

M.S., Department of Civil Engineering

Supervisor: Prof. Dr. Cem Topkaya

April 2016, 108 pages

The purpose of this thesis is to compare the stability provisions of AISC360 and EC3 specifications. AISC360 specification introduces two methods for member stability which are Effective Length Method (ELM) and Direct Analysis Method (DM). ELM uses effective length factor (K) which is a function of support and side-sway conditions and directly influences the buckling load. On the other hand, DM assumes the effective length factor K=1 for all support conditions. Moreover, due to inelasticity, DM uses reduced axial and bending stiffness. To take into account destabilizing effects (imperfections) on the structure, AISC360 offers notional load for both methods. Similarly, EC3 takes into account these destabilizing effects with sway and bow imperfections which consist of equivalent lateral loads. EC3 has a more direct approach which eliminates the use of effective length and therefore buckling checks. In this approach, additional notional loads are applied. In this thesis, individual fixed base members with different cross sections and two dimensional plane frames with different slenderness ratios were studied in detail according to these specifications. Results indicate that, DM, ELM and EC3 provisions give similar axial load capacities. Moreover, minor differences exist in moment capacities of DM and EC3. However, ELM gives smaller moment capacities compared to other analysis methods, generally.

Keywords: Buckling, Compression, Effective Length Method, Direct Analysis Method, Inelasticity, Imperfection, Notional Load, AISC360, EC3

ÖZ

AISC360 VE EC3 ŞARTNAMELERİNİN ELEMAN STABİLİTESİ KURALLARININ KARŞILAŞTIRILMASI

Kevran, Ömer
Yüksek Lisans, İnşaat Mühendisliği
Tez Yöneticisi: Prof. Dr. Cem Topkaya

Nisan 2016, 108 sayfa

Bu tezin amacı, AISC360 ve EC3 şartnamelerinde belirtilen stabilite ile ilgili kuralların karşılaştırılmasıdır. AISC360 şartnamesi eleman stabilitesi ile ilgili 2 yöntem olan Etkili Uzunluk Metodu ve Direkt Analiz Metodu'nu irdelemektedir. Etkili Uzunluk Metodu elemanın mesnetlenme, yanal ötelenme koşullarına bağlı olan ve burkulma yükünü direkt olarak etkileyen etkili uzunluk faktörünü kullanmaktadır. Diğer taraftan, Direkt Analiz Metodu etkili uzunluk faktörünü tüm mesnet koşulları için 1 kabul etmektedir. Ayrıca, inelastisiteden dolayı azaltılmış eksenel ve eğilme rijitliklerini kullanmaktadır. AISC360 şartnamesi her iki yöntem için de yapının stabilitesini bozan etkenleri dikkate almak için bir yatay yük tanımlamaktadır. Benzer olarak, EC3 şartnamesi de yapılardaki stabiliteyi etkileyen kusurları eşdeğer yatay yüklerden meydana gelen ötelenme (sway) ve bükülme (bow) düzensizlikleri olarak tanımlamaktadır. EC3 şartnamesi etkili uzunluk ve burkulma kontrollerini ortadan kaldıran daha açık bir yaklaşıma sahiptir. Bu yaklaşımda ilave yatay yükler etkitilmektedir. Bu tezde, farklı narinliklerdeki farklı kesite sahip münferit ankastre mesnetli elemanlar ve 2 boyutlu düzlem çerçeveler bu şartnamelere göre detaylı olarak incelenmiştir. Sonuçlara göre, Direkt Analiz Metodu, Etkili Uzunluk Metodu ve EC3 kuralları birbirine yakın eksenel yük kapasitesi vermektedir. Ayrıca, Direkt Analiz Metodu ve EC3'e göre yapılan analizden elde edilen moment kapasiteleri arasında küçük farklar bulunmaktadır. Fakat, Etkili Uzunluk Metodu diğer analiz metodlarına göre genellikle daha düşük moment kapasitesi vermektedir.

Anahtar Kelimeler: Burkulma, Basınç, Etkili Uzunluk Metodu, Direkt Analiz Metodu, İnelastisite, Kusur, Hayali Yük, AISC360, EC3

To My Love and Parents,

ACKNOWLEDGMENTS

The author deeply appreciates his supervisor Prof. Dr. Cem Topkaya for the continuous guidance and constructive criticism he has provided throughout the preparation of the thesis. Without his encouragement and patience, this thesis would not have been completed.

I would also like to express my sincere thanks to **Prof. Dr. Mehmet Utku**, **Assoc. Prof. Dr. Afşin Sarıtaş**, **Assoc. Prof. Dr. Eray Baran**, and **Asst. Prof. Dr. Burcu Güldür** for their suggestions and contributions during my thesis defense.

I should also thank my love Gizem Ünlü, my dearest friends Yusuf Dönmez, Meltem Tanış Dönmez, Ömer Faruk Işıkoğlu, Tuğçe Çavuşoğlu, Serdar Eser, Samet Kılıç and Derin Aykut for their great friendship and for giving moral and academic support.

The last but not least, the author wants to express his sincere thanks to his sister Kübra Kevran and his parents Mustafa Kevran and Ayten Kevran for the encouragement and love they have given him not only throughout the completion of this thesis but also his whole life.

TABLE OF CONTENTS

LIST OF TABLES

TABLES

LIST OF FIGURES

FIGURES

CHAPTER 1

INTRODUCTION AND BACKGROUND

Steel structures are widely used for different purposes around the world. Compared to reinforced concrete structures, most of the structural members are light and slender in a steel structure. Therefore, structural stability is an important concept for these structures.

High axial loads may result in unstable conditions for members that are subjected to compression. Also, residual stress, geometrical and structural imperfections are crucial parameters for determining the axial load capacity of a structural member. Specification for Structural Steel Buildings (AISC360-10) and Eurocode3 Design of Steel Structures (EC3) include some restrictions about stability of compression members. Member length, cross section properties (moment of inertia, section modulus, area, radius of gyration etc) are important parameters for buckling. These restrictions determine the load carrying capacity of the member. In addition to this, member imperfections that can be classified as residual stress, insufficiency of member verticality and eccentricities are being used for new generation analysis and design methods.

This thesis focuses on comparison of stability design approaches of AISC360-10 and EC3 specifications for individual members and frame systems. Columns with same sections but different slenderness ratios were studied to reveal the differences and similarities of AISC360-10 and EC3 specifications. These specifications have different approaches about structural stability. Effective Length Method is one of the most commonly used method for design of compression members. To determine axial load carrying capacity, this method focuses on slenderness ratio of member. ELM analysis can be performed by a computer program or hand calculations with nomographs depending on the side-sway conditions of the structure. ELM is the oldest method comparing to other analysis methods. To account for not only member

lengths but also inelasticity and imperfection items, AISC360-10 and EC3 provisions offer second order nonlinear analysis with some additional destabilizing forces. All restrictions given in these provisions were applied to members and explained in detail with case studies.

1.1 Plastic Behaviour of I Shapes

Mathematically, plastic moment of a section is defined as multiplication of yield stress and plastic section modulus. Theoretically, the maximum bending moment capacity can be defined as plastic moment capacity of the section in the absence of strain hardening. On the other hand, yield axial force is a function of gross area of the section and yield stress. Stress distribution of I shapes subjected to pure bending, pure compression and bending with compression was shown in Figure 1-1, Figure 1-2 and Figure 1-3 respectively.

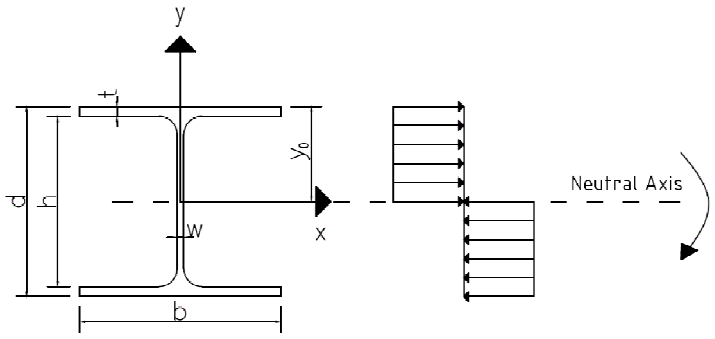

Figure 1-1 Stress Distribution of I Shape Subjected to Pure Bending

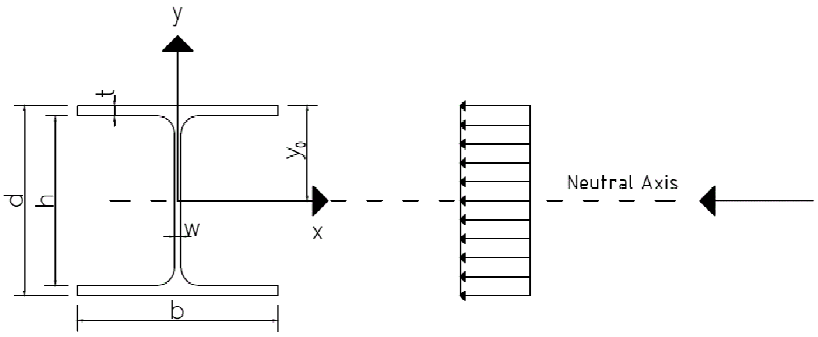

Figure 1-2 Stress Distribution of I Shape Subjected to Pure Compression

At the plasticity stage, all fibers in the cross-section reach to their yield stress and a plastic hinge is formed at the section. For wide-flange sections (i.e., those having constant flange thickness), the closed-form solution will vary depending on whether the neutral axis falls in the web ($y_o \leq h/2$) or the flange ($h/2 < y_o \leq d/2$). (Bruneau et al, 2011)

Equation (1-1) and (1-2) are closed form solution equations that determine the upper bound of normal force (P) and major axis bending moment (M) capacities of a section. These equations depend on the relation between $\frac{P}{P_y}$ and $\frac{A_w}{A}$ ratios.

$$\frac{M_{pr}}{M_p} = 1 - \left(\frac{P}{P_y}\right)^2 \frac{A^2}{4wZ_x} \qquad \text{for} \frac{P}{P_y} \leq \frac{A_w}{A} \tag{1-1}$$

$$\frac{M_{pr}}{M_p} = A\left(1 - \frac{P}{P_y}\right)\left(d - \frac{A}{2b}\left(1 - \frac{P}{P_y}\right)\right)\frac{1}{2Z_x} \qquad \text{for} \frac{P}{P_y} > \frac{A_w}{A} \tag{1-2}$$

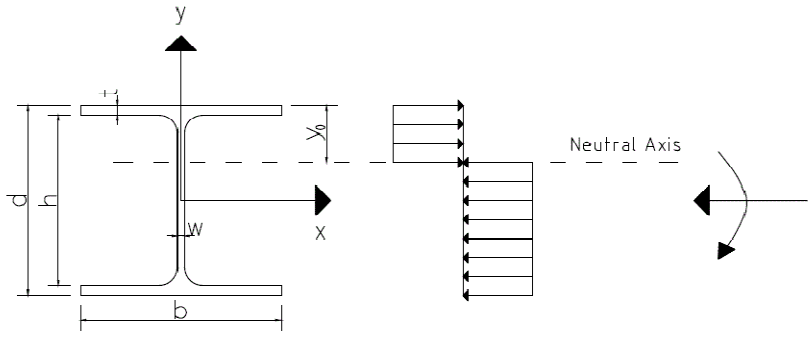

Figure 1-3 Stress Distribution of I Shape Subjected to Bending with Compression

Normalized M-P interaction equations can be obtained for wide flange sections in weak-axis bending following an approach similar to that presented above for strong-axis bending. Two cases must be considered, depending on whether the neutral axis falls in the web ($y_o \leq w/2$) or outside the web ($w/2 < y_o \leq b/2$). (Bruneau, Uang, Sabelli, 2011)

$$\frac{M_{pr}}{M_p} = 1 - \left(\frac{P}{P_y}\right)^2 \frac{A^2}{4wZ_y} \qquad \text{for} \frac{P}{P_y} \leq \frac{A_w}{A} \tag{1-3}$$

$$\frac{M_{pr}}{M_p} = \left(\frac{4bt}{A} - \left(1 - \frac{P}{P_y}\right)\right)\left(1 - \frac{P}{P_y}\right)\frac{A^2}{8tZ_y} \qquad \text{for } \frac{P}{P_y} > \frac{A_w}{A} \tag{1-4}$$

where;

P : applied force (kN), P_y : yield force (kN), M_p : plastic moment of the section (kNm), M_{pr} : plastic moment resistance of the section (kNm), A: section area (m^2), A_w : web area (m^2), Z_x : major axis plastic section modulus (m^3), Z_y : minor axis plastic section modulus (m^3), w: web thickness of the section (m), d : section depth (m), h : web height (m), b : flange width (m), y_0 : neutral axis depth (m)

1.2 Residual Stresses

Steel manufacturing processes mainly consist of heat treatment operations. High temperature is used in order to shape steel members. During the cooling stage of structural steel, thermal differences result in residual stress at the section. When the structural steel starts to cool, the external fibers of the section start to shrink.As the cooling stage at the external fiber is ongoing, internal fibers of section are still hot. For this reason, while the external fibers are exposed to tension forces, internal fibers are exposed to compression forces. This phenomenon causes the formation of residual stress at a cross-section. Due to existence of residual stresses, earlier yielding can be observed at the section. To account for the inelastic behavior resulting from residual stress, Direct Method offers a reduction on the bending stiffness and axial stiffness for compression members.

Members that can cool rapidly, such as thin steel plates, will be subjected to the largest magnitude of residual stresses, with values occasionally reaching up to the yield stress. However, in most rolled steel sections, the maximum residual stresses are approximately 33% of the yield stress. (Bruneau, Uang, Sabelli, 2011)

Residual stress causes the formation of partial yielding at the cross section. Partial yielding could strongly affect the stiffness of the member that are under high axial forces. For this reason, to account for the stiffness reduction effect, some parameters are considered in DM analysis. Bending stiffness of the section is modified with the

0.8 and τ_b coefficients. Moreover, modified axial stiffness, EA_{eff}, consist of 0.8 coefficient similar to flexural stiffness but τ_b coefficient is not included.

One of the most important component for the formation of column strength curves is initial residual stress distribution. The magnitude and distribution of initial residual stress in a section not only depend on the types of manufacturing process such as hot-rolled, welded or cold formed, they are also influenced by the types of cross-section, thickness of the section, cooling conditions, rolling temperature, straightening method and steel properties For a hot-rolled section, it is generally expected that for tension to form at centre of web and edge of flange because those place always cool fast whereas the web-flange junction, due to slow cooling process, contain tensile initial residual stresses. (Lu, 2011) Figure 1-4 shows the residual stress distribution of I shape cross-sections.

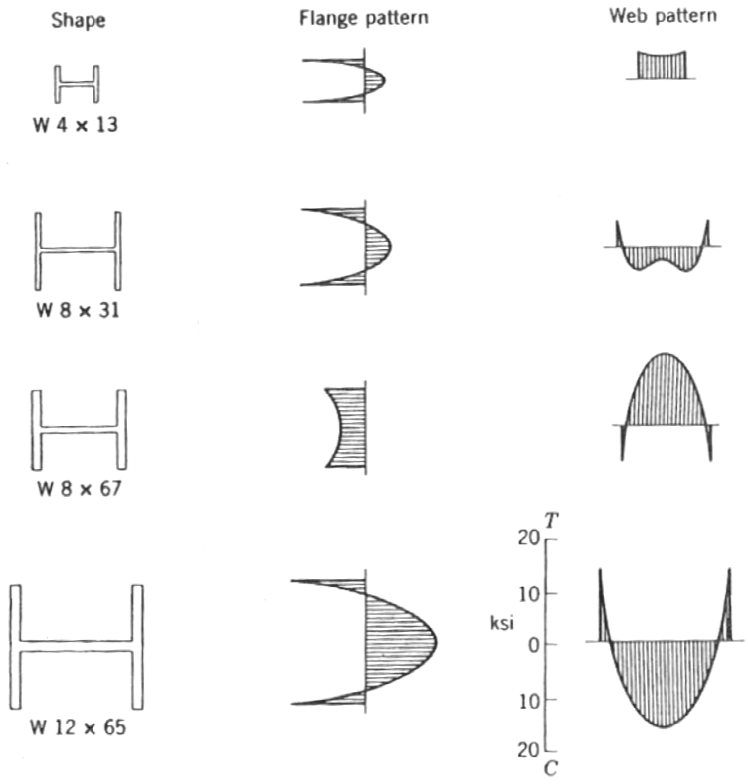

Figure 1-4 Initial Residual Stress Distribution of Sections (Adopted from Guide to Stability Design Criteria for Metal Structures)

1.3 Initial Imperfections

Initial imperfection is an another important destabilizing effect for structural members. It can be included in the system by obtaining an equivalent system with lateral loads. AISC360 and EC3 specifications define these lateral loads as notional load. Appropriate allowances should be incorporated in the structural analysis to cover the effects of imperfections including residual stress and geometrical imperfections such as lack of verticality, lack of straightness, lack of flatness, lack of fit and any minor eccentricities in joints of the unloaded structure.(Eurocode 3, 1993)

Definition of Notional Load :

Notional loads are unreal horizontal forces which are applied to the structural system at each storey level in the direction that contributes to the destabilizing effects of the load combination.

This method uses an equivalent lateral load to generate a larger than standard erection tolerance geometric deformation, intented to cover the effects of residual stresses, gradual yielding, local buckling and member imperfections that are not accounted for in the second order analysis. (Yuan, 2004)

AISC360-10 specification assumes a notional load which is equal to 0.002 times total gravity load at each storey. The magnitude of 0.002 comes from the allowable frame out of plumbness ratio of 1/500 of the storey height. On the other hand, EC specification offers a notional load depending on the storey height, gravity load acting on the column and number of columns in a row. For each specification, notional load parameters are shown in Figure 1-5.

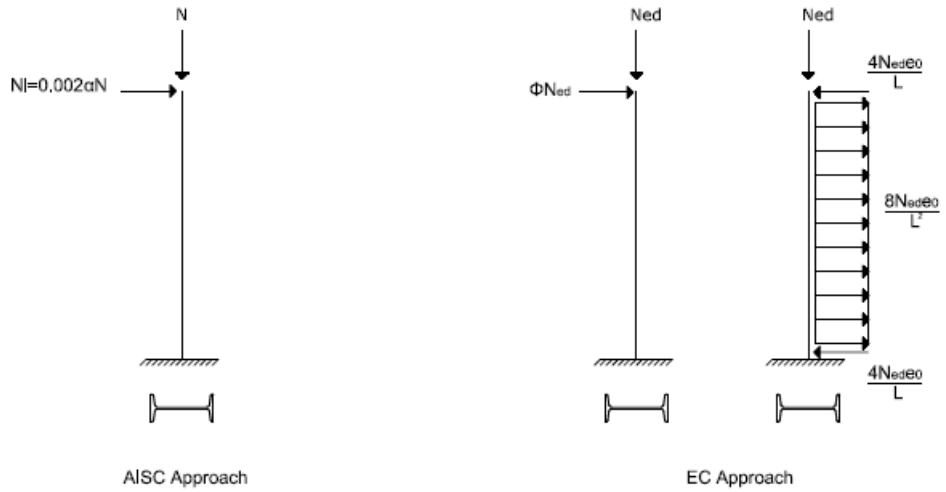

Figure 1-5 Notional Loads for AISC360 and EC3 specifications

1.4 Boundary Conditions

Slenderness ratio determines the axial load capacity of the compression members. With the elastic buckling analysis, axial load capacity of the column is calculated with Euler buckling equation. This equation includes effective length factor (K) which determines the effective buckling length of the member (KL). Euler buckling force is given in Equation (1-5).

$$P_E = \frac{\pi^2 EI}{(KL)^2} \tag{1-5}$$

For ideal columns, effective length factor can be determined by using alignment charts. As can be seen in the Equation (1-5), axial load capacity of a section is inversely proportional with the square of effective buckling length of column. For this reason, boundary conditions are important for determining the effective length factor and therefore axial strength of column member.

1.5 AISC360-10 Approaches for Stability of Frames

In this section, stability approaches of Effective Length Method and Direct Analysis Method are investigated in detail. First, general stability rules of AISC360 are mentioned. Then, Effective Length Method and Direct Analysis Method provisions

are studied specifically. Finally, a summary table is presented to show differences and similarities of each approach.

1.5.1 General Rules for Stability

This section summarises the stability rules which are valid both for Effective Length Method and Direct Analysis Method. These rules can be classified as member capacity curve equations, axial load carrying capacity of member and notional load concept. Second order analysis must be performed to account for the nonlinear effects on system. It can be performed with a appropriate computer program integrated with second order analysis. Moreover, it can be accomplished by amplifying the first order analysis results with B_1 and B_2 factors. B_1 multiplier to account for *P*-δ effects, determined for each member subject to compression and flexure, and each direction of bending of the member in accordance with Section 8.2.1. B_1 shall be taken as 1.0 for members not subject to compression. B_2 multiplier to account for *P*-Δ effects, determined for each story of the structure and each direction of lateral translation of the story in accordance with Section 8.2.2. (ANSI/AISC360-10, 2010)

In order to determine P-M axial force bending moment capacity curve of a member, column axial compressive strength P_n is used with the column bending moment strength M_n. Equation (1-6) and (1-7) are solved with second order analysis outputs of P_u and M_u.

$$\frac{P_u}{2P_n} + \frac{M_u}{M_n} = 1 \qquad \text{for } \frac{P_u}{P_n} < 0.2 \tag{1-6}$$

$$\frac{P_u}{P_n} + \frac{8M_u}{9M_n} = 1 \qquad \text{for } \frac{P_u}{P_n} \geq 0.2 \tag{1-7}$$

where;

P_u : required compression strength (kN), P_n : nominal compressive strength (kN)
M_u : major axis bending moment (kNm), M_n : nominal major axis bending moment (kNm)

The nominal compressive strength P_n, should be determined based on the limit state of flexural buckling. (ANSI/AISC360-10, 2010)

$$P_n = F_{cr}A_g \tag{1-8}$$

where;

F_{cr} : critical stress in accordance with the effective length of column (kN/m^2), A_g : gross area of the member (m^2)

Critical stress F_{cr} is a function of yield stress and Euler Buckling stress of the member. Depending on the slenderness ratio of the member, F_{cr} can be determined by the Equation (1-9) and (1-10).

$$\text{for} \quad \frac{KL}{r} \leq 4.71\sqrt{\frac{E}{F_y}} \qquad F_{cr} = (0.658^{\frac{F_y}{F_E}})F_E \tag{1-9}$$

$$\text{for} \quad \frac{KL}{r} > 4.71\sqrt{\frac{E}{F_y}} \qquad F_{cr} = 0.877F_E \tag{1-10}$$

Euler buckling stress of a member is defined in Equation (1-11).

$$F_E = \frac{\pi^2 E}{(\frac{KL}{r})^2} \tag{1-11}$$

where;

F_y : yield stress of member (kN/m^2); F_E : Euler Buckling stress of member (kN/m^2), E : Elastic modulus (kN/m^2); K : Effective length factor, L : Member length (m), r : radius of gyration (m)

There are some differences between the actual structure and the mathematical model caused by fabrication and erection processes. To take into account these differences, AISC360-10 provisions offer to apply a notional load in the transverse direction that is equal to 0.002 times total gravity load. Figure 1-6 shows the application of notional load with gravity loads on a typical frame system. The magnitude of 0.002 represents the maximum permitted value of frame out-of plumbness. An out of

plumbness of 1/500 represents the maximum tolerance on column plumbness ratio specified in the AISC Code of Standard Practice. (ANSI/AISC360-10, 2010)

$$N_i = 0.002\alpha_i Y_i \qquad (1\text{-}12)$$

where;

N_i : Notional load applied at level i, (kN), α_i : 1.0 for LRFD, 1.6 for ASD, Y_i : Gravity load applied at level i, (kN)

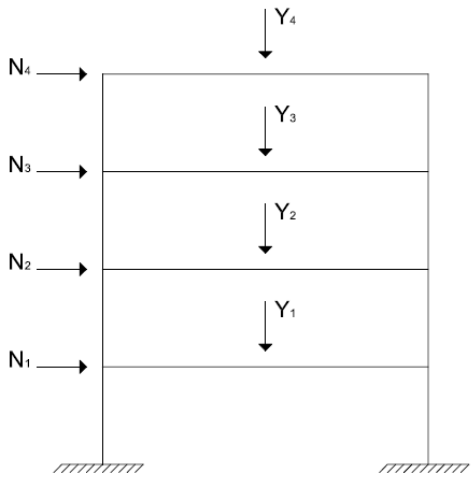

Figure 1-6 Typical Frame System

1.5.2 Effective Length Method (ELM)

For many years, Effective Length Method has been used as an inevitable method for design of compression members. In general, ELM calculates the nominal column buckling resistance using an effective length (KL) and the load effects are calculated based on either a rigorous or approximate second order analysis. (Ziemian, 2010)

The effective length method is probably the most well known method for stability analysis. However as the name implies, the effective length factor K must be calculated. This can become very complex even for relatively simple structures. The accuracy of the effective length method is critically linked to accurate calculation of the effective length factor. Various methods for determining K have been developed

but the most widely known is still the alignment charts. (Nelson, 2008) Effective buckling length KL of a member is determined with G factor defined in Equation (1-13).

$$G = \frac{\Sigma(^{E_c I_c}/_{L_c})}{\Sigma(^{E_b I_b}/_{L_b})} = \frac{\Sigma(^{EI}/_{L})_c}{\Sigma(^{EI}/_{L})_b} \tag{1-13}$$

The symbol Σ indicates a summation of all members rigidly connceted to that joint and located in the plane in which buckling of the column is being considered. E_c is the elastic modulus of the column, I_c is the moment of inertia of the column and L_c is the unsupported length of the column. E_g is the elastic modulus of the girder, I_g is moment of inertia of the girder, and L_g is the unsupported length of the girder or other restraining member. I_c and I_g are taken about axes perpendicular to the plane of buckling being considered. The alignment charts are valid for different materials if an appropriate effective rigidity, EI, is used in the calculation of G. (ANSI/AISC 360-10, 2010) K factor is determined by means of the nomographs given in Figure (1-7) and Figure (1-8) depending on structural system whether it is side-sway inhibited or not.

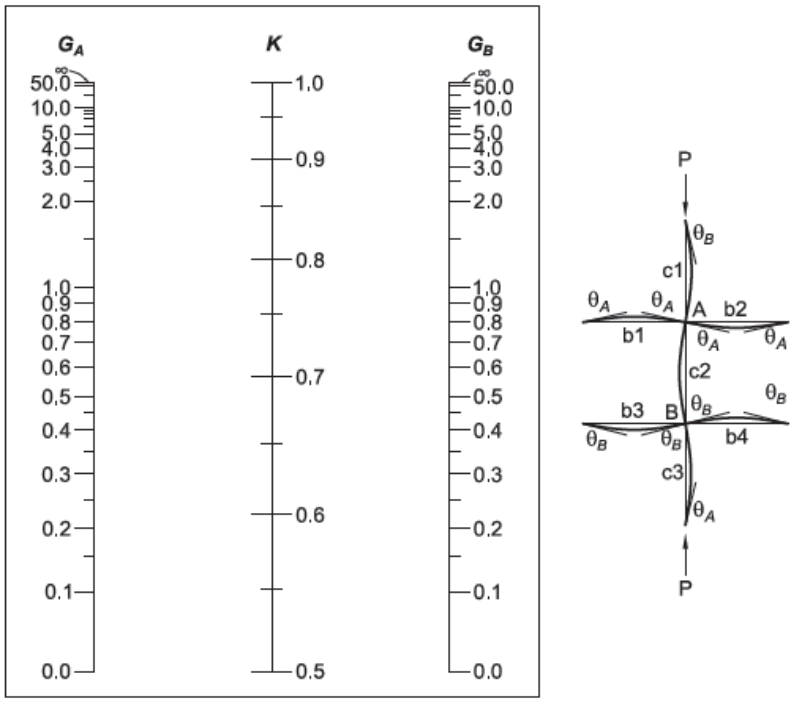

Figure 1-7 Alignment Chart-Sidesway Inhibited (Adopted from AISC 360-10)

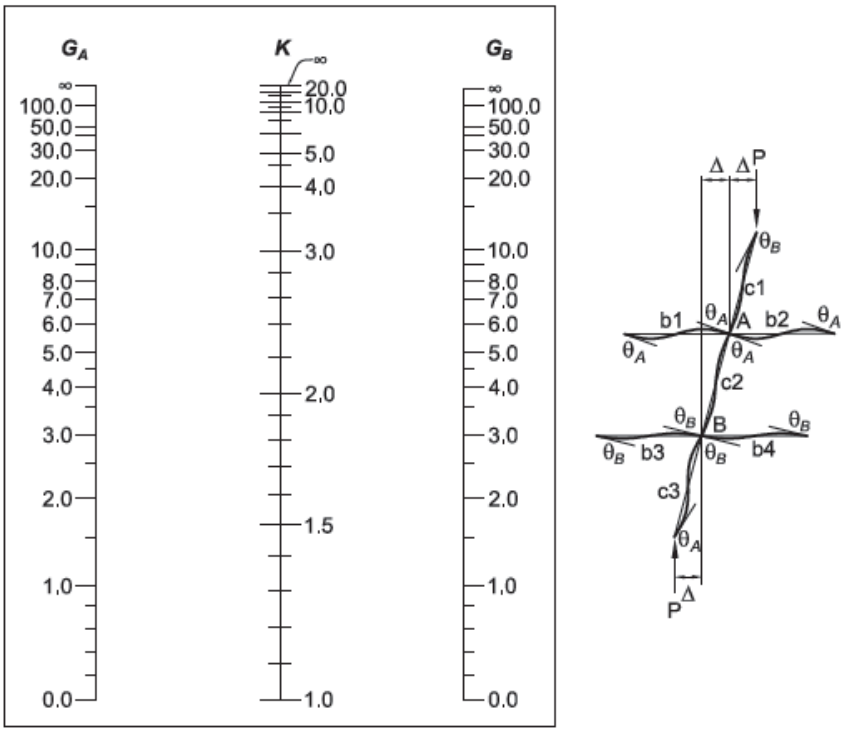

Figure 1-8 Alignment Chart-Sidesway Permitted (Adopted from AISC 360-10)

1.5.3 Direct Analysis Method (DM)

The goal of Direct Analysis Method is to assess stability of members without calculating effective length factor K. AISC360-10 states that, buckling length of the member is equal to the member actual length for Direct Analysis Method. In other words, effective length factor K is assumed as 1 for all boundary conditions of compression members.

As it has been stated in general rules, notional load represents geometrical imperfection of members. In addition to this, another important issue for Direct Analysis Method is inelasticity. AISC360-10 provisions state that, due to inelasticity flexural stiffness and axial stiffness should be modified in accordance with the magnitude of axial load acting on the member. To take into account inelastic behavior of cross section, EI and EA is reduced with a coefficient which is equal to 0.8. In addition to this, flexural rigidity is reduced with a τ_b factor which is a function of yielding force and the vertical load acting on the column. If the ratio of resisting force to yielding force smaller than 0.5, τ_b coeffecient is assumed as one.

Otherwise, computation of τ_b with respect to applied axial load is needed. In other words, relatively high loads require the calculation of τ_b. As a result, main subjects of Direct Analysis Method are using modified stiffness parameters and eliminating the calculation of effective length factor. Modified axial stiffness is illustrated in Equation 1-14.

$$EA^* = 0.8EA \tag{1-14}$$

Modified flexural stiffness is shown in Equation 1-15.

$$EI^* = 0.8\tau_b EI \tag{1-15}$$

As shown in Equation 1-16 and 1-17, τ_b coefficient is computed depending on the ratio of applied axial force to member yield force.

$$\frac{\alpha P_r}{P_y} < 0.5 \qquad \tau_b = 1 \tag{1-16}$$

$$\frac{\alpha P_r}{P_y} > 0.5 \qquad \tau_b = 4\frac{\alpha P_r}{P_y}\left(1 - \frac{\alpha P_r}{P_y}\right) \tag{1-17}$$

where;
α = 1.0 (for LRFD); α = 1.6 (for ASD)

Stiffness modification is not an essential rule for Direct Analysis Method. Nominal axial and flexural stiffness values can be used with the application of additional notional load to the structure. It is permitted when $\frac{\alpha P_r}{P_y} > 0.5$ ($\tau_b = 1$). In this case, a total of 0.003 times the notional load is applied to each storey.

1.5.4 Comparison of ELM and DM

As mentioned in the previous sections in detail, Table 1-1 was prepared to represent the similarities and disparities of ELM and DM.

Table 1-1 Summary Table of ELM and DM

	Effective Length Method (ELM)	**Direct Analysis Method (DM)**
AISC Specification Reference	Appendix 7	Chapter C
Limitation on the Use of this Method	$\frac{\Delta_{2nd\ order}}{\Delta_{1st\ order}}$ or $B_2 \leq 1.5$ $B_2 = \frac{1}{1-\frac{\alpha P_{storey}}{P_{estorey}}}$	None
Analysis Type	Second order elastic	Second order elastic
Structure Geometry in the Analysis	Nominal	Nominal
Notional Loads in the Analysis	$0.002Y_i$	$0.002Y_i$
Member Stiffnesses in the Analysis	Use Nominal EA and EI	Use $EA^* = 0.8EA$ Use $EI^* = 0.8\tau_b EI$ $\tau_b = 1.0$; $\frac{\alpha P_r}{P_y} \leq 0.5$ $\tau_b = 4\frac{\alpha P_r}{P_y}(1-\frac{\alpha P_r}{P_y})$; $\frac{\alpha P_r}{P_y} > 0.5$

The above table shows the Effective Length Method and Direct Analysis Method criteria about member stability. There is a limitation of using Effective Length Method if sidesway amplification factor B_2 is greater than 1.5. In other words, in order to use ELM, the proportion of side-sway displacements obtained from second order analysis to first order analysis must be smaller than 1.5. While all the requirements for AISC stability analysis are covered with this method, slight

variations in each requirement are allowed and discussed in further detail. One major advantage of the direct analysis method is that it has been developed and verified for application to all types of structural systems and therefore has no limitations for use. (Maleck and White, 2003)

1.6 EUROCODE 1993-1-1 (EC3) Approaches for Stability of Frames

Member resistance and cross section resistance of compression members are investigated in different chapters in EC3. With the determination of compression resistance of section, buckling checks can be neglected by taking into consideration of sway and bow imperfections. EC3 (Section 5.2.2) establishes that the verification of the stability of frames and their parts should be carried out considering imperfections and second order effects. (Yong et al, 2006)

1.6.1 EC3 Buckling Resistance of Compression Member

EC3 compression member design provisions states that design value of compression force N_{Ed} must be smaller than the buckling resistance of the member.

$$\frac{N_{Ed}}{N_{b,Rd}} \leq 1.0 \qquad (1\text{-}18)$$

where;

N_{Ed} : design value of compression force, $N_{b,Rd}$: buckling resistance of member

Buckling resistance of a member is related with the cross section classification.AISC360-10 and EC3 covers the flexural buckling with a non-dimensional slenderness coefficient λ. AISC360-10 gives the strength of single column with a one curve. On the other hand, EC3 defines five different column strength curves to determine the capacity of member. Nominal axial load capacity of flexural buckling can be determined with Equation (1-19).

$$P_n = \chi F_y A_g \quad \text{(AISC360-10 and EC3)} \qquad (1\text{-}19)$$

The non-dimensional slenderness ratio (λ) can be defined as :

$$\lambda = \sqrt{\frac{P_{cr}}{F_y A_g}} = \frac{\pi r}{KL}\sqrt{\frac{E}{F_y}} \quad (1\text{-}20)$$

Reduction factor χ stated in AISC360 and EC3 specificationsis given in Equation (1-21) and (1-22).

$$\chi = 0.658^{\lambda^2} \quad \lambda \leq 1.5 \qquad \chi = \frac{0.877}{\lambda^2} \quad \lambda > 1.5 \quad \text{(AISC360-10)} \quad (1\text{-}21)$$

$$\chi = \frac{1}{\phi + \sqrt{\phi^2 - \lambda^2}} \qquad \phi = 0.5(1 + \alpha(\lambda - 0.2) + \lambda^2) \quad \text{(EC3)} \quad (1\text{-}22)$$

EC3 utilizes an imperfection coefficient (α) to distinguish between different column strength curves. For flexural buckling, five cases termed as ao, a, b, c, d are given for which the α values are 0.13, 0.21, 0.34, 0.49, and 0.76, respectively. The choice as to which buckling curve to adopt is dependent upon the geometry and material properties of the cross section and upon the axis of buckling. The rules for selecting the appropriate column strength curve are tabulated in EC3. (Topkaya C. Şahin S, 2009)

Table 1-2 shows the selection of buckling curve for a cross section.

Table 1-2 Selection of Buckling Curve for a Cross-Section (Adopted from EC3)

Cross section		Limits		Buckling about axis	Buckling curve: S 235 S 275 S 355 S 420	Buckling curve: S 460
Rolled sections	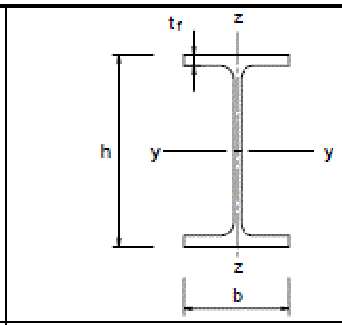	$h/b > 1,2$	$t_f \leq 40$ mm	y – y z – z	a b	a_0 a_0
			40 mm < $t_f \leq 100$	y – y z – z	b c	a a
		$h/b \leq 1,2$	$t_f \leq 100$ mm	y – y z – z	b c	a a
			$t_f >$ 100 mm	y – y z – z	d d	c c
Welded I-sections	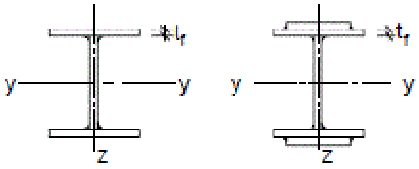	$t_f \leq 40$ mm		y – y z – z	b c	b c
		$t_f > 40$ mm		y – y z – z	c d	c d
Hollow sections		hot finished		any	a	a_0
		cold formed		any	c	c
Welded box sections	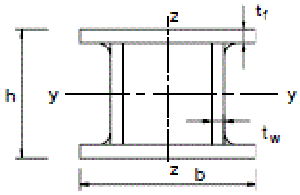	generally (except as below)		any	b	b
		thick welds: $a > 0,5t_f$ $b/t_f < 30$ $h/t_w < 30$		any	c	c
U-, T- and solid sections	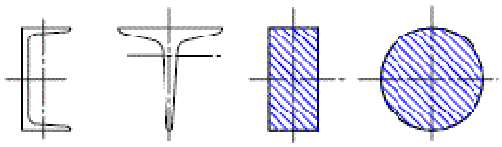			any	c	c
L-sections	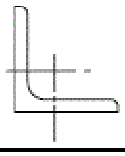			any	b	b

Buckling curves of different types of sections are determined depending on the ratio of height of section to flange width ($\frac{h}{b}$), material quality and limitation of flange thickness criteria. Moreover, buckling resistance of a member depends on its end conditions. EC3 does not provide alignment chart to determine effective buckling length of a member. Some information for determining effective length factor can be found in BS 5950. Elastic critical buckling resistance of the section can be determined with the Equation (1-23).

$$N_{cr} = \frac{\pi^2 EI}{(KL)^2} \qquad (1\text{-}23)$$

where;

N_{cr} : Elastic critical buckling force (kN)

Imperfection factor α is determined with using the appropriate buckling curve. Column strength curves given in AISC360-10 and EC3 are compared in Figure 1-9.

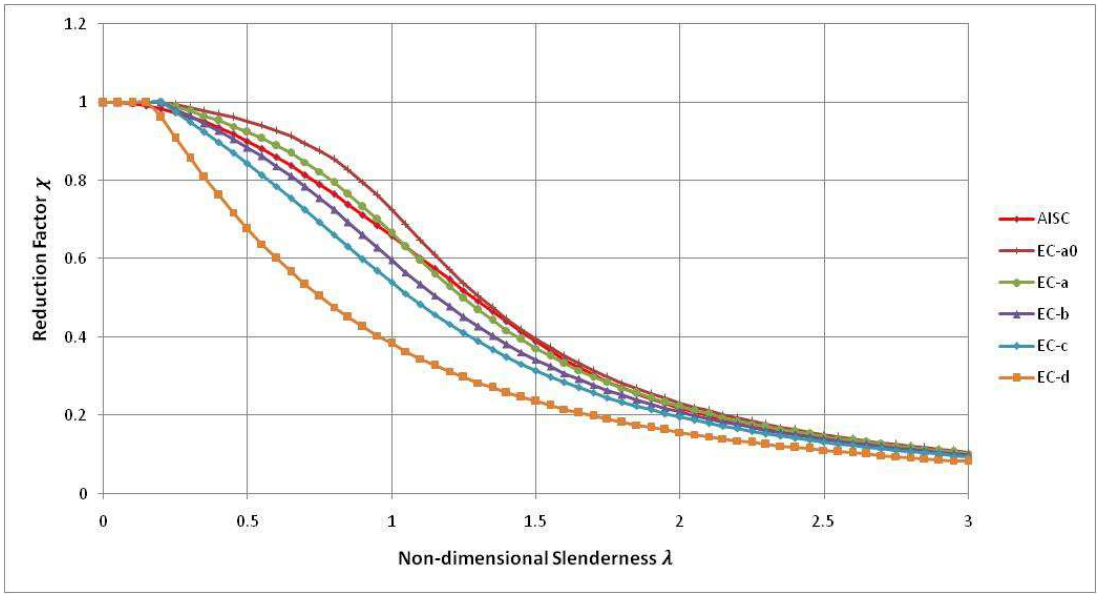

Figure 1-9 Comparison of Reduction Factors Given in AISC360-10 and EC3 for Flexural Buckling

1.6.2 EC3 Cross Section Resistance of Compression and Flexural Members

Major axis bending moment capacity of the compression members is determined with the Equations (1-24), (1-25) and (1-26).

$$M_{N,y,Rd} = M_{pl,y,Rd}\frac{(1-n)}{(1-0.5a)} \qquad M_{N,y,Rd} \leq M_{pl,y,Rd} \qquad (1\text{-}24)$$

On the other hand, minor axis bending moment capacity of the compression member is determined with the Equations (1-25), (1-26) and (1-27).

$$\text{for } n \leq a\ ;\ M_{N,z,Rd} = M_{pl,z,Rd} \tag{1-25}$$

$$\text{for } n > a\ ; \quad M_{N,z,Rd} = M_{pl,z,Rd}\left[1 - \left(\frac{n-a}{1-a}\right)^2\right] \tag{1-26}$$

where;

$$n = \frac{N_{Ed}}{N_{pl,Rd}} \qquad a = \frac{A-2bt_f}{A}\ a \leq 0.5 \tag{1-27}$$

N_{Ed} : Design value of compression force, (kN)

$N_{pl,Rd}$: Design plastic resistance to normal forces of gross cross section, (kN)

$M_{N,y,Rd}$: Reduced design value of resistance to strong axis bending moment for the presence of normal force, (kNm)

$M_{pl,y,Rd}$: Strong axis plastic moment resistance, (kNm)

$M_{N,z,Rd}$: Reduced design value of resistance to weak axis bending moment for the presence of normal force, (kNm)

$M_{pl,z,Rd}$: Weak axis plastic moment resistance, (kNm)

1.6.3 Initial Sway Imperfection

Initial sway imperfection parameters stands for lack of member verticality, eccentricities and lack of fit. The system can be analyzed with two ways. First method is rotating the member with an angle of ϕ. Then, compression force is applied to rotated system and analysis is performed with respect to rotated system. Second method is converting the system into an equivalent system with lateral forces. Analysis is performed with respect to the undeformed system with lateral forces. The ϕ parameter includes a basic constant value of $\frac{1}{200}$, reduction factor for height, α_h, and reduction factor for number of column α_m, according to Equation (1-28).

$$\Phi = \Phi_0 * \alpha_h * \alpha_m \qquad \alpha_h = \frac{2}{\sqrt{h}}\left(\frac{2}{3} \leq \alpha_h \leq 1\right) \qquad \alpha_m = \sqrt{0.5 * (1 + \frac{1}{m})} \tag{1-28}$$

where;

h : column height in meters, m : number of columns in a row

Sway imperfection loading is presented in Figure 1-10.

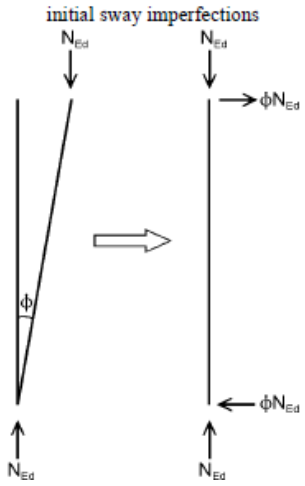

Figure 1-10 Sway Imperfection (Adopted from EC3)

These initial sway imperfections should be applied in all relevant horizontal directions, but need only be considered in one direction at a time. (Eurocode3, 1993)

1.6.4 Local Bow Imperfection

Local bow imperfection represents flexural buckling of the compression member. To account for the local bow imperfection, lateral distributed load is applied along the member in the transverse direction. Initial bow imperfection depends on column length L, maximum amplitude of a member imperfection e_0 and compression force acting on the member.

Bow imperfection loading is presented in Figure 1-11.

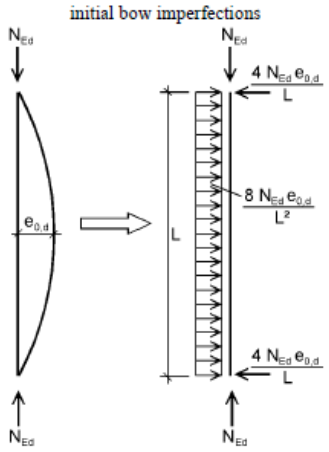

Figure 1-11 Bow Imperfection (Adopted from EC3)

Design values of local bow imperfections are illustrated in Table 1-3.

Table 1-3 Design Values of Local Bow Imperfections (Adopted from EC3)

Design Values of Local Bow Imperfection		
Buckling Curve Acc. To Table 1-2	**Elastic Analysis (e_0/L)**	**Plastic Analysis (e_0/L)**
a_0	1/350	1/300
a	1/300	1/250
b	1/250	1/200
c	1/200	1/150
d	1/150	1/100

To combine notional loads resulting from initial sway imperfection and local bow imperfection, lateral forces are superposed.

1.7 Scope of Thesis

The goal of this thesis is to compare the stability design approaches given in AISC360-10 and EC3 specifications with different sections and case studies. First chapter explains closed form solution of I shapes, destabilizing effects on structures, ELM, DM and EC3 provisions about stability. In the second chapter, benchmark problems given in AISC360-10 are studied in detail with second order analysis. A comparison and verification of SAP2000 outputs and benchmark solutions are tabulated. Also, accuracy of SAP2000 for second order analysis solutions are

discussed. Then, stability provisions given in AISC360-10 and EC3 specifications were discussed in Chapter 3. Differences and similarities of Effective Length Method and Direct Analysis Method are evaluated. W10x26, W10x60, W14x605 and W18x192 sections with idealized boundary conditions are investigated both for strong axis and weak axis with the slenderness ratio of KL/r = 40, 80, 120, 160 and 200. Column members that are part of a two dimensional plane frame system are studied in Chapter 4. Direct Analysis Method, Effective Length Method and EC3 analysis were performed for column member of two dimensional plane frames. Also, effect of effective length factor on axial load capacity is discussed in Chapter 4. Finally, conclusions and recommendations are given in Chapter 5.

CHAPTER 2

VERIFICATION OF SAP2000 FOR SECOND ORDER ANALYSIS USING BENCHMARK PROBLEMS

2.1 Problem Definition

In this chapter, benchmark problems given in AISC360-10 specification were analyzed in order to make a comparison of target base moment values with analysis results obtained from SAP2000. These problems consist of members subjected to lateral and axial compression loads. Also, each of these problems has different boundary conditions. Benchmark problem definitions and loading parameters are presented in Figure 2-1 and Figure 2-2. Second order nonlinear analysis was performed to take into account relative lateral displacement between start and end nodes. Nonlinear analysis with P-Δ effects which is also known as kinematic nonlinearity effects depends on the loading and boundary conditions of the system. Therefore, during the analysis process, the axial load is applied incrementally.

The first benchmark problem shown in Figure 2-1 is a pin and roller supported beam-column subjected to an axial force at its roller end. In addition to this, there is a uniformly distributed load along the member in the transverse direction. For different axial load values, target span moments given by AISC360-10 were compared with midspan moment values obtained from SAP2000 analysis results.

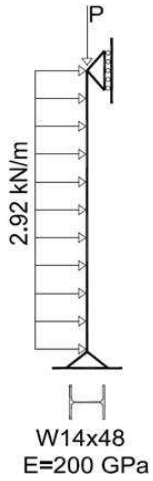

Figure 2-1 Benchmark Problem 1

For the first benchmark problem, target span moments and tip displacement values are given in Table 2-1.

Table 2-1 Target Results of Benchmark Problem 1(Adopted from AISC360-10)

Axial Load P (kN)	0	667	1334	2001
Lateral Load (kN/m)	2.92	2.92	2.92	2.92
M_{span} (kNm)	26.6	30.5	35.7	43
Δ_{tip} (mm)	5.13	5.86	6.84	8.21
Analysis include axial, flexural and shear deformations				

The second benchmark problem is a fixed base cantilever column subjected to a lateral load with an axial compression load at its free end. Similar to first benchmark problem, target base moments given by AISC360-10 for different axial compression forces were compared with SAP2000 analysis results. This problem shown in Figure 2-2.

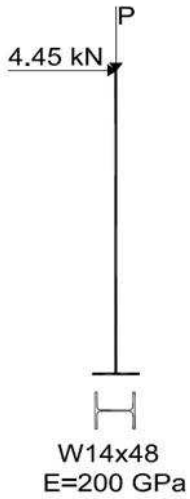

Figure 2-2 Benchmark Problem 2

For the second benchmark problem, target base moment and tip displacement values are given in Table 2-2.

Table 2-2 Target Results of Benchmark Problem 2(Adopted from AISC360-10)

Axial Load P (kN)	0	445	667	890
Lateral Load (kN)	4.45	4.45	4.45	4.45
M_{base} (kNm)	38	53.2	68.1	97.2
Δ_{tip} (mm)	23.1	34.2	45.1	66.6
Analysis include axial, flexural and shear deformations				

2.2 Solutions for Benchmark Problem Case 1

To obtain analysis results of Problem 1, five structural models were analysed separately. Figure 2-3 shows the structural analysis models for benchmark problem 1. For the case with one element per member, if there is no axial load on the system, target span moment and analysis result of midspan moment are identical. In other words, if the member is subjected only 2.92 kN/m laterally distributed load, SAP2000 gives reasonable results comparing to AISC360-10. On the other hand, if the axial force on the system increases, second order effects become important. Therefore, to obtain close results with target span moments beam-column was divided into five elements.

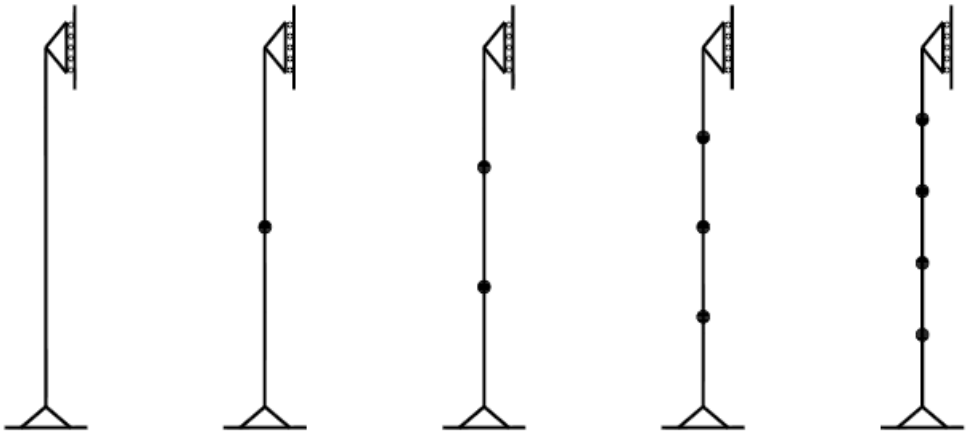

Figure 2-3 Analysis Models for Benchmark Problem 1

Analysis results for the first benchmark problem were shown in Table 2-3.

Table 2-3 SAP2000 Analysis Results for Benchmark Problem 1

Applied Axial Load (kN)	Applied Lateral Load (kN/m)	P/P_{cr} (%)	Target Span Moment (kNm)	Sap2000 P-Δ Analysis Span Moment Results (kNm)				
				1 Element	2 Elements	3 Elements	4 Elements	5 Elements
0	2.92	0	26.6	26.56	26.56	26.56	26.56	26.56
667	2.92	27%	30.5	29.49	30.37	30.42	30.44	30.44
1334	2.92	54%	35.7	33.17	35.44	35.54	35.59	35.59
2001	2.92	81%	43	37.73	42.44	42.65	42.75	42.76
				% Error				
				1 Element	2 Elements	3 Elements	4 Elements	5 Elements
				0.16	0.16	0.16	0.16	0.16
				3.30	0.42	0.27	0.21	0.19
				7.08	0.72	0.45	0.31	0.30
				12.25	1.30	0.81	0.58	0.56

2.3 Solutions for Benchmark Problem Case 2

Second benchmark problem was solved similar to first problem. Structural analysis models for benchmark problem 2 were shown in Figure 2-4. Analysis results show that, error percentage decreases when the element is divided into more than two elements. Also, when the column exposed to relatively high axial loads the error percentage increases considerably.

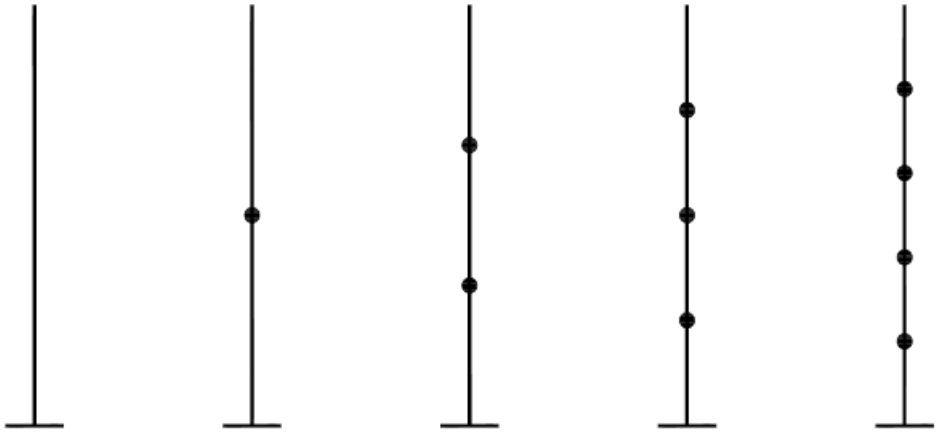

Figure 2-4 Analysis Models for Benchmark Problem 2

Analysis results for second benchmark problem were illustrated in Table 2-4.

Table 2-4 Analysis Results for Benchmark Problem 2

Applied Axial Load (kN)	Applied Lateral Load (kN)	P/P_{cr} (%)	Target Base Moment (kNm)	Sap2000 P-Δ Analysis Base Moment Results (kNm)				
				1 Element	2 Elements	3 Elements	4 Elements	5 Elements
0	4.45	0	38	37.96	37.96	37.96	37.96	37.96
445	4.45	37%	53.2	52.87	52.90	52.90	52.90	52.90
667	4.45	56%	68.1	66.82	67.36	67.37	67.38	67.38
890	4.45	81%	97.2	94.66	95.13	95.17	95.18	95.19
				% Error				
				1 Element	2 Elements	3 Elements	4 Elements	5 Elements
				0.11	0.11	0.11	0.11	0.11
				0.61	0.57	0.56	0.56	0.56
				1.88	1.08	1.07	1.06	1.06
				2.61	2.13	2.09	2.07	2.07

2.4 Conclusion

For benchmark problem 1, analysis results obtained from one element model are not close to target span moment under high axial loads. There is a consistency between target span moments and SAP2000 analysis results when dividing the member into more than two segments. For benchmark problem 2, analysis results are compatible with target base moment values when the gravity load is relatively low. Analysis results are close to target base moments when the element is divided into more than two elements. Generally, the errors are small for each benchmark problem. However,

in order to make a precise analysis, all compression members were divided into five elements for the rest of the analysis presented in this thesis.

CHAPTER 3

COMPARISON OF STABILITY APPROACHES OF AISC360-10 AND EC3 SPECIFICATIONS FOR A MEMBER UNDER IDEALIZED BOUNDARY CONDITIONS

In this chapter, cantilever members with different sections and different slenderness ratios were studied. W10x60, W10x26, W14x605 and W18x192 sections were investigated depending on the AISC360 and EC3 stability provisions for strong and weak axis bending. The purpose of using these cross sections is to compare AISC360 and EC3 approaches for different initial bow imperfection values of EC3 specification. Bow imperfection values are determined with respect to axis of bending as well as flange thickness and $\frac{h}{b}$ ratio of the section. In Chapter 1, Table 1-2 shows the imperfection values depending on those criteria. For each section and case study, EC3 bow imperfection loading parameters were determined and are presented in Table 3-1.

Table 3-1 Determination of Initial Bow Imperfection Parameters

Section	Flange Thickness (mm)	h/b	EC3 Bow Imperfection	
			Strong Axis	Weak Axis
W10x60	17.272	1.014	b	c
W10x26	11.176	1.790	a	b
W14x605	105.664	1.201	d	d
W18x192	44.450	1.777	b	c

With the determination of loading parameters, each cross section was analysed to present the effect of EC3 imperfections on P-M capacity values. Steel design specifications emphasize the importance of horizontal (notional) loads resulting from initial and geometrical imperfections in different ways. For this reason, main purpose of this chapter is to determine P-M capacities of sections with destabilizing effects of AISC360 and EC3 provisions. For each specification, notional load parameters

depend on imperfections factors and axial load subjected to column member. Comparison of major axis bending moment and vertical base reactions are shown at the end of each case study. Analysis were performed with SAP2000 software by taking into consideration of nonlinear P-Δ effects. Members were subdivided into 5 elements in all studies.

3.1 Member Under Strong Axis Bending

In this section, W10x60, W10x26, W14x605 and W18x192 sections under strong axis bending with different slenderness ratios were studied according to AISC360-10 and EC3 stability provisions. Using the effective length factor K=2, columns that have slenderness ratio of KL/r = 40, 80, 120, 160 and 200 were investigated for each section. Results are presented in graphs which include closed form solution curve, EC3 strong axis bending capacity curve, AISC360 DM and ELM strong axis bending capacity curves with related analysis results. Closed form solution curve for major axis bending was obtained with Equations (1-1) and (1-2). Also, EC3 curve was obtained with Equation (1-24). In addition to this, AISC360 curves were obtained by using Equation (1-6) and (1-7). Figure 3.1 shows the member under strong axis bending with compression.

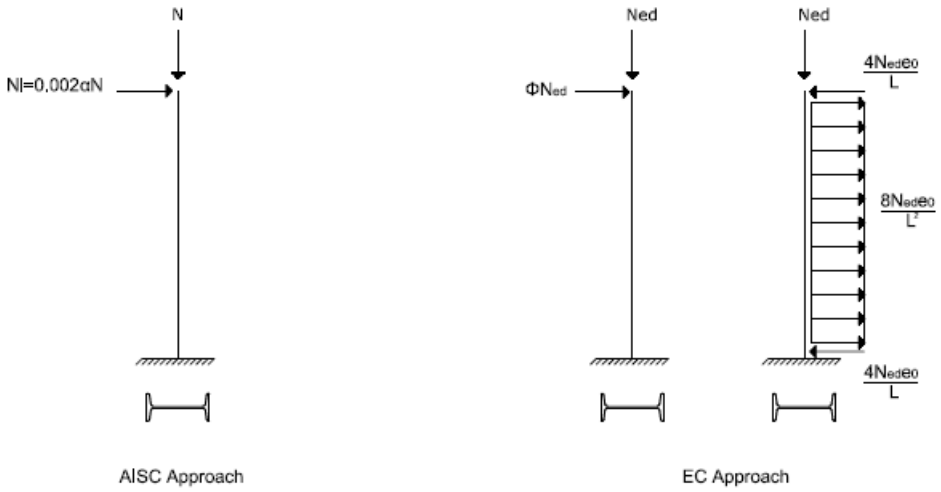

Figure 3-1 Members Under Strong Axis Bending with Compression

3.2 Member Under Weak Axis Bending

In this section, same procedures valid for strong axis bending analysis were applied to members under weak axis bending. Also, cross section properties, slenderness of column members and loading parameters for AISC360 and EC3 specifications are identical with the strong axis bending case. Figure 3-2 shows the member under weak axis bending with compression.

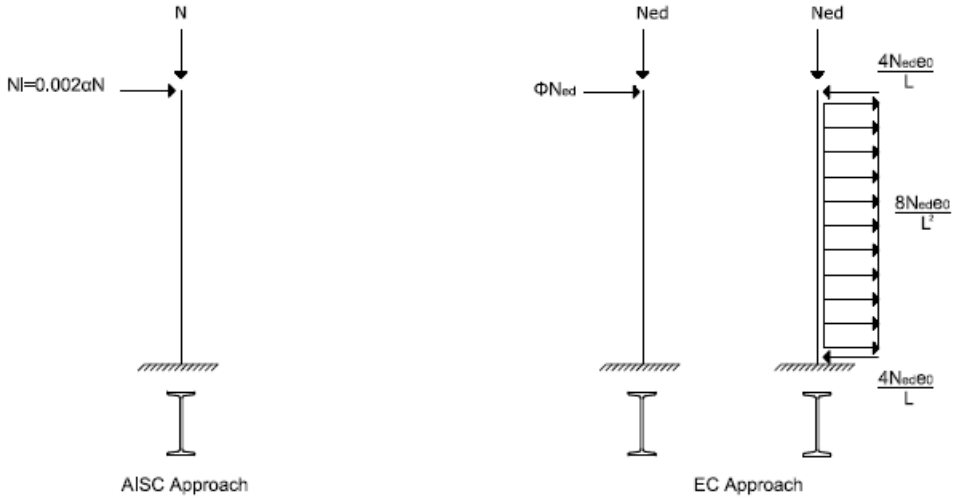

Figure 3-2 Members Under Weak Axis Bending with Compression

3.3 Comparison of EC3 Sway and Bow Imperfections

EC3 structural stability provisions include imperfection concepts for systems that are under compression. As mentioned before, these concepts named as sway and bow imperfections resulting from residual stress, lack of straightness, lack of verticality and some eccentricities on the members. For frames sensitive to buckling in a sway mode the effect of imperfections should be allowed for in frame analysis by means of an equivalent imperfection in the form of an initial sway imperfection and individual bow imperfections of members. (EC3, Design of Steel Structures, 1993) These imperfections are represented with random directions in EC3. W10x60 column with KL/r=80 was studied specifically to compare P-M capacities obtained from sway+bow and sway-bow loadings. Each loading results were plotted in Figure 3-3. Results show that, sway-bow loading gives the lowest capacity when all loading

directions are considered. For this reason, all analysis about EC3 provisions were performed by considering sway-bow loading.

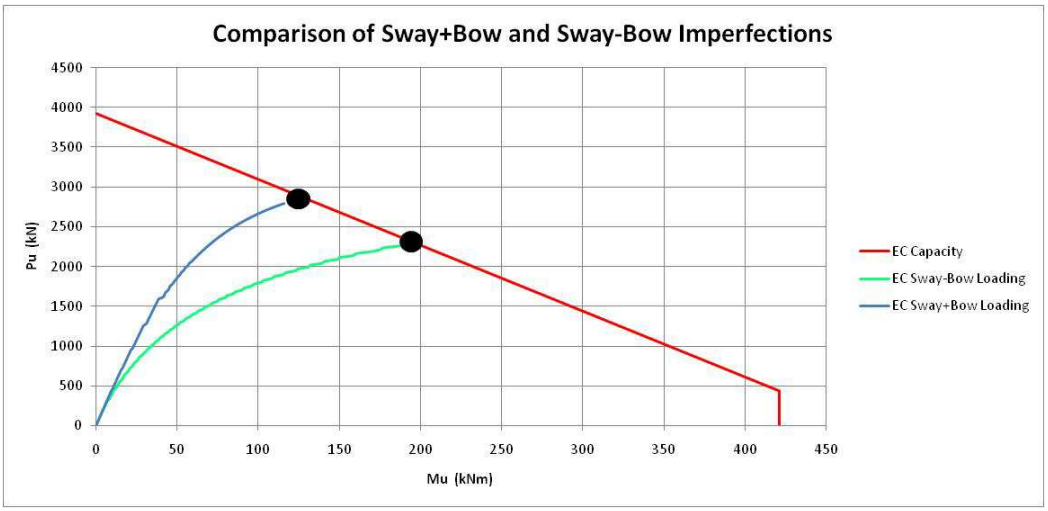

Figure 3-3 Comparison of EC3 Sway-Bow and Sway+Bow Loadings for KL/r=80 W10x60 Column

3.4 Investigation of W10x60

This section includes investigation individual W10x60 column members that are under strong axis bending. Cross section properties of W10x60 are shown in Table 3-2.

Table 3-2 Cross Section Properties of W10x60

E : elastic modulus	200 GPa
F_y : yield strength	345 MPa
b : width of flange	256.032 mm
h : total heigth	259.588 mm
t_f : flange thickness	17.272 mm
t_w : web thickness	10.668 mm
A : cross section area	$11.4x10^3$ mm^2
I_x : moment of inertia about x direction	$1.419x10^8$ mm^4
I_y : moment of inertia about y direction	$4.828x10^7$ mm^4
r_x : radius of gyration in x direction	111.8 mm
r_y : radius of gyration in y direction	65.2 mm
S_x : section modulus about x direction	$1.094x10^6$ mm^3
S_y : section modulus about y direction	$3.772x10^5$ mm^3
Z_x : plastic section modulus about x axis	$1.222x10^6$ mm^3
Z_y : plastic section modulus about y axis	$5.735x10^5$ mm^3

For each case study, member lengths for major and minor axis bendings are presented in Table 3-3.

Table 3-3 Individual Member Properties with W10x60 Section

Case Study	**KL/r**	**Column Profile**	**Column Height**	
			Strong Axis	**Weak Axis**
L/r =20	40	W10x60	2.236 m	1.304 m
L/r = 40	80	W10x60	4.472 m	2.608 m
L/r = 60	120	W10x60	6.708 m	3.912 m
L/r = 80	160	W10x60	8.944 m	5.216 m
L/r = 100	200	W10x60	11.180 m	6.520 m

With the determination of member lengths, strong axis bending loading parameters for AISC360 and EC3 specifications are shown in Table 3-4. AISC360 notional load, τ_b and modified stiffness parameters were calculated depending on the applied axial force. Loading parameters needed for EC3 provisions were obtained depending on the applied axial load. As it has been given in Table 3-1, strong axis bending of W10x60 bow imperfection loading parameters were obtained with imperfection *b* which is $\frac{e_0}{L} = \frac{1}{250}$. On the other hand, loading parameters of this section for weak axis bending were obtained by using imperfection *c* which is $\frac{e_0}{L} = \frac{1}{200}$.

Table 3-4 Strong Axis Bending Loading Parameters for AISC360 and EC3

Case Study	AISC Loading Parameters					EC Loading Parameters			
	Applied Axial Force P (kN)	Applied Notional Load Ni (kN)	Modified Stiffness Parameters			Applied Axial Force Ned (kN)	Sway Imperfection Load (kN)	Bow Imperfection Loads	
			τ_b	EI*	EA*			$\frac{4N_{ed}e_0}{L}$ (kN)	$\frac{8N_{ed}e_0}{L^2}$ ($\frac{kN}{m}$)
KL/r = 40	3500	7	0.39	0.31EI	0.80EA	3500	17.50	46.67	41.74
KL/r = 80	2400	4.8	0.95	0.76EI	0.80EA	2400	11.35	32.00	14.31
KL/r = 120	1500	3	1.00	0.80EI	0.80EA	1500	5.79	20.00	5.96
KL/r = 160	800	1.6	1.00	0.80EI	0.80EA	800	2.68	10.67	2.39
KL/r = 200	750	1.5	1.00	0.80EI	0.80EA	750	2.50	10.00	1.79

Table 3-5 shows loading values of minor axis bending of AISC360 and EC3 specifications.

Table 3-5 Weak Axis Bending Loading Parameters for AISC360 and EC3

Case Study	AISC Loading Parameters					EC Loading Parameters			
	Applied Axial Force P (kN)	Applied Notional Load Ni (kN)	Modified Stiffness Parameters			Applied Axial Force Ned (kN)	Sway Imperfection Load (kN)	Bow Imperfection Loads	
			τ_b	EI*	EA*			$\frac{4N_{ed}e_0}{L}$ (kN)	$\frac{8N_{ed}e_0}{L^2}$ ($\frac{kN}{m}$)
KL/r = 40	3500	7	0.39	0.31EI	0.80EA	3500	17.50	46.67	41.74
KL/r = 80	2400	4.8	0.95	0.76EI	0.80EA	2400	11.35	32.00	14.31
KL/r = 120	1500	3	1.00	0.80EI	0.80EA	1500	5.79	20.00	5.96
KL/r = 160	800	1.6	1.00	0.80EI	0.80EA	800	2.68	10.67	2.39
KL/r = 200	750	1.5	1.00	0.80EI	0.80EA	750	2.50	10.00	1.79

3.4.1 Strong Axis Bending Analysis Results According to AISC360-10 and EC3 Specifications

This section shows axial compression major axis bending capacity curves of fixed base columns. Capacity curves include loading curves of each method for members with KL/r=40, 80, 120, 160 and 200 respectively. Horizontal axis shows the ultimate moment in terms of kNm. On the other hand, vertical axis shows ultimate axial compression force in terms of kN. Results are presented in Figures 3-4, 3-5, 3-6, 3-7 and 3-8.

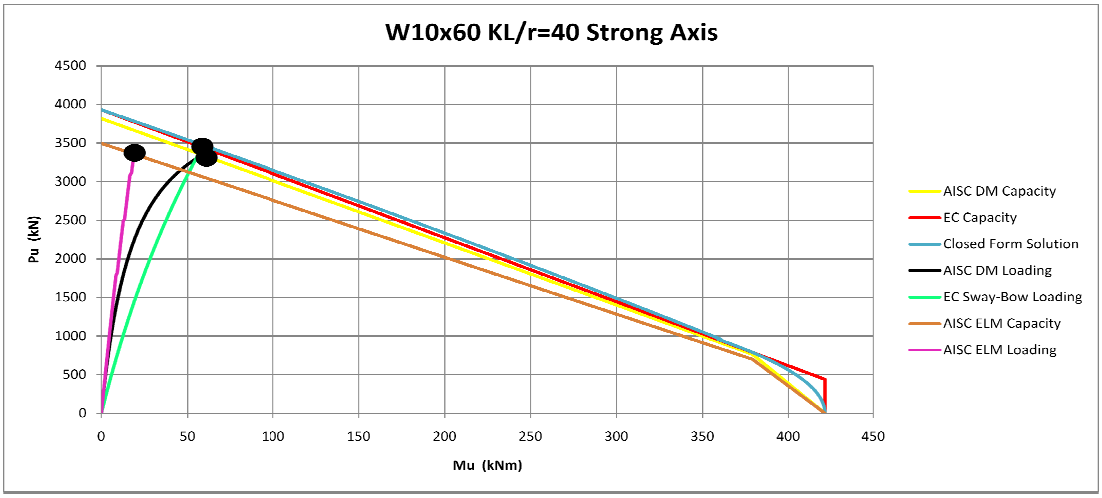

Figure 3-4 Strong Axis Interaction Diagram for KL/r=40 W10x60 Column

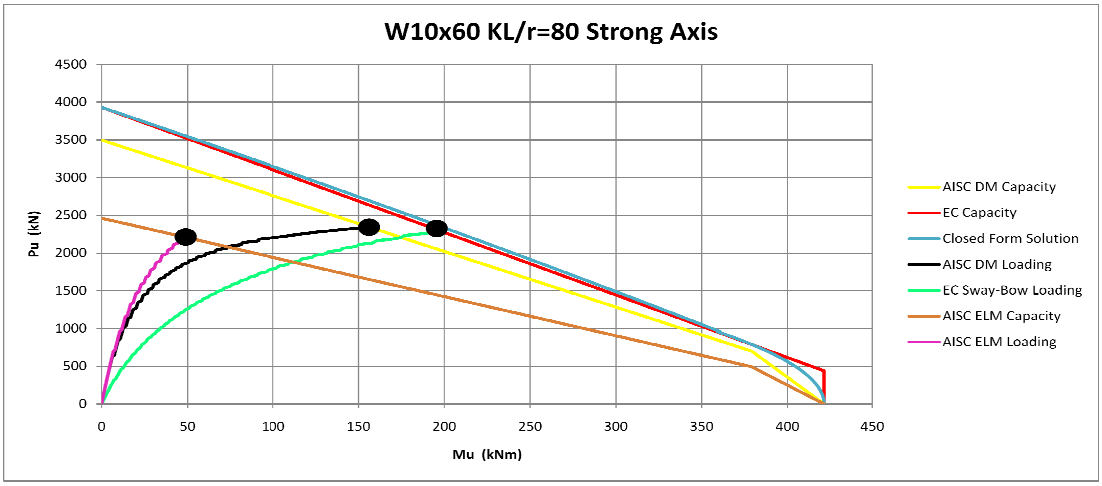

Figure 3-5 Strong Axis Interaction Diagram for KL/r=80 W10x60 Column

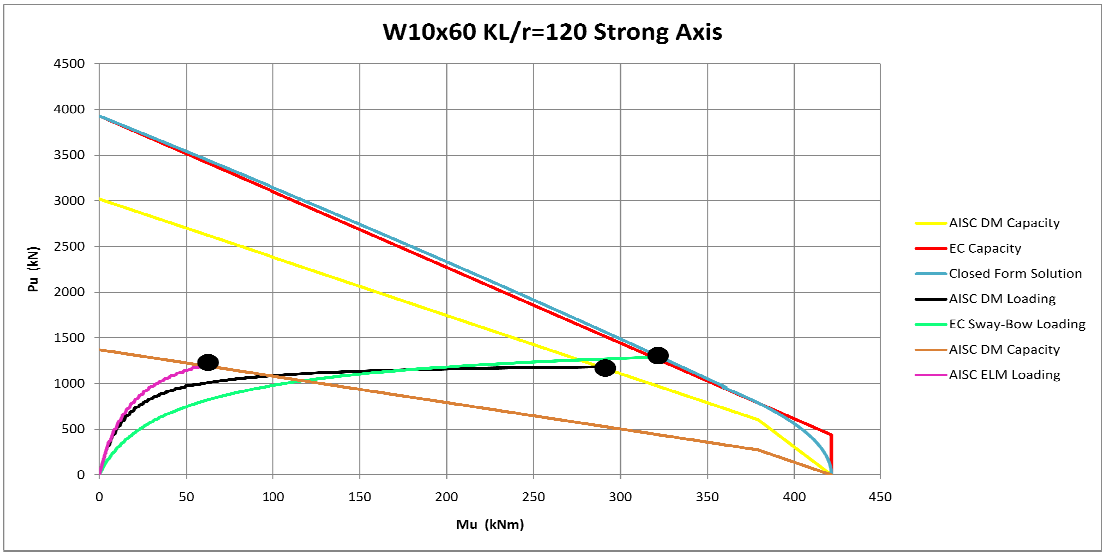

Figure 3-6 Strong Axis Interaction Diagram for KL/r=120 W10x60 Column

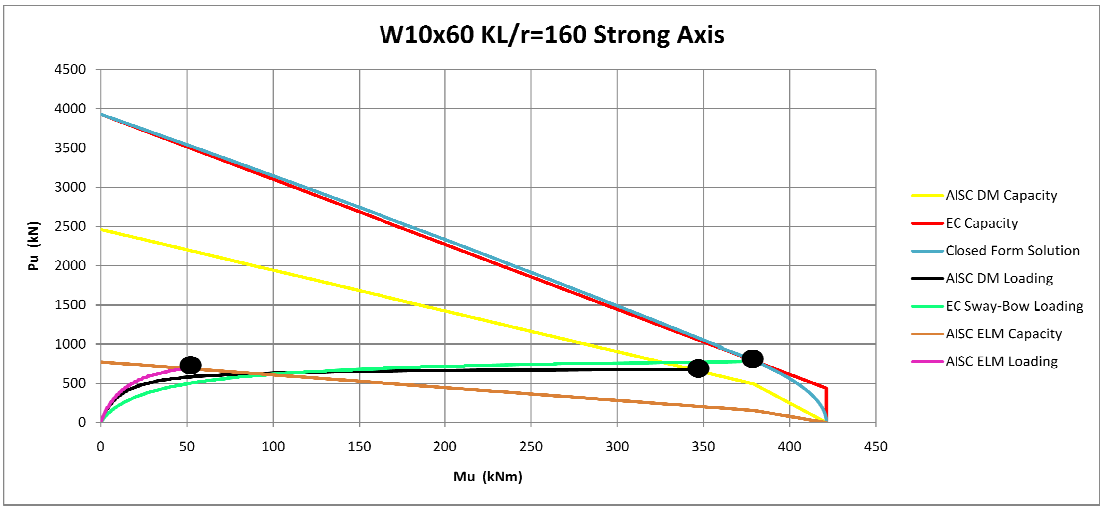

Figure 3-7 Strong Axis Interaction Diagram for KL/r=160 W10x60 Column

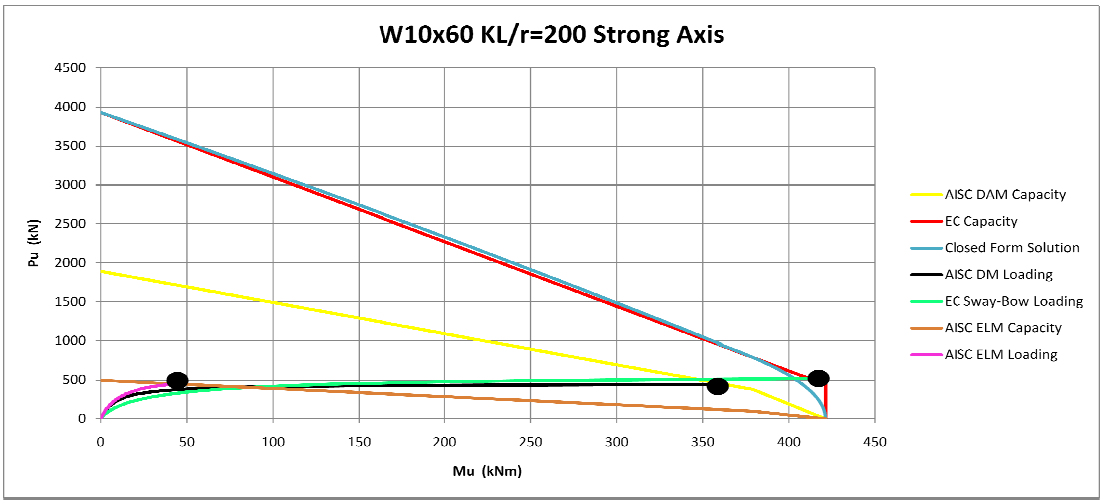

Figure 3-8 Strong Axis Interaction Diagram for KL/r=200 W10x60 Column

For five case studies, P-M capacities were obtained from intersection points of capacity and loading curves. These values are presented in Table 3-6, Table 3-7 and Table 3-8. Tables include τ_b values for DM analysis, maximum bending moment and axial load for each case. Also, to compare capacity values, ratio of bending moments and axial loads obtained by using AISC360 and EC3 provisions are given for each method.

Table 3-6 Comparison of AISC360-10 DM & EC3 Strong Axis Analysis Results

Case Study	Intersection Points						
	AISC360-10 DM Capacity			EC3 Capaciy		AISC DM/EC3 RATIO	
	τb	M (kNm)	P (kN)	M (kNm)	P (kN)	M	P
KL/r=40	0.39	60.9	3326.0	61.7	3419.0	0.99	0.97
KL/r=80	0.95	157.4	2335.0	198.0	2350.0	0.79	0.99
KL/r=120	1.00	289.6	1185.0	317.6	1336.0	0.91	0.89
KL/r=160	1.00	344.7	671.0	382.1	763.0	0.90	0.88
KL/r=200	1.00	359.4	457.0	411.7	518.0	0.87	0.88

Table 3-7 Comparison of AISC360-10 DM & ELM Strong Axis Analysis Results

Case Study	Intersection Points						
	AISC360-10 DM Capacity			AISC360-10 ELM Capacity		AISC DM/AISC ELM RATIO	
	τb	M (kNm)	P (kN)	M (kNm)	P (kN)	M	P
KL/r=40	0.39	60.9	3326.0	22.5	3330.0	2.70	1.00
KL/r=80	0.95	157.4	2335.0	49.8	2203.0	3.16	1.06
KL/r=120	1.00	289.6	1185.0	63.1	1188.0	4.59	1.00
KL/r=160	1.00	344.7	671.0	48.5	692.0	7.11	0.97
KL/r=200	1.00	359.4	457.0	43.6	448.0	8.25	1.02

Table 3-8 Comparison of EC3 & AISC360-10 ELM Strong Axis Analysis Results

Case Study	Intersection Points					
	EC3 Capaciy		AISC360-10 ELM Capacity		EC3/AISC ELM RATIO	
	M (kNm)	P (kN)	M (kNm)	P (kN)	M	P
KL/r=40	61.7	3419.0	22.5	3330.0	2.74	1.03
KL/r=80	198.0	2350.0	49.8	2203.0	3.98	1.07
KL/r=120	317.6	1336.0	63.1	1188.0	5.03	1.12
KL/r=160	382.1	763.0	48.5	692.0	7.88	1.10
KL/r=200	411.7	518.0	43.6	448.0	9.45	1.16

Table 3-6 shows the comparison of Direct Method and EC3 analysis results. Although each specification has a different point of view about imperfection concept, axial load and major axis bending moment values are close to each other. Moreover, DM and ELM analysis results are presented in Table 3-7. DM and ELM results are compatible in terms of axial load capacities. On the other hand, the major axis bending moment capacities are different from each other. As KL/r increases, there is a considerable difference between bending moment capacities. Finally, Table 3-8 compares the P-M capacity values of ELM and EC3 analysis results. For small KL/r values, ratio of axial compression capacities are close one. On the other hand, bending moment capacities are not close to each other. ELM provides lower bending

moments when compared with DM and EC3 curves. For this reason, as KL/r increases, ratio of moment capacities increase significantly.

As it has been stated above, each specification covers stability provisions in different ways. Results show that, there is a minor difference between AISC360 and EC3 axial compression capacities. Furthermore, the bending moments at the point of failure are close to each other.

3.4.2 Weak Axis Bending Analysis Results According to AISC360-10 and EC3 Specifications

Weak axis bending analysis results are presented in the figures below.

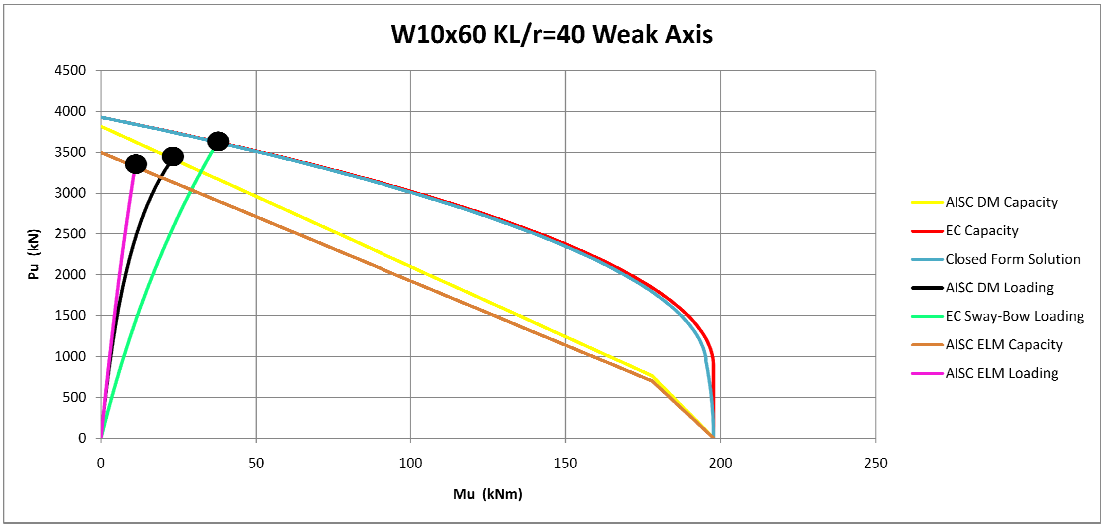

Figure 3-9 Weak Axis Interaction Diagram for KL/r= 40 W10x60 Column

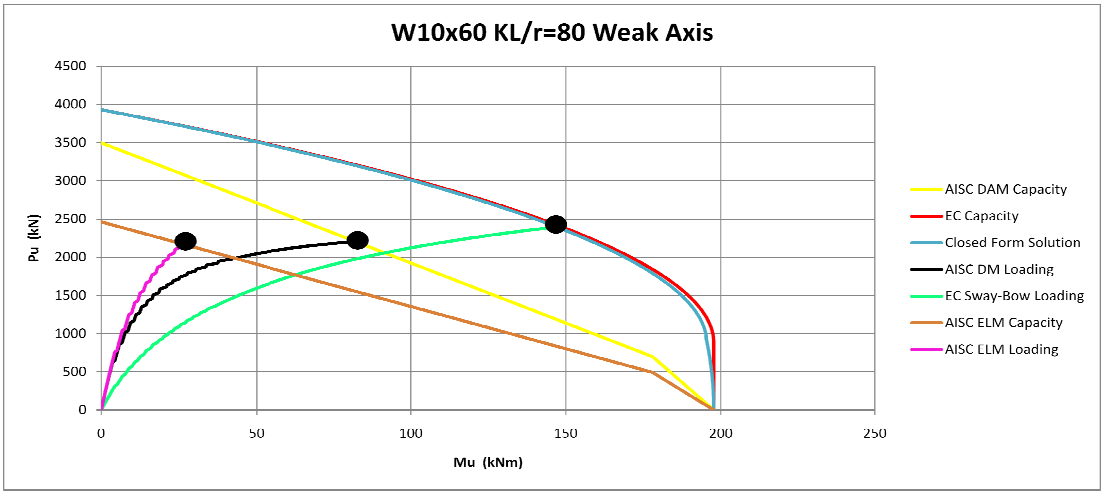

Figure 3-10 Weak Axis Interaction Diagram for KL/r= 80 W10x60 Column

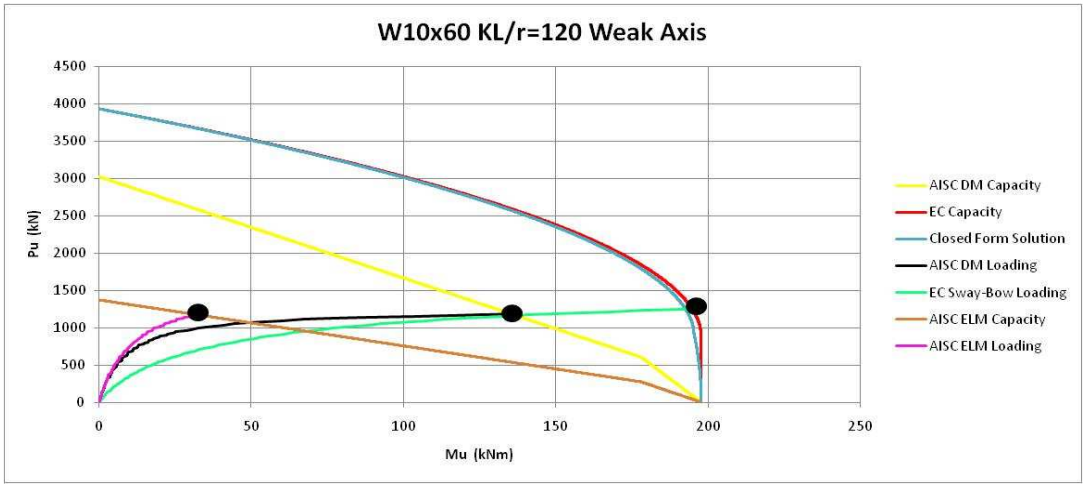

Figure 3-11 Weak Axis Interaction Diagram for KL/r= 120 W10x60 Column

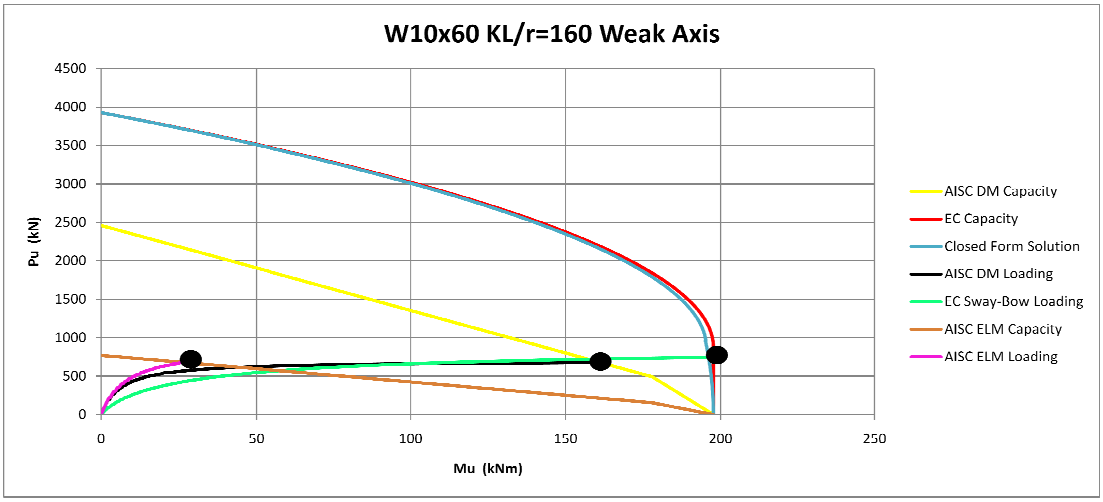

Figure 3-12 Weak Axis Interaction Diagram for KL/r= 160 W10x60 Column

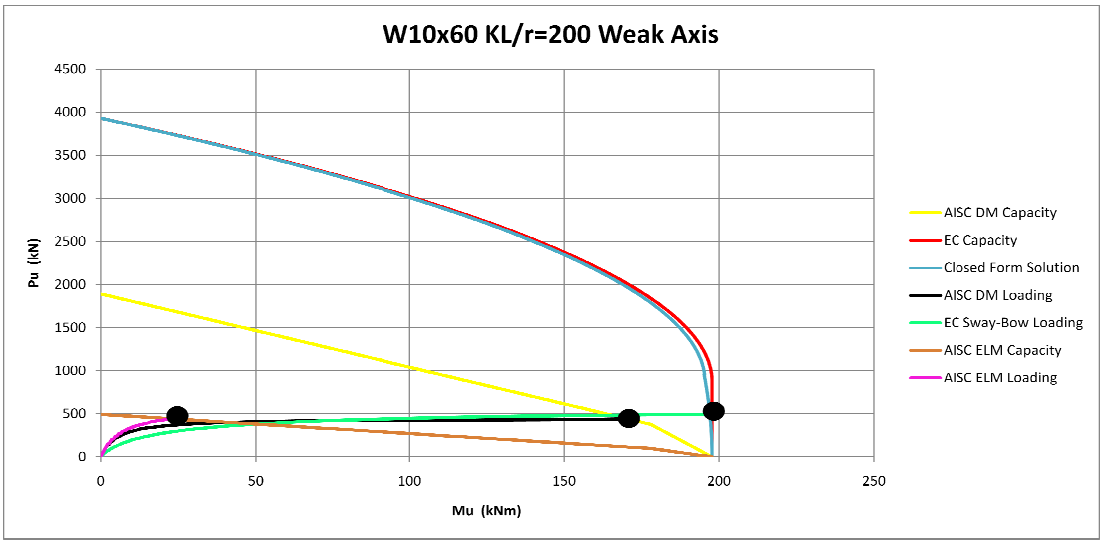

Figure 3-13 Weak Axis Interaction Diagram for KL/r= 200 W10x60 Column

Weak axis bending capacity values are illustrated in Table 3-9, Table 3-10 and Table 3-11, respectively.

Table 3-9 Comparison of AISC360-10 DM & EC3 Weak Axis Analysis Results

Case Study	Intersection Points						
	AISC360-10 DM Capacity			EC3 Capaciy		AISC DM/EC3 RATIO	
	τb	M (kNm)	P (kN)	M (kNm)	P (kN)	M	P
KL/r=40	0.47	24.9	3389.0	38.6	3612.0	0.65	0.94
KL/r=80	0.90	84.1	2175.0	148.4	2375.0	0.57	0.92
KL/r=120	1.00	133.3	1211.0	192.4	1258.0	0.69	0.96
KL/r=160	1.00	161.3	677.0	196.2	724.0	0.82	0.94
KL/r=200	1.00	170.8	439.0	197.7	465.0	0.86	0.94

Table 3-10 Comparison of AISC360-10 DM & ELM Weak Axis Analysis Results

Case Study	Intersection Points						
	AISC360-10 DM Capacity			AISC360-10 ELM Capacity		AISC DM/AISC ELM RATIO	
	τb	M (kNm)	P (kN)	M (kNm)	P (kN)	M	P
KL/r=40	0.47	24.9	3389.0	12.8	3295.0	1.95	1.03
KL/r=80	0.90	84.1	2175.0	28.1	2151.0	2.99	1.01
KL/r=120	1.00	133.3	1211.0	30.8	1170.0	4.33	1.04
KL/r=160	1.00	161.3	677.0	27.7	675.0	5.83	1.00
KL/r=200	1.00	170.8	439.0	25.4	437.0	6.72	1.00

Table 3-11 Comparison of EC3 & AISC360-10 ELM Weak Axis Analysis Results

Case Study	Intersection Points					
	EC3 Capaciy		AISC360-10 ELM Capacity		EC3/AISC ELM RATIO	
	M (kNm)	P (kN)	M (kNm)	P (kN)	M	P
KL/r=40	38.6	3612.0	12.8	3295.0	3.01	1.10
KL/r=80	148.4	2375.0	28.1	2151.0	5.29	1.10
KL/r=120	192.4	1258.0	30.8	1170.0	6.26	1.08
KL/r=160	196.2	724.0	27.7	675.0	7.09	1.07
KL/r=200	197.7	465.0	25.4	437.0	7.78	1.06

For weak axis bending analysis, comparison of AISC360-10 Direct Analysis Method and EC3 analysis show that,approximately 8% difference exists between axial load capacities for all slenderness ratios. On the other hand, there is no consistency between moment capacities for small slenderness ratios. Table 3-9 shows that, consistent moment capacities were obtained with relatively high slenderness ratios. DM and ELM analysis results are presented for each case in Table 3-10. DM and ELM are compatible in terms of the axial load capacities. For each case study, the ratio of axial compression is close to one. On the other hand, this is not valid for weak axis bending moment capacities. There is a major difference between moment values. Finally, comparison of ELM and EC3 analysis results shown in Table 3-11. Except KL/r=200 case, there is approximately 10 % difference between axial compression capacities. Major differences exist in moment capacities for each case.

3.5 Investigation of W10x26

This part includes the investigation of W10x26 section for strong and weak axis bending analysis. Cross section properties of W10x26 are shown in Table 3-12.

Table 3-12 Cross Section Properties of W10x26

E : elastic modulus	200 GPa
F_y : yield strength	345 MPa
b : width of flange	146.558 mm
h : total heigth	262.382 mm
t_f : flange thickness	11.176 mm
t_w : web thickness	6.604 mm
A : cross section area	$4.91x10^3$ mm^2
I_x : moment of inertia about x direction	$5.994x10^7$ mm^4
I_y : moment of inertia about y direction	$5.869x10^6$ mm^4
r_x : radius of gyration in x direction	110.5 mm
r_y : radius of gyration in y direction	34.6 mm
S_x : section modulus about x direction	$4.569x10^5$ mm^3
S_y : section modulus about y direction	$8.009x10^4$ mm^3
Z_x : plastic section modulus about x axis	$5.129x10^5$ mm^3
Z_y : plastic section modulus about y axis	$1.229x10^5$ mm^3

For each case study, member lengths for major and minor axis bendings are presented in Table 3-13.

Table 3-13 Individual Member Properties with W10x26 Section

Case Study	**KL/r**	**Column Profile**	**Column Height**	
			Strong Axis	**Weak Axis**
L/r =20	40	W10x26	2.210 m	0.692 m
L/r = 40	80	W10x26	4.420 m	1.384 m
L/r = 60	120	W10x26	6.630 m	2.076 m
L/r = 80	160	W10x26	8.840 m	2.768 m
L/r = 100	200	W10x26	11.050 m	3.460 m

According to Table 3-1, strong axis bending of W10x26 of bow imperfection loading parameters were obtained with imperfection *a* which is $\frac{e_0}{L} = \frac{1}{300}$. On the other hand, loading parameters of this section for weak axis bending were obtained by using imperfection *b* which is $\frac{e_0}{L} = \frac{1}{250}$.

With the determination of member lengths, loading parameters for strong axis bending of AISC360 and EC3 specifications are shown in Table 3-14.

Table 3-14 Strong Axis Loading Table of AISC360 and EC3

Case Study	AISC Loading Parameters					EC Loading Parameters			
	Applied Axial Force P (kN)	Applied Notional Load Ni (kN)	Modified Stiffness Parameters			Applied Axial Force Ned (kN)	Sway Imperfection Load (kN)	Bow Imperfection Loads	
			τ_b	EI*	EA*			$\frac{4N_{ed}e_0}{L}$ (kN)	$\frac{8N_{ed}e_0}{L^2}$ ($\frac{kN}{m}$)
KL/r = 40	1500	3.00	0.40	0.32EI	0.80EA	1500	7.50	28.00	18.10
KL/r = 80	1100	2.20	0.91	0.73EI	0.80EA	1300	6.18	17.33	7.84
KL/r = 120	800	1.60	1.00	0.80EI	0.80EA	800	3.11	10.67	3.22
KL/r = 160	600	1.20	1.00	0.80EI	0.80EA	600	2.02	8.00	1.81
KL/r = 200	400	0.80	1.00	0.80EI	0.80EA	400	1.33	5.33	0.97

Table 3-15 shows loading parameters for weak axis bending of W10x26.

Table 3-15 Weak Axis Loading Table of AISC360 and EC3

Case Study	AISC Loading Parameters					EC Loading Parameters			
	Applied Axial Force P (kN)	Applied Notional Load Ni (kN)	Modified Stiffness Parameters			Applied Axial Force Ned (kN)	Sway Imperfection Load (kN)	Bow Imperfection Loads	
			τ_b	EI*	EA*			$\frac{4N_{ed}e_0}{L}$ (kN)	$\frac{8N_{ed}e_0}{L^2}$ ($\frac{kN}{m}$)
KL/r = 40	1480	2.96	0.44	0.35EI	0.80EA	1600	8.00	25.60	73.99
KL/r = 80	1000	2.00	0.97	0.77EI	0.80EA	1300	6.50	20.80	30.06
KL/r = 120	900	1.80	1.00	0.80EI	0.80EA	900	4.50	14.40	13.87
KL/r = 160	650	1.30	1.00	0.80EI	0.80EA	650	3.91	10.40	7.51
KL/r = 200	300	0.60	1.00	0.80EI	0.80EA	300	1.61	4.80	2.77

3.5.1 Strong Axis Bending Analysis Results According to AISC360-10 and EC3 Specifications

This section shows P-M major axis bending capacity curves with related analysis of fixed base W10x26 members. Capacity curves for each KL/r value are shown in Figure 3-14, Figure 3-15, Figure 3-16, Figure 3-17 and Figure 3-18.

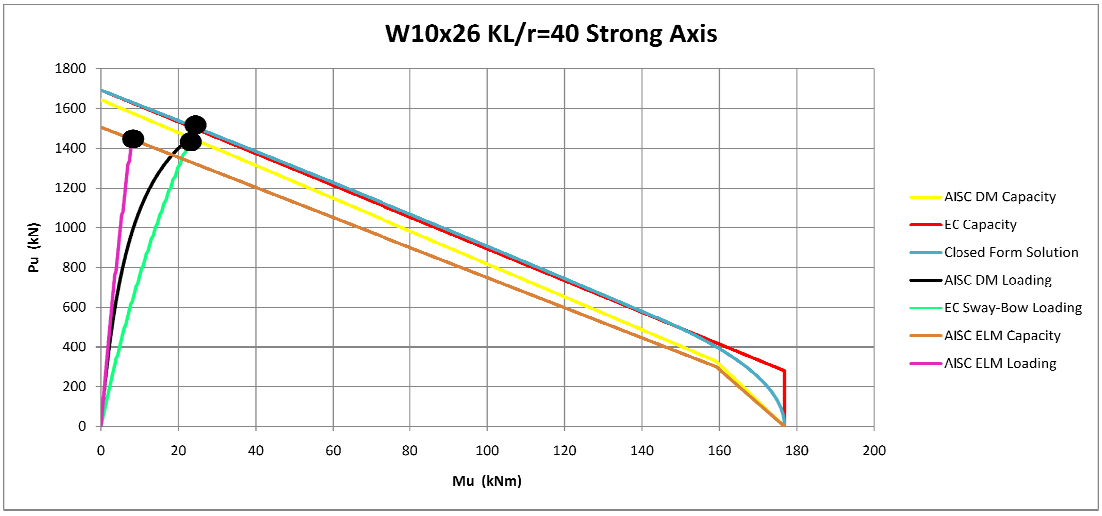

Figure 3-14 Strong Axis Interaction Diagram for KL/r=40 W10x26 Column

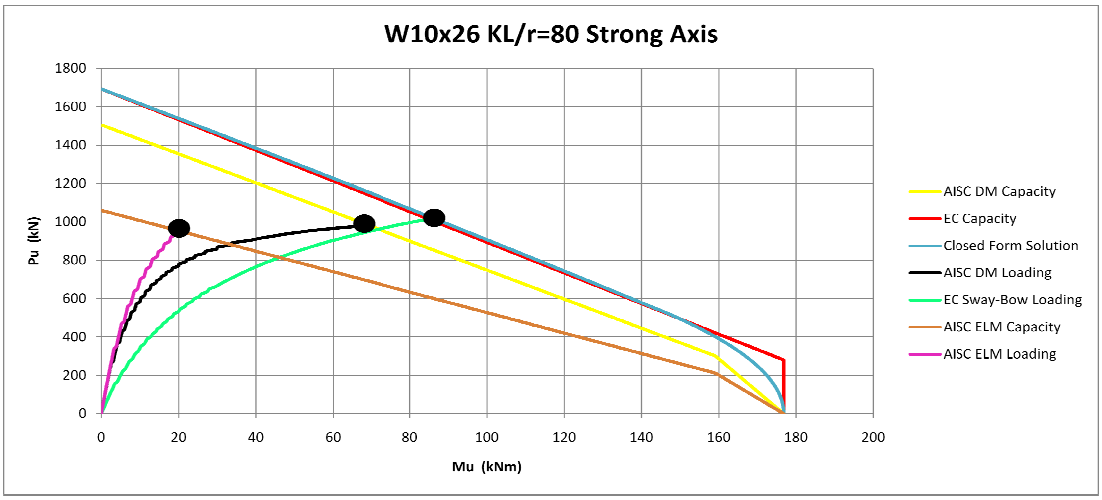

Figure 3-15 Strong Axis Interaction Diagram for KL/r=80 W10x26 Column

Figure 3-16 Strong Axis Interaction Diagram for KL/r=120 W10x26 Column

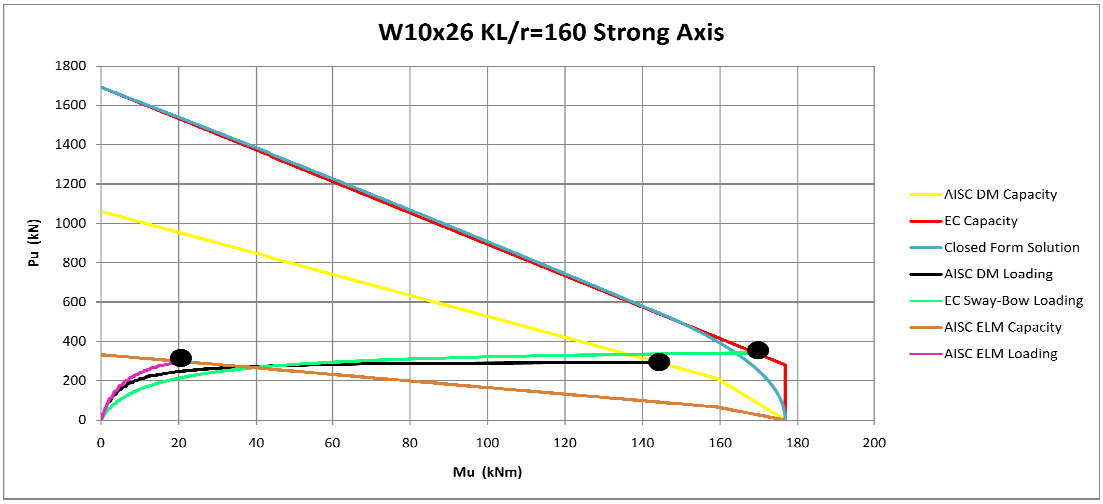

Figure 3-17 Strong Axis Interaction Diagram for KL/r=160 W10x26 Column

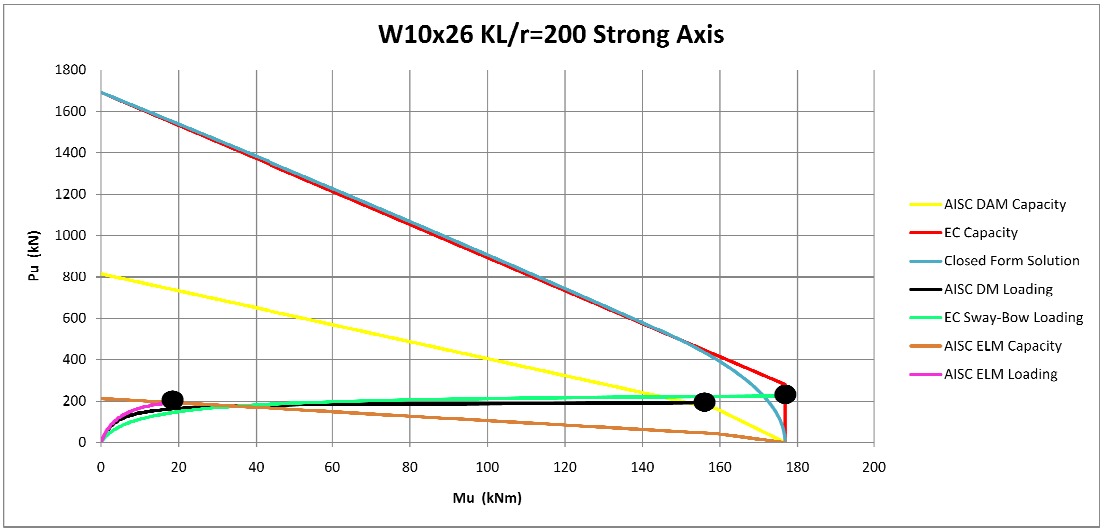

Figure 3-18 Strong Axis Interaction Diagram for KL/r=200 W10x26 Column

Strong axis bending moment and axial compression capacities are illustrated in Table 3-16, Table 3-17 and Table 3-18.

Table 3-16 Comparison of AISC360-10 DM & EC3 Strong Axis Analysis Results

Case Study	Intersection Points						
	AISC360-10 DM Capacity			EC3 Capaciy		AISC DM/EC3 RATIO	
	τb	M (kNm)	P (kN)	M (kNm)	P (kN)	M	P
KL/r=40	0.40	24.4	1442.0	25.6	1496.0	0.95	0.96
KL/r=80	0.91	67.0	979.0	83.3	1042.0	0.80	0.94
KL/r=120	1.00	121.4	507.0	141.4	567.0	0.86	0.89
KL/r=160	1.00	145.8	283.0	170.6	330.0	0.85	0.86
KL/r=200	1.00	153.5	186.0	176.8	210.0	0.87	0.89

Table 3-17 Comparison of AISC360-10 DM & ELM Strong Axis Analysis Results

Case Study	Intersection Points						
	AISC360-10 DM Capacity			AISC360-10 ELM Capacity		AISC DM/AISC ELM RATIO	
	τ_b	M (kNm)	P (kN)	M (kNm)	P (kN)	M	P
KL/r=40	0.40	24.4	1442.0	9.8	1432.0	2.51	1.01
KL/r=80	0.91	67.0	979.0	18.1	964.0	3.71	1.02
KL/r=120	1.00	121.4	507.0	26.5	512.0	4.58	0.99
KL/r=160	1.00	145.8	283.0	18.4	288.0	7.94	0.98
KL/r=200	1.00	153.5	186.0	19.2	192.0	8.00	0.97

Table 3-18 Comparison of EC3 & AISC360-10 ELM Strong Axis Analysis Results

Case Study	Intersection Points					
	EC3 Capaciy		AISC360-10 ELM Capacity		EC3/AISC ELM RATIO	
	M (kNm)	P (kN)	M (kNm)	P (kN)	M	P
KL/r=40	25.6	1496.0	9.8	1432.0	2.63	1.04
KL/r=80	83.3	1042.0	18.1	964.0	4.61	1.08
KL/r=120	141.4	567.0	26.5	512.0	5.33	1.11
KL/r=160	170.6	330.0	18.4	288.0	9.29	1.15
KL/r=200	176.8	210.0	19.2	192.0	9.21	1.09

DM and EC3 analysis results were compared in Table 3-16. Axial compression capacities are consistent with relatively small slenderness ratios. Except KL/r=40 and KL/r=80, P ratios are not close to each other. In Table 3-17, DM and ELM analysis results were presented for each case studies. Axial compression capacities of DM and ELM methods are compatible for each case. On the other hand, there is a major difference between bending moment capacities of W10x26 with relatively high slenderness ratio. Finally, P-M capacity values of ELM and EC3 were compared in Table 3-18. Results show that, there is a consistency between axial compression capacities of KL/r=40 and 80. For other cases, there is approximately 10 % difference between P values. On the other hand, bending moment capacities are not close to each other.

3.5.2 Weak Axis Bending Analysis Results According to AISC360-10 and EC3 Specifications

Minor axis bending analysis results of fixed base W10x26 columns are illustrated in Figure 3-19, Figure 3-20, Figure 3-21, Figure 3-22 and Figure 3-23.

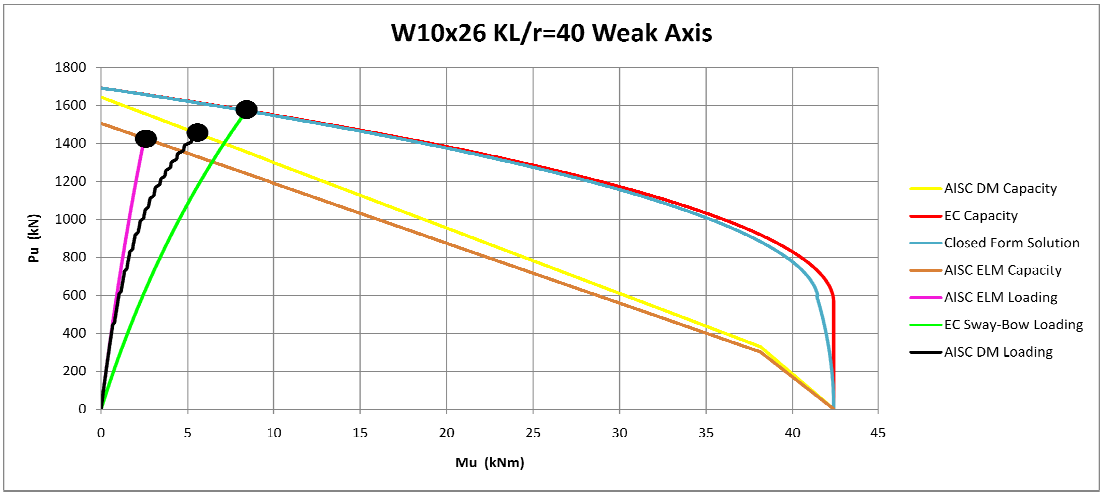

Figure 3-19 Weak Axis Interaction Diagram for KL/r= 40 W10x26 Column

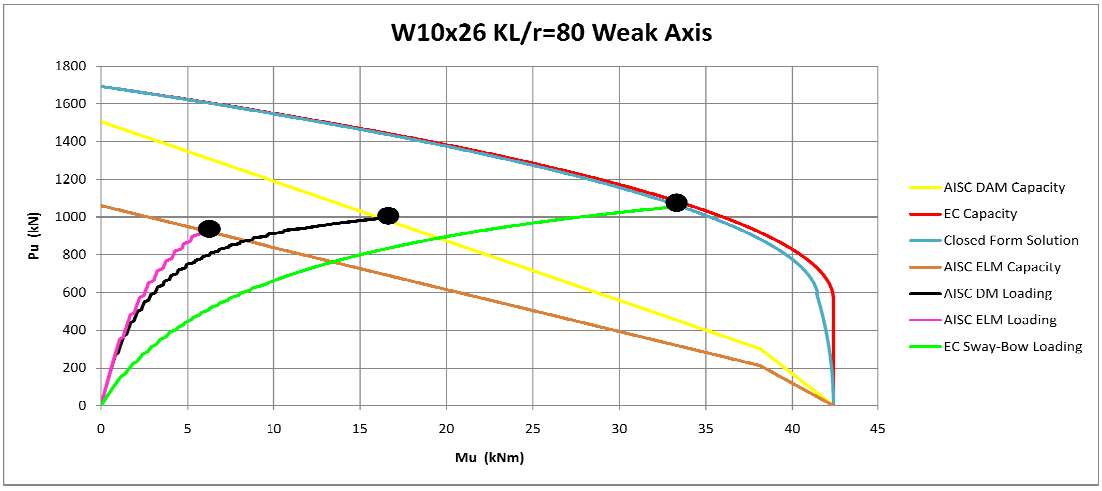

Figure 3-20 Weak Axis Interaction Diagram for KL/r= 80 W10x26 Column

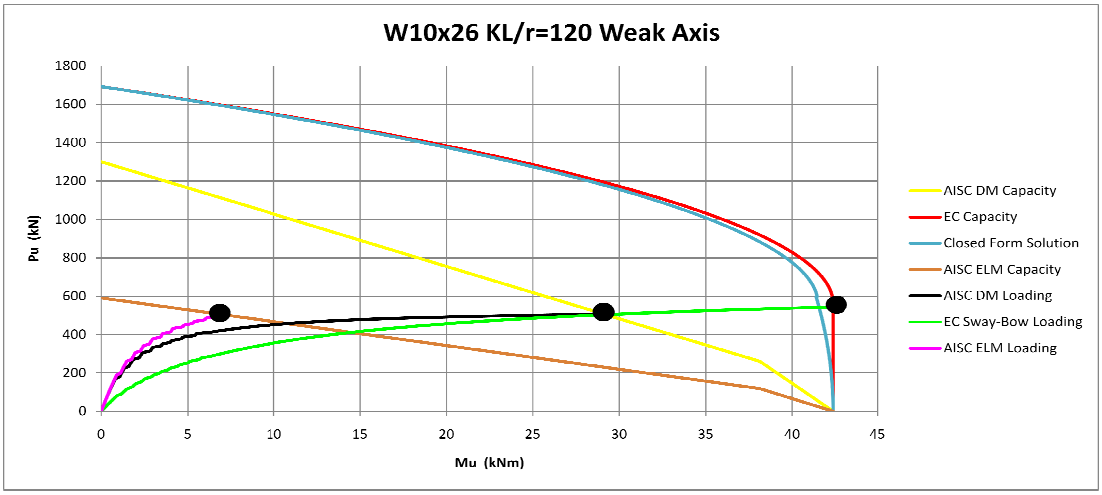

Figure 3-21 Weak Axis Interaction Diagram for KL/r= 120 W10x26 Column

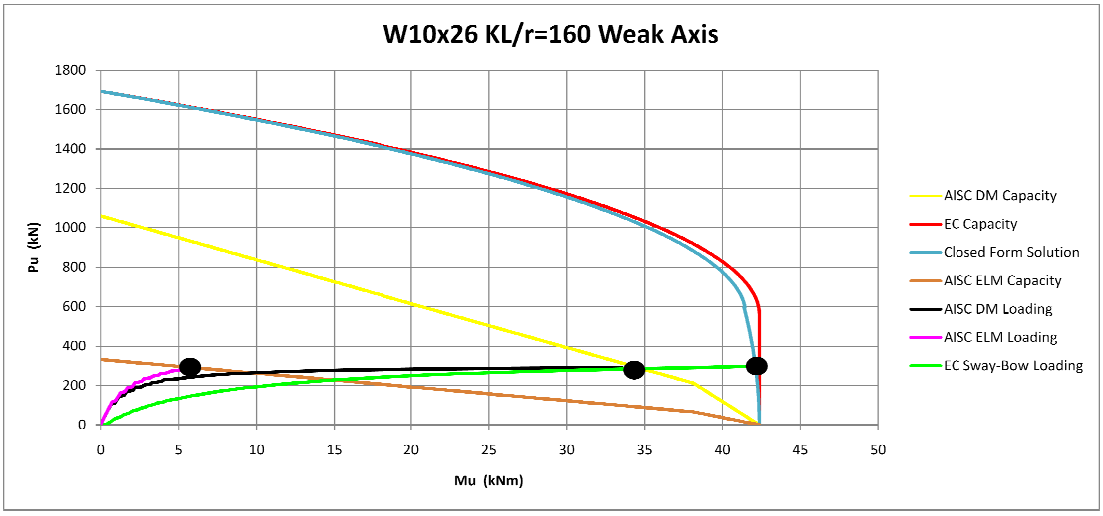

Figure 3-22 Weak Axis Interaction Diagram for KL/r= 160 W10x26 Column

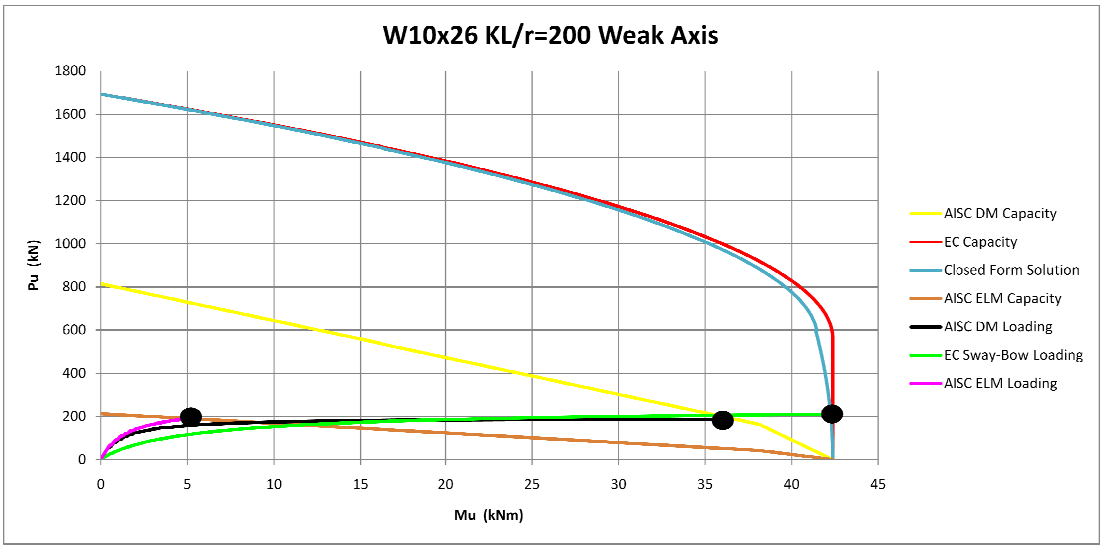

Figure 3-23 Weak Axis Interaction Diagram for KL/r= 200 W10x26 Column

Comparison of weak axis analysis results are shown in Table 3-19, Table 3-20 and Table 3-21 respectively.

Table 3-19 Comparison of AISC360-10 DM & EC3 Weak Axis Analysis Results

Case Study	Intersection Points						
	AISC360-10 DM Capacity			EC3 Capaciy		AISC DM/EC3 RATIO	
	τb	M (kNm)	P (kN)	M (kNm)	P (kN)	M	P
KL/r=40	0.44	5.9	1442.0	8.6	1572.0	0.68	0.92
KL/r=80	0.97	16.6	982.0	34.5	1049.0	0.48	0.94
KL/r=120	1.00	29.5	497.0	42.4	531.0	0.70	0.94
KL/r=160	1.00	33.6	312.0	42.4	315.3	0.79	0.99
KL/r=200	1.00	36.3	194.0	42.4	204.0	0.86	0.95

Table 3-20 Comparison of AISC360-10 DM & ELM Weak Axis Analysis Results

Case Study		Intersection Points					
		AISC360-10 DM Capacity		AISC360-10 ELM Capacity		AISC DM/AISC ELM RATIO	
	τ_b	M (kNm)	P (kN)	M (kNm)	P (kN)	M	P
KL/r=40	0.44	5.9	1441.0	2.8	1416.0	2.07	1.02
KL/r=80	0.97	15.9	990.0	6.2	923.0	2.57	1.07
KL/r=120	1.00	29.5	497.0	7.1	503.0	4.16	0.99
KL/r=160	1.00	33.6	312.0	5.5	294.0	6.16	1.06
KL/r=200	1.00	36.3	194.0	5.5	188.0	6.62	1.03

Table 3-21 Comparison of EC3 & AISC360-10 ELM Weak Axis Analysis Results

Case Study	Intersection Points					
	EC3 Capaciy		AISC360-10 ELM Capacity		EC3/AISC ELM RATIO	
	M (kNm)	P (kN)	M (kNm)	P (kN)	M	P
KL/r=40	8.8	1569.0	2.8	1416.0	3.08	1.11
KL/r=80	33.1	1053.0	6.2	923.0	5.36	1.14
KL/r=120	42.4	531.0	7.1	503.0	5.98	1.06
KL/r=160	42.4	315.3	5.5	294.0	7.76	1.07
KL/r=200	42.4	204.0	5.5	188.0	7.72	1.09

AISC360 DM and EC3 weak axis bending results are compared in Table 3-19. There is approximately 5% difference between axial compression capacities except KL/r=40 case. On the other hand, difference between moment capacities decrease with high slenderness ratios. In Table 3-20, AISC360 DM and ELM results are compared. Axial compression capacities of DM and ELM are close to each other. It can be seen from Table 3-20 that, ratio of these values are close to one. It can be interpreted that, DM and ELM are reliable methods for determining axial compression capacities of a member. Yet, these are not accurate for bending moment capacities. Moreover EC3 and AISC360 ELM analysis results were presented in Table 3-21. Approximately 10 % difference exists in axial compression capacities. Effective Length Method gives smaller moment capacities comparing to DM and EC3 methods. For this reason, capacity ratio of bending moments are always greater than 1.

3.6 Investigation of W14x605

In this section, cantilever members with W14x605 sections were studied for major axis and minor axis bending. Cross-section properties of W14x605 section is given in Table 3-22.

Table 3-22 Cross Section Properties of W14x605

E : elastic modulus	200 GPa
F_y : yield strength	345 MPa
b : width of flange	442.341 mm
h : total heigth	531.368 mm
t_f : flange thickness	105.664 mm
t_w : web thickness	65.913 mm
A : cross section area	$11.5x10^4$ mm^2
I_x : moment of inertia about x direction	$4.495x10^9$ mm^4
I_y : moment of inertia about y direction	$1.532x10^9$ mm^4
r_x : radius of gyration in x direction	197.8 mm
r_y : radius of gyration in y direction	115.5 mm
S_x : section modulus about x direction	$1.692x10^7$ mm^3
S_y : section modulus about y direction	$6.926x10^6$ mm^3
Z_x : plastic section modulus about x axis	$2.163x10^7$ mm^3
Z_y : plastic section modulus about y axis	$1.068x10^7$ mm^3

Depending on the slenderness ratios, member lengths for major axis and minor axis bendings are presented in Table 3-23.

Table 3-23 Individual Member Properties with W14x605 Section

Case Study	KL/r	Column Profile	Column Height	
			Strong Axis	Weak Axis
L/r =20	40	W14x605	3.956 m	2.310 m
L/r = 40	80	W14x605	7.912 m	4.620 m
L/r = 60	120	W14x605	11.868 m	6.930 m
L/r = 80	160	W14x605	15.824 m	9.240 m
L/r = 100	200	W14x605	19.780 m	11.550 m

According to Table 3-1, strong axis bending of W14x605 of bow imperfection loading parameters were obtained with imperfection *d* which is $\frac{e_0}{L} = \frac{1}{150}$. On the

other hand, loading parameters of this section for weak axis bending were obtained by using imperfection *d* which is $\frac{e_0}{L} = \frac{1}{150}$.

For W14x605 section, loading parameters for strong axis bending of AISC360 and EC3 specifications are shown in Table 3-24.

Table 3-24 Strong Axis Loading Table for AISC360 and EC3

Case Study	AISC Loading Parameters					EC Loading Parameters			
	Applied Axial Force P (kN)	Applied Notional Load Ni (kN)	Modified Stiffness Parameters			Applied Axial Force Ned (kN)	Sway Imperfection Load (kN)	Bow Imperfection Loads	
			τ_b	EI*	EA*			$\frac{4N_{ed}e_0}{L}$ (kN)	$\frac{8N_{ed}e_0}{L^2}$ ($\frac{kN}{m}$)
KL/r = 40	34500	69	0.45	0.36EI	0.80EA	35000	175.00	933.33	471.86
KL/r = 80	27000	54	0.87	0.69EI	0.80EA	30000	106.65	800.00	202.22
KL/r = 120	25000	50	0.93	0.74EI	0.80EA	25000	83.33	666.67	112.35
KL/r = 160	18000	36	1.00	0.80EI	0.80EA	18000	60.00	480.00	60.67
KL/r = 200	10000	20	1.00	0.80EI	0.80EA	10000	33.33	266.67	26.96

Table 3-25 illustrates loading values for minor axis bending of AISC360 and EC3 specifications.

Table 3-25 Weak Axis Loading Table for AISC360 and EC3

Case Study	AISC Loading Parameters					EC Loading Parameters			
	Applied Axial Force P (kN)	Applied Notional Load Ni (kN)	Modified Stiffness Parameters			Applied Axial Force Ned (kN)	Sway Imperfection Load (kN)	Bow Imperfection Loads	
			τ_b	EI*	EA*			$\frac{4N_{ed}e_0}{L}$ (kN)	$\frac{8N_{ed}e_0}{L^2}$ ($\frac{kN}{m}$)
KL/r = 40	34000	68	0.48	0.39	0.80EA	36000	180.00	960.00	831.17
KL/r = 80	23500	47	0.96	0.77	0.80EA	30000	139.57	800.00	346.32
KL/r = 120	20000	40	1.00	0.80	0.80EA	20000	75.97	533.33	153.92
KL/r = 160	12000	24	1.00	0.80	0.80EA	12000	40.02	320.00	69.26
KL/r = 200	6000	12	1.00	0.80	0.80EA	6000	20.10	160.00	27.71

3.6.1 Strong Axis Bending Analysis Results According to AISC360-10 and EC3 Specifications

AISC360-10 DM, ELM and EC3 strong axis bending results of W14x605 members are shown in Figure 3-24, Figure 3-25, Figure 3-26, Figure 3-27 and Figure 3-28.

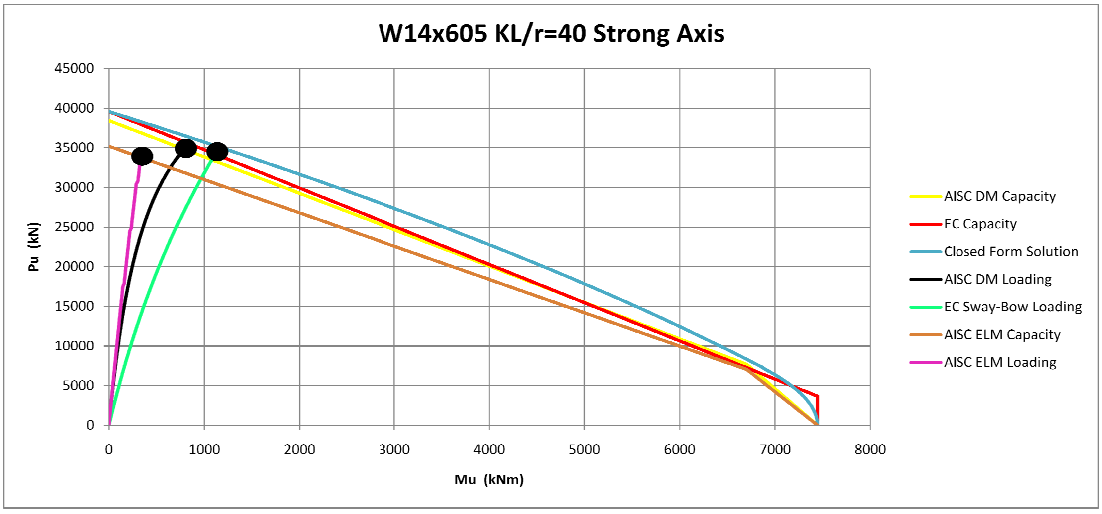

Figure 3-24 Strong Axis Interaction Diagram for KL/r=40 W14x605 Column

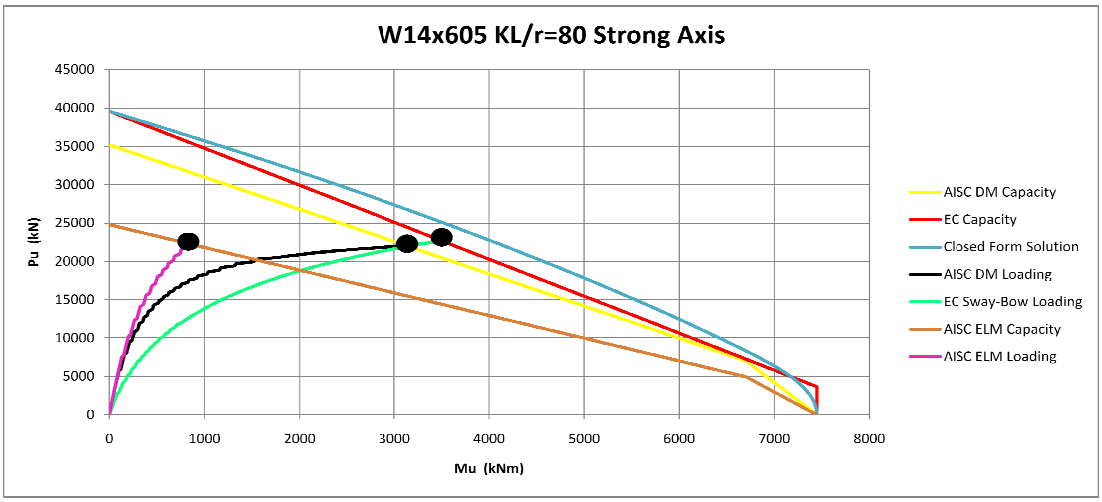

Figure 3-25 Strong Axis Interaction Diagram for KL/r=80 W14x605 Column

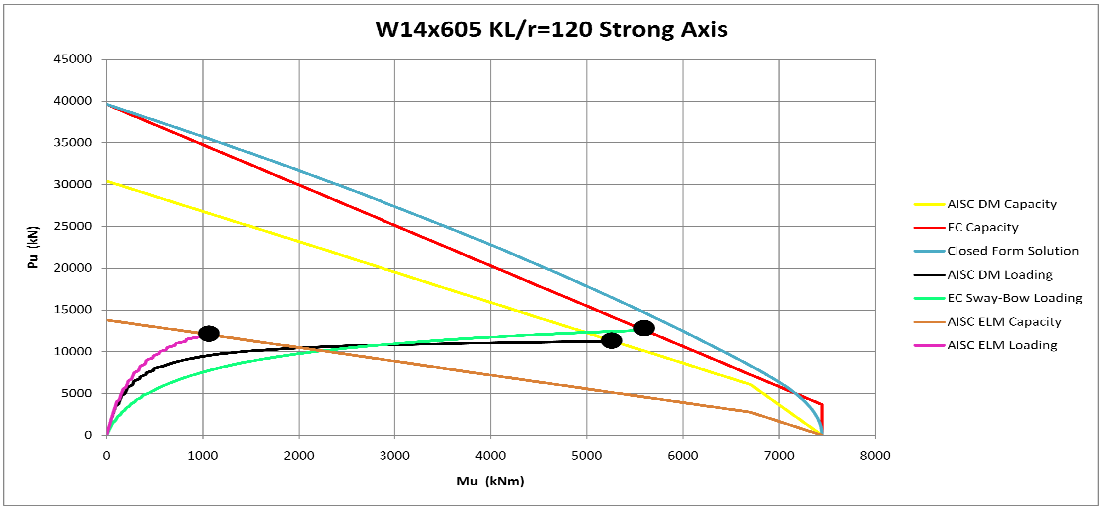

Figure 3-26 Strong Axis Interaction Diagram for KL/r=120 W14x605 Column

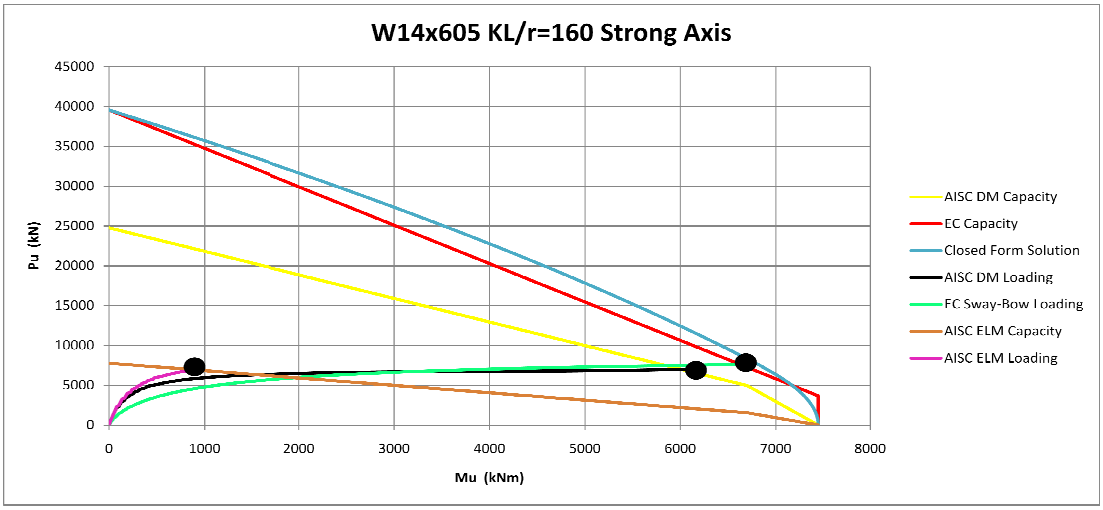

Figure 3-27 Strong Axis Interaction Diagram for KL/r=160 W14x605 Column

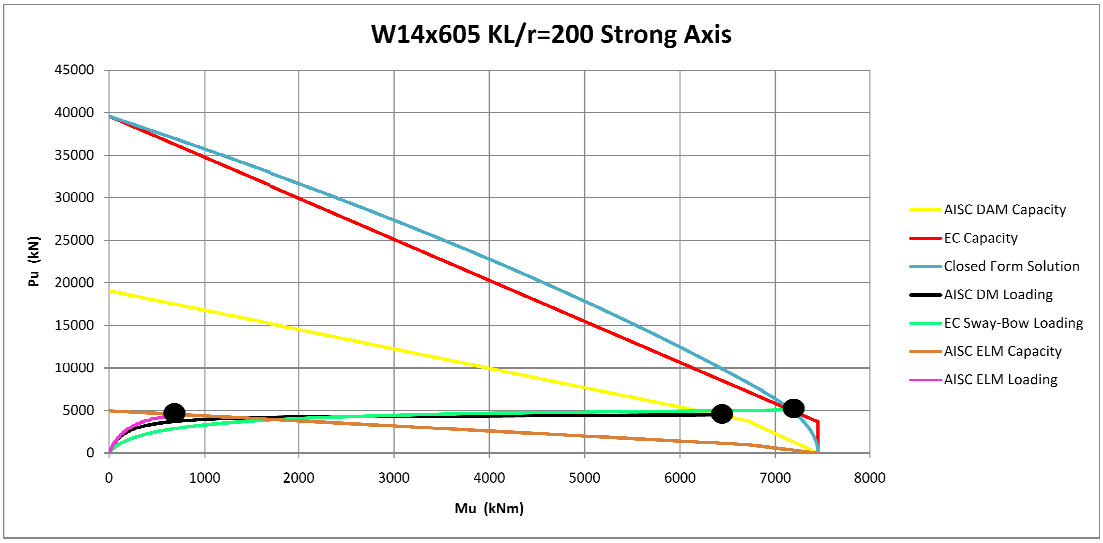

Figure 3-28 Strong Axis Interaction Diagram for KL/r=200 W14x605 Column

For each method, axial compression and major axis bending moment capacities of W14x605 members are presented in Table 3-26, Table 3-27 and Table 3-28.

Table 3-26 Comparison of AISC360-10 DM & EC3 Strong Axis Analysis Results

Case Study	Intersection Points						
	AISC360-10 DM Capacity			EC3 Capaciy		AISC DM/EC3 RATIO	
	τb	M (kNm)	P (kN)	M (kNm)	P (kN)	M	P
KL/r=40	0.45	839.9	34582.0	1161.8	33974.0	0.72	1.02
KL/r=80	0.87	3080.2	22262.0	3557.6	22422.0	0.87	0.99
KL/r=120	0.93	5305.4	11154.0	5621.5	12470.0	0.94	0.89
KL/r=160	1.00	6083.6	6787.0	6647.7	7522.0	0.92	0.90
KL/r=200	1.00	6442.6	4400.0	7179.8	4922.0	0.90	0.89

Table 3-27 Comparison of AISC360-10 DM & ELM Strong Axis Analysis Results

Case Study	Intersection Points						
	AISC360-10 DM Capacity			AISC360-10 ELM Capacity		AISC DM/AISC ELM RATIO	
	τb	M (kNm)	P (kN)	M (kNm)	P (kN)	M	P
KL/r=40	0.45	839.9	34582.0	403.9	33510.0	2.08	1.03
KL/r=80	0.87	3080.2	22262.0	865.4	22228.0	3.56	1.00
KL/r=120	0.93	5305.4	11154.0	1041.6	12000.0	5.09	0.93
KL/r=160	1.00	6083.6	6787.0	816.7	6840.0	7.45	0.99
KL/r=200	1.00	6442.6	4400.0	666.2	4400.0	9.67	1.00

Table 3-28 Comparison of EC3 & AISC360-10 ELM Strong Axis Analysis Results

Case Study	Intersection Points					
	EC3 Capaciy		AISC360-10 ELM Capacity		EC3/AISC ELM RATIO	
	M (kNm)	P (kN)	M (kNm)	P (kN)	M	P
KL/r=40	1161.8	33974.0	403.9	33510.0	2.88	1.01
KL/r=80	3557.6	22422.0	865.4	22228.0	4.11	1.01
KL/r=120	5621.5	12470.0	1041.6	12000.0	5.40	1.04
KL/r=160	6647.7	7522.0	816.7	6840.0	8.14	1.10
KL/r=200	7179.8	4922.0	666.2	4400.0	10.78	1.12

Comparison of AISC DM and EC3 analysis are presented in Table 3-26. Except KL/r=40 and 80 cases, there is a 10% difference between axial compression capacities. Similarly, there is approximately 10% difference between moment capacities except KL/r =40 case. Table 3-27 shows the comparison of AISC360 DM and ELM P-M capacities. Similar to other DM and ELM comparisons, axial compression capacities are consistent with each other. On the other hand, there is no consistency between major axis bending moment capacities. EC3 and AISC360 ELM analysis results are compared in Table 3-28. For the first three cases, axial compression values are close to each other. For KL/r =160 and 200 cases, axial compression capacity values of ELM are 10% lower than EC3 axial compression capacity values. Table 3-28 shows that, moment capacities of EC3 analysis are increasing with slenderness ratio at the same time. On the other hand, ELM has the highest moment capacity at KL/r=120. As a result, moment capacities are not close to each other for all cases.

3.6.2 Weak Axis Bending Analysis Results According to AISC360-10 and EC3 Specifications

Weak axis bending analysis results are presented in Figure 3-29, Figure 3-30, Figure 3-31, Figure 3-32 and Figure 3-33 respectively.

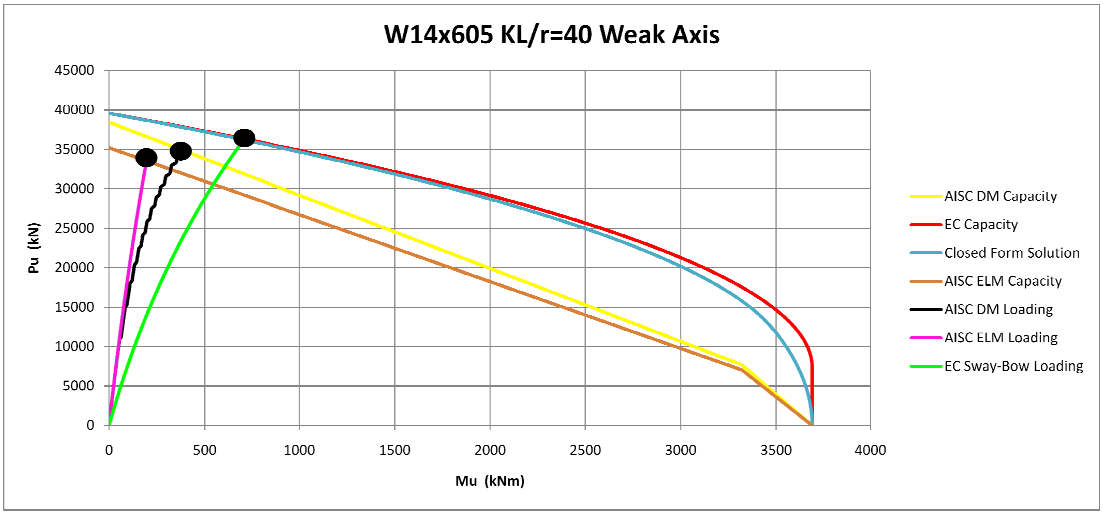

Figure 3-29 Weak Axis Interaction Diagram for KL/r= 40 W14x605 Column

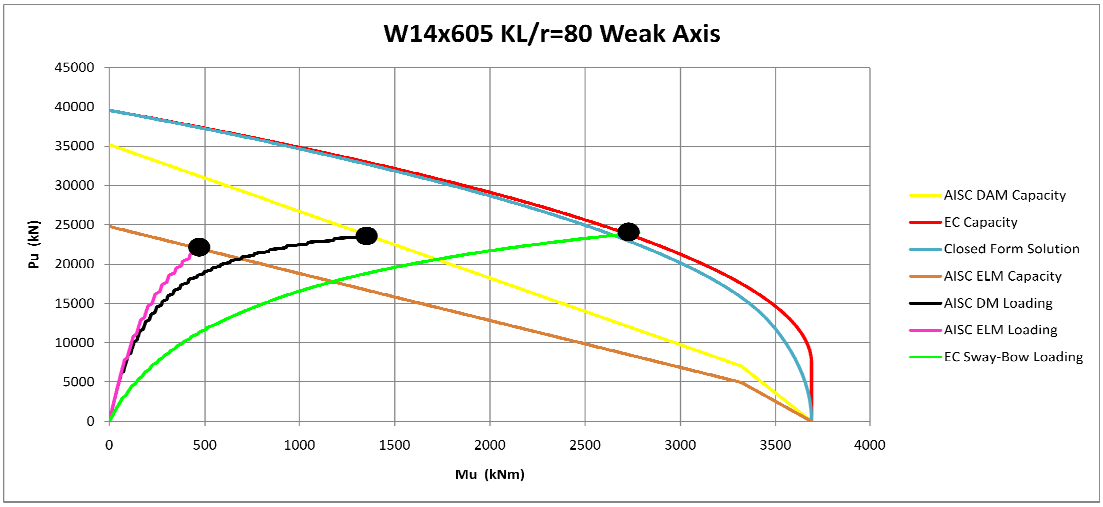

Figure 3-30 Weak Axis Interaction Diagram for KL/r= 80 W14x605 Column

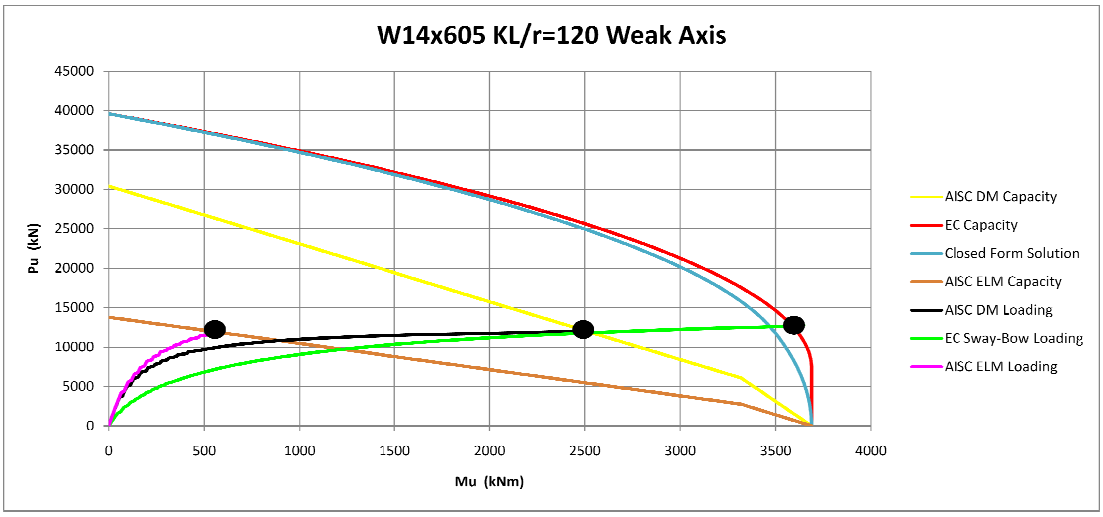

Figure 3-31 Weak Axis Interaction Diagram for KL/r= 120 W14x605 Column

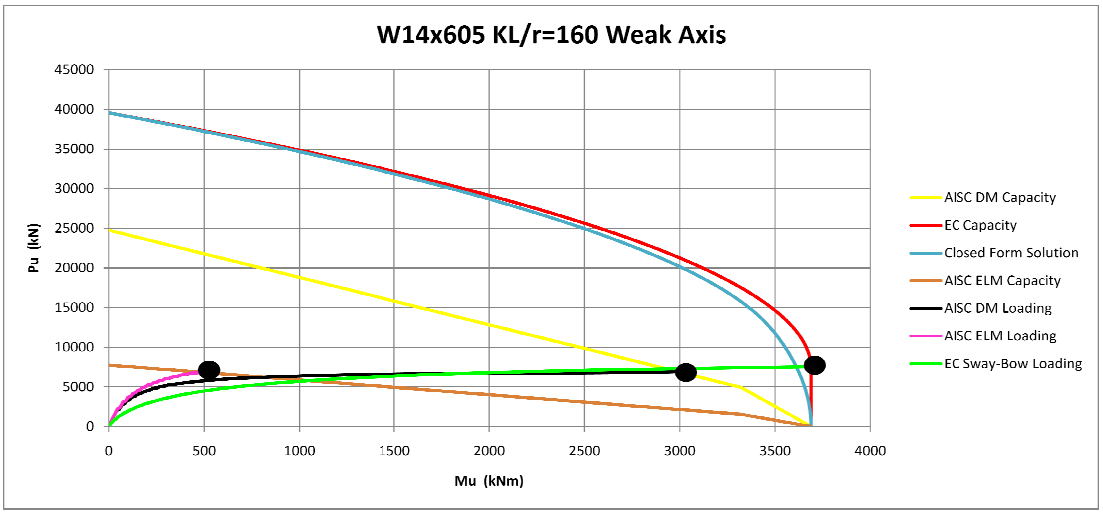

Figure 3-32 Weak Axis Interaction Diagram for KL/r= 160 W14x605 Column

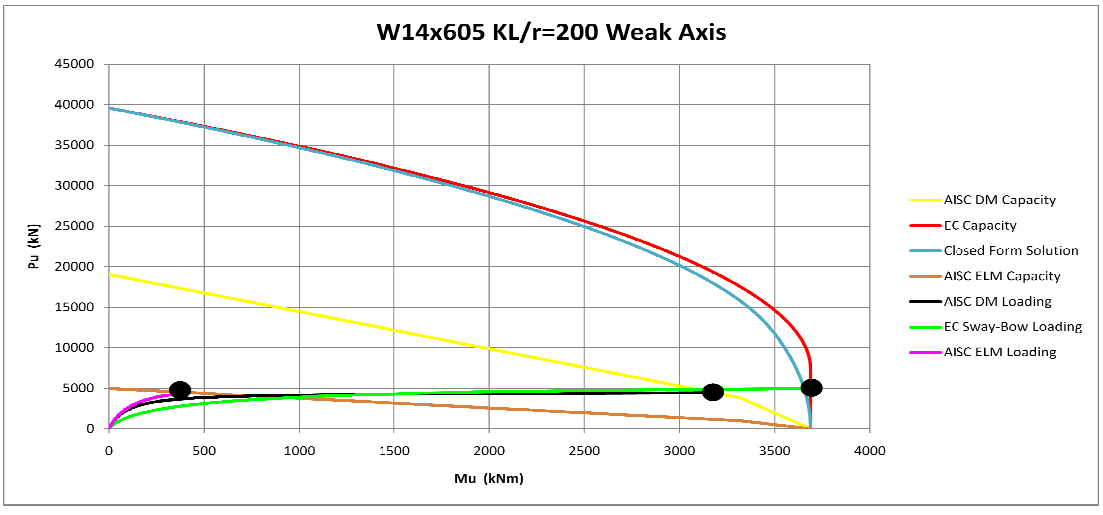

Figure 3-33 Weak Axis Interaction Diagram for KL/r= 200 W14x605 Column

Minor axis bending moment and axial compression capacities are illustrated in Table 3-29, Table 3-30 and Table 3-31.

Table 3-29 Comparison of AISC360-10 DM & EC3 Weak Axis Analysis Results

Case Study	Intersection Points						
	AISC360-10 DM Capacity			EC3 Capaciy		AISC DM/EC3 RATIO	
	τb	M (kNm)	P (kN)	M (kNm)	P (kN)	M	P
KL/r=40	0.48	400.3	34728.0	675.1	35276.6	0.59	0.98
KL/r=80	0.96	1379.7	23500.0	2746.6	23632.0	0.50	0.99
KL/r=120	1.00	2495.7	12125.0	3599.8	12346.0	0.69	0.98
KL/r=160	1.00	2982.0	6976.0	3688.7	7468.0	0.81	0.93
KL/r=200	1.00	3159.0	4549.0	3688.7	5058.0	0.86	0.90

Table 3-30 Comparison of AISC360-10 DM & ELM Weak Axis Analysis Results

Case Study	Intersection Points						
	AISC360-10 DM Capacity			AISC360-10 ELM Capacity		ISC DM/AISC ELM RATI	
	τb	M (kNm)	P (kN)	M (kNm)	P (kN)	M	P
KL/r=40	0.48	400.3	34728.0	225.8	33292.0	1.77	1.04
KL/r=80	0.96	1379.7	23500.0	508.0	21754.0	2.72	1.08
KL/r=120	1.00	2495.7	12125.0	588.4	11844.0	4.24	1.02
KL/r=160	1.00	2982.0	6976.0	475.6	6840.0	6.27	1.02
KL/r=200	1.00	3159.0	4549.0	423.8	4461.0	7.45	1.02

Table 3-31 Comparison of EC3 & AISC360-10 ELM Weak Axis Analysis Results

Case Study	Intersection Points					
	EC3 Capaciy		AISC360-10 ELM Capacity		EC3/AISC ELM RATIO	
	M (kNm)	P (kN)	M (kNm)	P (kN)	M	P
KL/r=40	675.1	35276.6	225.8	33292.0	2.99	1.06
KL/r=80	2746.6	23632.0	508.0	21754.0	5.41	1.09
KL/r=120	3599.8	12346.0	588.4	11844.0	6.12	1.04
KL/r=160	3688.7	7468.0	475.6	6840.0	7.76	1.09
KL/r=200	3688.7	5058.0	423.8	4461.0	8.70	1.13

In Table 3-29, difference between axial compression capacities of AISC360 DM and EC3 increase when KL/r=160 and 200. In other words, ratio of axial compression capacities are close to one when KL/r=40, 80 and 120. On the other hand, ratio of moment capacities are inconsistent with each other. EC3 moment capacities are always greater than moment capacities obtained with AISC360 DM analysis. Table 3-30 shows the comparison of AISC360 DM and ELM analysis results. In this table, axial compression capacities are close to each other for all cases. On the other hand, moment capacities are not consistent for all cases. Comparison of EC3 and AISC360

ELM capacities are illustrated in Table 3-31. As it has been seen from the P ratios, there is a consistency between axial load capacities. On the other hand, difference between moment capacities increase with slenderness ratio proportionaly.

3.7 Investigation of W18x192

In this section, procedures presented above applied for W18x192 section. Cross-section properties of W18x192 is given in Table 3-32.

Table 3-32 Cross Section Properties of W18x192

E : elastic modulus	200 GPa
Fy : yield strength	345 MPa
b : width of flange	290.957 mm
h : total heigth	516.89 mm
t_f : flange thickness	44.45 mm
t_w : web thickness	24.384 mm
A : cross section area	$36.4x10^3$ mm^2
I_x : moment of inertia about x direction	$1.611x10^9$ mm^4
I_y : moment of inertia about y direction	$1.831x10^8$ mm^4
r_x : radius of gyration in x direction	210.4 mm
r_y : radius of gyration in y direction	70.9 mm
S_x : section modulus about x direction	$6.233x10^6$ mm^3
S_y : section modulus about y direction	$1.259x10^6$ mm^3
Z_x : plastic section modulus about x axis	$7.243x10^6$ mm^3
Z_y : plastic section modulus about y axis	$1.95x10^6$ mm^3

Member lengths for major and minor axis bendings are presented for each slenderness ratio in Table 3-33.

Table 3-33 Individual Member Properties with W18x192 Section

Case Study	**KL/r**	**Column Profile**	**Column Height**	
			Strong Axis	**Weak Axis**
L/r =20	40	W18x192	4.208 m	1.418 m
L/r = 40	80	W18x192	8.416 m	2.836 m
L/r = 60	120	W18x192	12.624 m	4.254 m
L/r = 80	160	W18x192	16.832 m	5.672 m
L/r = 100	200	W18x192	21.040 m	7.090 m

Depending on Table 3-1, strong axis bending of W18x192 of bow imperfection loading parameters were obtained with imperfection *b* which is $\frac{e_0}{L} = \frac{1}{250}$. On the other hand, loading parameters of this section for weak axis bending were obtained by using imperfection *c* which is $\frac{e_0}{L} = \frac{1}{200}$.

For W18x192 strong axis bending analysis, loading parameters of AISC360 and EC3 specifications are shown in Table 3-34.

Table 3-34 Strong Axis Loading Table of AISC360 and EC3

Case Study	AISC Loading Parameters					EC Loading Parameters			
	Applied Axial Force P (kN)	Applied Notional Load Ni (kN)	Modified Stiffness Parameters			Applied Axial Force Ned (kN)	Sway Imperfection Load (kN)	Bow Imperfection Loads	
			τ_b	EI*	EA*			$\frac{4N_{ed}e_0}{L}$ (kN)	$\frac{8N_{ed}e_0}{L^2}$ ($\frac{kN}{m}$)
KL/r = 40	11000	22	0.43	0.35EI	0.80EA	11700	57.04	187.20	88.97
KL/r = 80	8000	16	0.92	0.74EI	0.80EA	9000	31.02	144.00	34.22
KL/r = 120	7000	14	0.99	0.79EI	0.80EA	7000	23.33	112.00	17.74
KL/r = 160	4000	8	1.00	0.80EI	0.80EA	4000	13.33	64.00	7.60
KL/r = 200	2000	4	1.00	0.80EI	0.80EA	2000	6.67	32.00	3.04

Table 3-35 illustrates loading values for minor axis bending of AISC360 and EC3 specifications.

Table 3-35 Weak Axis Loading Table of AISC360 and EC3

Case Study	AISC Loading Parameters					EC Loading Parameters			
	Applied Axial Force P (kN)	Applied Notional Load Ni (kN)	Modified Stiffness Parameters			Applied Axial Force Ned (kN)	Sway Imperfection Load (kN)	Bow Imperfection Loads	
			τ_b	EI*	EA*			$\frac{4N_{ed}e_0}{L}$ (kN)	$\frac{8N_{ed}e_0}{L^2}$ ($\frac{kN}{m}$)
KL/r = 40	11000	22	0.43	0.35EI	0.80EA	11600	58.00	232.00	327.22
KL/r = 80	8000	16	0.92	0.74EI	0.80EA	8000	40.00	160.00	112.83
KL/r = 120	5000	10	1.00	0.80EI	0.80EA	5000	24.24	100.00	47.01
KL/r = 160	3000	6	1.00	0.80EI	0.80EA	3000	12.60	60.00	21.16
KL/r = 200	2500	5	1.00	0.80EI	0.80EA	2500	9.39	50.00	14.10

3.7.1 Strong Axis Bending Analysis Results According to AISC360-10 and EC3 Specifications

Capacity curves of W18x192 strong axis bending are shown in Figure 3-34, Figure 3-35, Figure 3-36, Figure 3-37 and Figure 3-38.

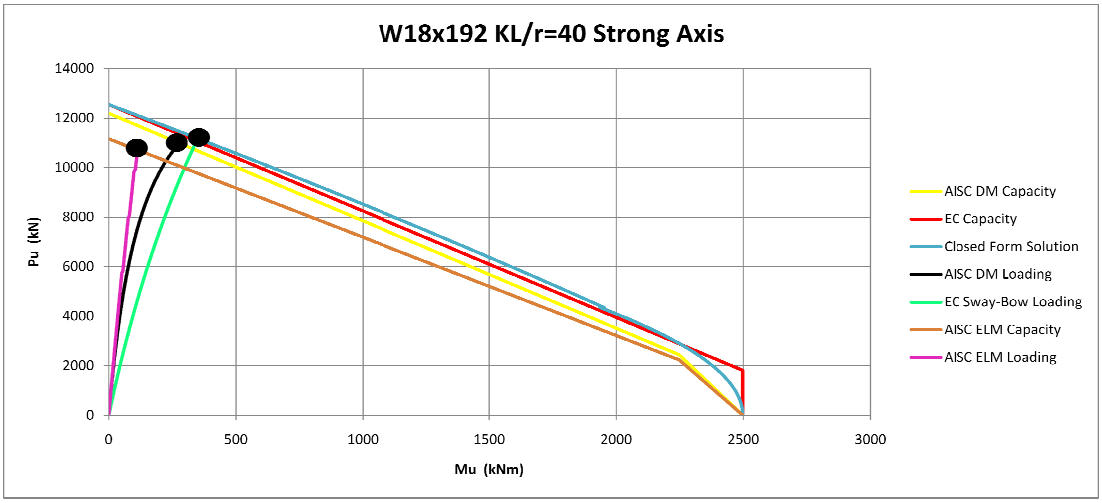

Figure 3-34 Strong Axis Interaction Diagram for KL/r=40 W18x192 Column

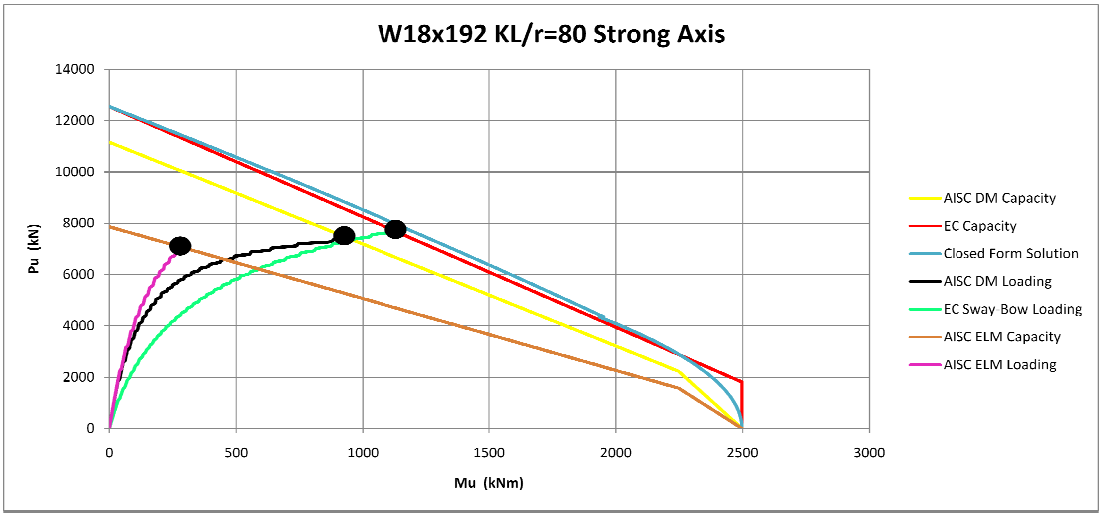

Figure 3-35 Strong Axis Interaction Diagram for KL/r=80 W18x192 Column

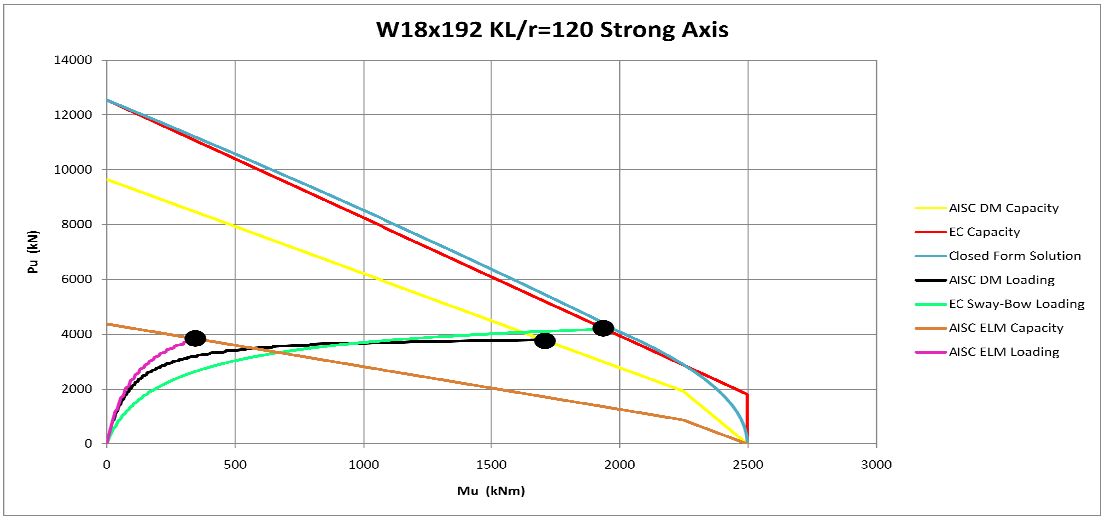

Figure 3-36 Strong Axis Interaction Diagram for KL/r=120 W18x192Column

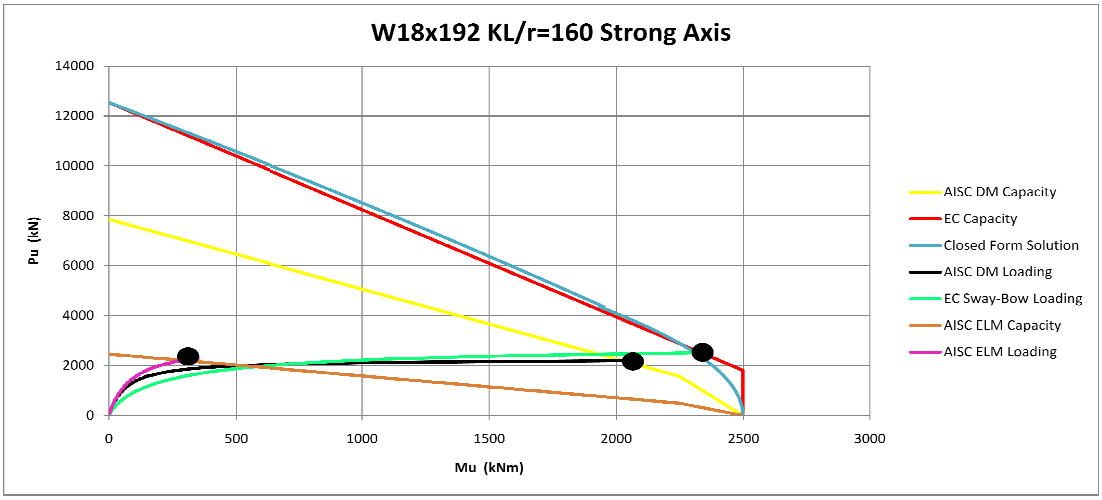

Figure 3-37 Strong Axis Interaction Diagram for KL/r=160 W18x192 Column

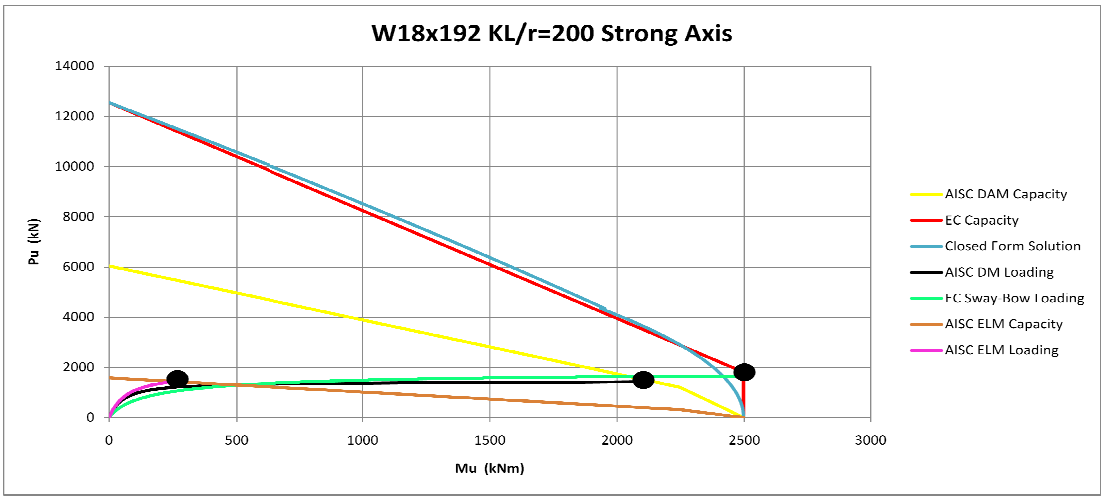

Figure 3-38 Strong Axis Interaction Diagram for KL/r=200 W18x192 Column

Strong axis capacity curve intersection points are illustrated in Table 3-36, Table 3-37 and Table 3-38.

Table 3-36 Comparison of AISC360-10 DM & EC3 Strong Axis Analysis Results

Case Study	Intersection Points						
	AISC360-10 DM Capacity			EC3 Capaciy		AISC DM/EC3 RATIO	
	τb	M (kNm)	P (kN)	M (kNm)	P (kN)	M	P
KL/r=40	0.43	304.7	10865.0	363.8	10984.0	0.84	0.99
KL/r=80	0.92	955.0	7368.0	1136.9	7659.0	0.84	0.96
KL/r=120	0.99	1720.4	3738.0	1958.9	4124.0	0.88	0.91
KL/r=160	1.00	2047.5	2131.0	2349.8	2443.0	0.87	0.87
KL/r=200	1.00	2113.0	1497.0	2496.9	1750.0	0.85	0.86

Table 3-37 Comparison of AISC360-10 DM & ELM Strong Axis Analysis Results

Case Study	Intersection Points						
	AISC360-10 DM Capacity			AISC360-10 ELM Capacity		AISC DM/AISC ELM RATIO	
	τb	M (kNm)	P (kN)	M (kNm)	P (kN)	M	P
KL/r=40	0.43	304.7	10865.0	144.8	10588.0	2.10	1.03
KL/r=80	0.92	955.0	7368.0	309.1	6995.0	3.09	1.05
KL/r=120	0.99	1720.4	3738.0	366.5	3805.0	4.69	0.98
KL/r=160	1.00	2047.5	2131.0	325.8	2176.0	6.29	0.98
KL/r=200	1.00	2113.0	1497.0	287.7	1414.0	7.35	1.06

Table 3-38 Comparison of EC3 & AISC360-10ELM Strong Axis Analysis Results

Case Study	Intersection Points					
	EC3 Capaciy		AISC360-10 ELM Capacity		EC3/AISC ELM RATIO	
	M (kNm)	P (kN)	M (kNm)	P (kN)	M	P
KL/r=40	363.8	10984.0	144.8	10588.0	2.51	1.04
KL/r=80	1136.9	7659.0	309.1	6995.0	3.68	1.09
KL/r=120	1958.9	4124.0	366.5	3805.0	5.35	1.08
KL/r=160	2349.8	2443.0	325.8	2176.0	7.21	1.12
KL/r=200	2496.9	1750.0	287.7	1414.0	8.68	1.24

Table 3-36 shows that axial compression capacities are consistent in KL/r=40 and 80 cases. On the other hand, there is 15% difference between bending moment capacities. Comparison of AISC360 DM and ELM were presented in Table 3-37. Similar to other DM and ELM comparisons, axial compression capacities are suitable with each other. Yet, there is no consistency between moment capacities. Finally, Table 3-38 shows the comparison of EC3 and AISC360 ELM P-M capacities. Except KL/r=200 and 160 cases, axial compression capacities are suitable with each other. Moment capacities are different for all cases.

3.7.2 Weak Axis Bending Analysis Results According to AISC360-10 and EC3 Specifications

Capacity curves for weak axis bending analysis are presented according to slenderness ratio of members.

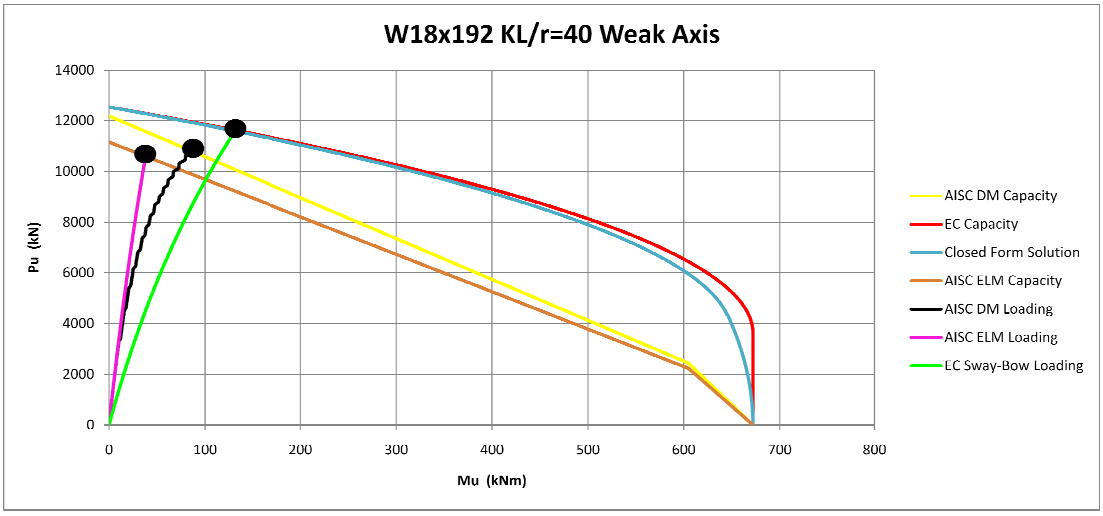

Figure 3-39 Weak Axis Interaction Diagram for KL/r= 40 W18x192 Column

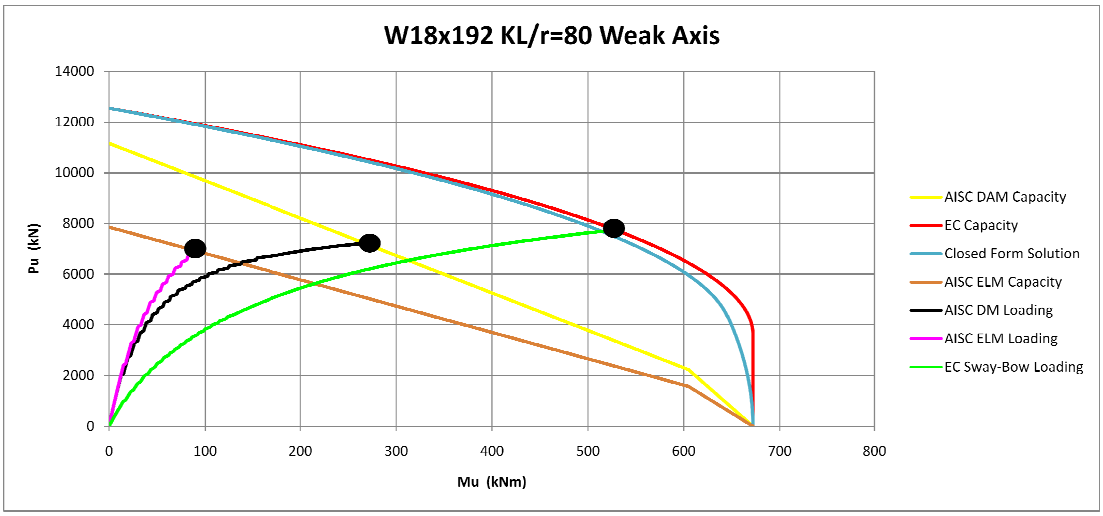

Figure 3-40 Weak Axis Interaction Diagram for KL/r= 80 W18x192 Column

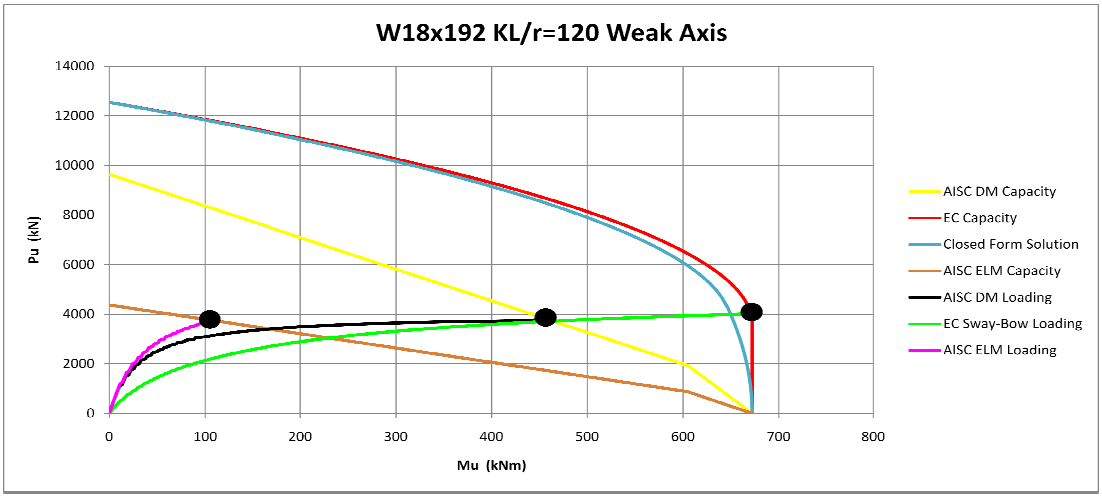

Figure 3-41 Weak Axis Interaction Diagram for KL/r= 120 W18x192 Column

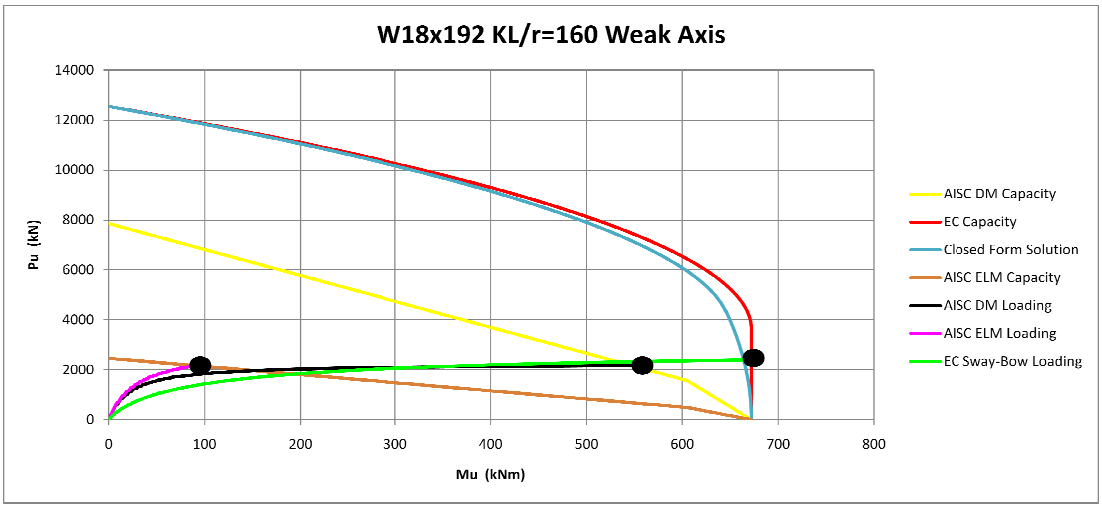

Figure 3-42 Weak Axis Interaction Diagram for KL/r= 160 W18x192 Column

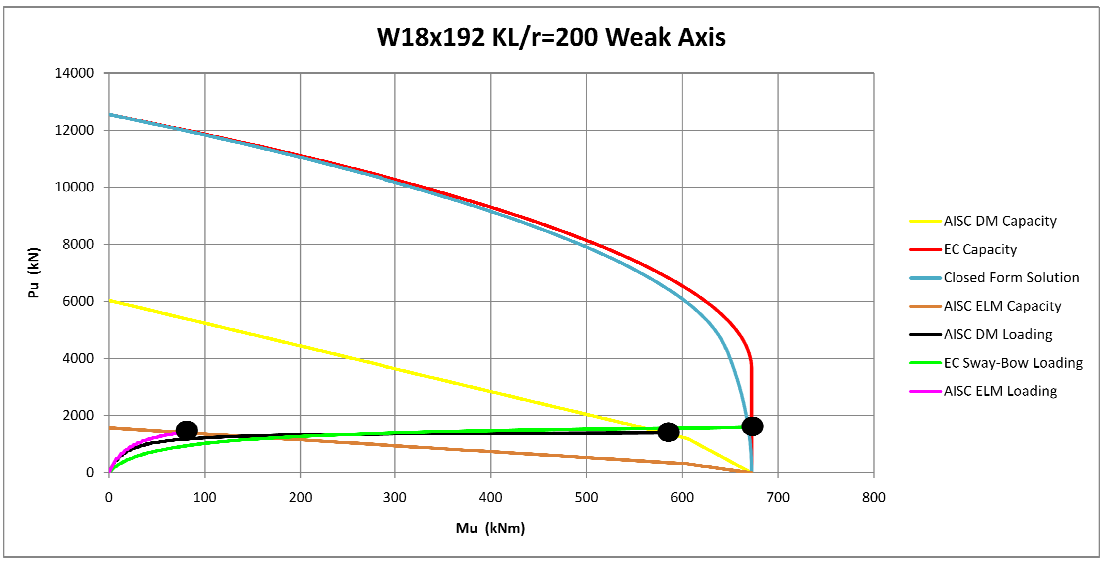

Figure 3-43 Weak Axis Interaction Diagram for KL/r= 200 W18x192 Column

Weak axis capacity curve intersection points are illustrated in Table 3-39, Table 3-40 and Table 3-41 respectively.

Table 3-39 Comparison of AISC360-10 DM & EC3Weak Axis Analysis Results

Case Study	Intersection Points						
	AISC360-10 DM Capacity			EC3 Capaciy		AISC DM/EC3 RATIO	
	τb	M (kNm)	P (kN)	M (kNm)	P (kN)	M	P
KL/r=40	0.43	96.6	10630.0	141.3	11555.0	0.68	0.92
KL/r=80	0.92	270.5	7170.0	531.5	7705.0	0.51	0.93
KL/r=120	1.00	463.3	3736.0	671.8	3852.0	0.69	0.97
KL/r=160	1.00	551.5	2128.0	672.2	2268.0	0.82	0.94
KL/r=200	1.00	586.9	1353.0	672.2	1419.0	0.87	0.95

Table 3-40 Comparison of AISC360-10 DM & ELMWeak Axis Analysis Results

Case Study	Intersection Points						
	AISC360-10 DM Capacity			AISC360-10 ELM Capacity		AISC DM/AISC ELM RATIO	
	τb	M (kNm)	P (kN)	M (kNm)	P (kN)	M	P
KL/r=40	0.43	90.0	10736.0	45.7	10630.0	1.97	1.01
KL/r=80	0.92	269.0	7193.0	98.1	7170.0	2.74	1.00
KL/r=120	1.00	459.1	3800.0	113.7	3736.0	4.04	1.02
KL/r=160	1.00	553.0	2113.0	96.3	2128.0	5.74	0.99
KL/r=200	1.00	582.4	1389.0	83.7	1353.0	6.96	1.03

Table 3-41 Comparison of EC3 & AISC360-10 ELMWeak Axis Analysis Results

Case Study	Intersection Points					
	EC3 Capaciy		AISC360-10 ELM Capacity		EC3/AISC ELM RATIO	
	M (kNm)	P (kN)	M (kNm)	P (kN)	M	P
KL/r=40	127.1	11367.0	45.7	10630.0	2.78	1.07
KL/r=80	531.4	7760.0	98.1	7170.0	5.42	1.08
KL/r=120	671.0	4004.0	113.7	3736.0	5.90	1.07
KL/r=160	672.2	2275.0	96.3	2128.0	6.98	1.07
KL/r=200	672.2	1419.0	83.7	1353.0	8.03	1.05

For weak axis bending analysis, comparison of AISC360-10 DM and EC3 analysis was shown in Table 3-39. Axial compression capacities are close to each other except KL/r=40 and 80 cases. There is no consistency between moment capacities except KL/r=200 case. Table 3-40 shows the comparison of AISC360 DM and ELM capacity values. As it can be seen from P ratios, axial compression capacities are close to each other. However, this is not valid for moment capacities. Finally, EC3 and AISC360 ELM comparison are given in Table 3-41. Axial compression capacities are comparable with each other. Yet, weak axis bending moment values are different for each method. For this reason, the ratio of bending moments are always greater than one.

3.8 Effect of EC3 Imperfections on Axial Force and Bending Moment Capacities

The purpose of this study is to compare AISC DM and EC3 capacity values with different EC3 imperfection values. W10x60, W10x26, W14x605 and W18x192 sections were studied with the EC3 "a, b, c, d" imperfection values. For each section, maximum and minimum P-M ratios were determined in order to make a statistical comparison between imperfection values. In addition to this, each imperfection value was evaluated in terms of P-M ratios among all cross sections. For each cross section, strong axis and weak axis bending analysis results are given in below tables.

Investigation of W10x60-Strong Axis Bending

W10x60 strong axis bending analysis results are illustrated Table 3-42, Table 3-43 Table 3-44 and Table 3-45.

Table 3-42 Comparison of AISC360-10 DM & EC3 Strong Axis Bending Capacities with W10x60-Imperfection "a"

Case Study	Intersection Points						
	AISC360-10 DM Capacity			EC3 Capaciy		AISC DM/EC3 RATIO	
	τ_b	M (kNm)	P (kN)	M (kNm)	P (kN)	M	P
KL/r=40	0.39	60.9	3326.0	62.6	3411.0	0.97	0.98
KL/r=80	0.95	157.4	2335.0	194.9	2328.0	0.81	1.00
KL/r=120	1.00	289.6	1185.0	319.7	1280.0	0.91	0.93
KL/r=160	1.00	344.7	671.0	381.0	772.0	0.90	0.87
KL/r=200	1.00	359.4	457.0	416.5	517.5	0.86	0.88
					max	0.97	1.00
					min	0.81	0.87
					average	0.89	0.93
					standard deviation	0.06	0.06

Table 3-43 Comparison of AISC360-10 DM & EC3 Strong Axis Bending Capacities with W10x60-Imperfection "b"

Case Study	Intersection Points						
	AISC360-10 DM Capacity			EC3 Capaciy		AISC DM/EC3 RATIO	
	τb	M (kNm)	P (kN)	M (kNm)	P (kN)	M	P
KL/r=40	0.39	60.9	3326.0	61.0	3455.0	1.00	0.96
KL/r=80	0.95	157.4	2335.0	198.0	2350.0	0.79	0.99
KL/r=120	1.00	289.6	1185.0	317.6	1336.0	0.91	0.89
KL/r=160	1.00	344.7	671.0	382.1	763.0	0.90	0.88
KL/r=200	1.00	359.4	457.0	411.7	518.0	0.87	0.88
					max	1.00	0.99
					min	0.79	0.88
					average	0.90	0.92
					standard deviation	0.07	0.05

Table 3-44 Comparison of AISC360-10 DM & EC3 Strong Axis Bending Capacities with W10x60-Imperfection "c"

Case Study	Intersection Points						
	AISC360-10 DM Capacity			EC3 Capaciy		AISC DM/EC3 RATIO	
	τb	M (kNm)	P (kN)	M (kNm)	P (kN)	M	P
KL/r=40	0.39	60.9	3326.0	63.3	3405.0	0.96	0.98
KL/r=80	0.95	157.4	2335.0	206.3	2220.0	0.76	1.05
KL/r=120	1.00	289.6	1185.0	323.9	1245.0	0.89	0.95
KL/r=160	1.00	344.7	671.0	385.1	738.0	0.90	0.91
KL/r=200	1.00	359.4	457.0	417.4	470.0	0.86	0.97
					max	0.96	1.05
					min	0.76	0.91
					average	0.88	0.97
					standard deviation	0.07	0.05

Table 3-45 Comparison of AISC360-10 DM & EC3 Strong Axis Bending Capacities with W10x60-Imperfection "d"

Case Study	Intersection Points						
	AISC360-10 DM Capacity			EC3 Capaciy		AISC DM/EC3 RATIO	
	τb	M (kNm)	P (kN)	M (kNm)	P (kN)	M	P
KL/r=40	0.39	60.9	3326.0	67.0	3375.0	0.91	0.99
KL/r=80	0.95	157.4	2335.0	212.2	2171.0	0.74	1.08
KL/r=120	1.00	289.6	1185.0	328.9	1204.0	0.88	0.98
KL/r=160	1.00	344.7	671.0	388.0	714.0	0.89	0.94
KL/r=200	1.00	359.4	457.0	415.8	484.0	0.86	0.94
					max	0.91	1.08
					min	0.74	0.94
					average	0.86	0.99
					standard deviation	0.07	0.05

Investigation of W10x60-Weak Axis Bending

W10x60 weak axis bending analysis results are illustrated Table 3-46, Table 3-47, Table 3-48 and Table 3-49.

Table 3-46 Comparison of AISC360-10 DM & EC3 Weak Axis Bending Capacities with W10x60-Imperfection "a"

Case Study	Intersection Points						
	AISC360-10 DM Capacity			EC3 Capaciy		AISC DM/EC3 RATIO	
	τb	M (kNm)	P (kN)	M (kNm)	P (kN)	M	P
KL/r=40	0.47	24.9	3389.0	34.2	3653.0	0.73	0.93
KL/r=80	0.90	84.1	2175.0	144.7	2458.0	0.58	0.88
KL/r=120	1.00	133.3	1211.0	195.0	1234.0	0.68	0.98
KL/r=160	1.00	161.3	677.0	197.7	716.0	0.82	0.95
KL/r=200	1.00	170.8	439.0	197.7	472.0	0.86	0.93
					max	0.86	0.98
					min	0.58	0.88
					average	0.73	0.93
					standard deviation	0.11	0.03

Table 3-47 Comparison of AISC360-10 DM & EC3 Weak Axis Bending Capacities with W10x60-Imperfection "b"

Case Study	Intersection Points						
	AISC360-10 DM Capacity			EC3 Capaciy		AISC DM/EC3 RATIO	
	τb	M (kNm)	P (kN)	M (kNm)	P (kN)	M	P
KL/r=40	0.47	24.9	3389.0	35.5	3642.0	0.70	0.93
KL/r=80	0.90	84.1	2175.0	147.4	2417.0	0.57	0.90
KL/r=120	1.00	133.3	1211.0	195.5	1201.0	0.68	1.01
KL/r=160	1.00	161.3	677.0	197.7	700.0	0.82	0.97
KL/r=200	1.00	170.8	439.0	197.7	459.0	0.86	0.96
					max	0.86	1.01
					min	0.57	0.90
					average	0.73	0.95
					standard deviation	0.12	0.04

Table 3-48 Comparison of AISC360-10 DM & EC3 Weak Axis Bending Capacities with W10x60-Imperfection "c"

Case Study	Intersection Points						
	AISC360-10 DM Capacity			EC3 Capaciy		AISC DM/EC3 RATIO	
	τb	M (kNm)	P (kN)	M (kNm)	P (kN)	M	P
KL/r=40	0.47	24.9	3389.0	38.6	3612.0	0.65	0.94
KL/r=80	0.90	84.1	2175.0	148.4	2375.0	0.57	0.92
KL/r=120	1.00	133.3	1211.0	192.4	1258.0	0.69	0.96
KL/r=160	1.00	161.3	677.0	196.2	724.0	0.82	0.94
KL/r=200	1.00	170.8	439.0	197.1	465.0	0.87	0.94
					max	0.87	0.96
					min	0.57	0.92
					average	0.72	0.94
					standard deviation	0.12	0.02

Table 3-49 Comparison of AISC360-10 DM & EC3 Weak Axis Bending Capacities with W10x60-Imperfection "d"

Case Study	Intersection Points						
	AISC360-10 DM Capacity			EC3 Capaciy		AISC DM/EC3 RATIO	
	τb	M (kNm)	P (kN)	M (kNm)	P (kN)	M	P
KL/r=40	0.47	24.9	3389.0	38.8	3614.0	0.64	0.94
KL/r=80	0.90	84.1	2175.0	153.4	2340.0	0.55	0.93
KL/r=120	1.00	133.3	1211.0	195.7	1185.0	0.68	1.02
KL/r=160	1.00	161.3	677.0	197.7	682.0	0.82	0.99
KL/r=200	1.00	170.8	439.0	197.7	445.0	0.86	0.99
					max	0.86	1.02
					min	0.55	0.93
					average	0.71	0.97
					standard deviation	0.13	0.04

Investigation of W10x26-Strong Axis Bending

W10x26 strong axis bending analysis results are illustrated Table 3-50, Table 3-51, Table 3-52 and Table 3-53.

Table 3-50 Comparison of AISC360-10 DM & EC3 Strong Axis Bending Capacities with W10x26-Imperfection "a"

Case Study	Intersection Points						
	AISC360-10 DM Capacity			EC3 Capaciy		AISC DM/EC3 RATIO	
	τb	M (kNm)	P (kN)	M (kNm)	P (kN)	M	P
KL/r=40	0.40	24.4	1442.0	25.6	1496.0	0.95	0.96
KL/r=80	0.91	67.0	979.0	83.3	1042.0	0.80	0.94
KL/r=120	1.00	121.4	507.0	141.4	567.0	0.86	0.89
KL/r=160	1.00	145.8	283.0	170.6	330.0	0.85	0.86
KL/r=200	1.00	153.5	186.0	176.8	210.0	0.87	0.89
					max	0.95	0.96
					min	0.80	0.86
					average	0.87	0.91
					standard deviation	0.05	0.04

Table 3-51 Comparison of AISC360-10 DM & EC3 Strong Axis Bending Capacities with W10x26-Imperfection "b"

Case Study	Intersection Points						
	AISC360-10 DM Capacity			EC3 Capaciy		AISC DM/EC3 RATIO	
	τb	M (kNm)	P (kN)	M (kNm)	P (kN)	M	P
KL/r=40	0.40	24.4	1442.0	26.1	1492.0	0.93	0.97
KL/r=80	0.91	67.0	979.0	84.3	1034.0	0.80	0.95
KL/r=120	1.00	121.4	507.0	142.7	556.0	0.85	0.91
KL/r=160	1.00	145.8	283.0	170.5	331.0	0.86	0.85
KL/r=200	1.00	153.5	186.0	176.8	222.2	0.87	0.84
					max	0.93	0.97
					min	0.80	0.84
					average	0.86	0.90
					standard deviation	0.05	0.06

Table 3-52 Comparison of AISC360-10 DM & EC3 Strong Axis Bending Capacities with W10x26-Imperfection "c"

Case Study	Intersection Points						
	AISC360-10 DM Capacity			EC3 Capaciy		AISC DM/EC3 RATIO	
	τb	M (kNm)	P (kN)	M (kNm)	P (kN)	M	P
KL/r=40	0.40	24.4	1442.0	26.9	1486.0	0.91	0.97
KL/r=80	0.91	67.0	979.0	86.3	1018.0	0.78	0.96
KL/r=120	1.00	121.4	507.0	145.4	535.0	0.84	0.95
KL/r=160	1.00	145.8	283.0	172.0	319.0	0.85	0.89
KL/r=200	1.00	153.5	186.0	176.8	220.0	0.87	0.85
					max	0.91	0.97
					min	0.78	0.85
					average	0.85	0.92
					standard deviation	0.05	0.05

Table 3-53 Comparison of AISC360-10 DM & EC3 Strong Axis Bending Capacities with W10x26-Imperfection "d"

Case Study	Intersection Points						
	AISC360-10 DM Capacity			EC3 Capaciy		AISC DM/EC3 RATIO	
	τb	M (kNm)	P (kN)	M (kNm)	P (kN)	M	P
KL/r=40	0.40	24.4	1442.0	28.2	1476.0	0.87	0.98
KL/r=80	0.91	67.0	979.0	89.9	989.0	0.75	0.99
KL/r=120	1.00	121.4	507.0	146.0	530.0	0.83	0.96
KL/r=160	1.00	145.8	283.0	172.5	315.0	0.85	0.90
KL/r=200	1.00	153.5	186.0	176.8	219.9	0.87	0.85
					max	0.87	0.99
					min	0.75	0.85
					average	0.83	0.93
					standard deviation	0.05	0.06

Investigation of W10x26-Weak Axis Bending

W10x26 weak axis bending analysis results are illustrated Table 3-54, Table 3-55, Table 3-56 and Table 3-57.

Table 3-54 Comparison of AISC360-10 DM & EC3 Weak Axis Bending Capacities with W10x26-Imperfection "a"

Case Study	Intersection Points						
	AISC360-10 DM Capacity			EC3 Capaciy		AISC DM/EC3 RATIO	
	τb	M (kNm)	P (kN)	M (kNm)	P (kN)	M	P
KL/r=40	0.44	5.9	1441.0	8.6	1569.0	0.69	0.92
KL/r=80	0.97	15.9	990.0	34.0	1079.0	0.47	0.92
KL/r=120	1.00	29.5	497.0	42.4	535.0	0.70	0.93
KL/r=160	1.00	33.6	312.0	42.4	369.0	0.79	0.85
KL/r=200	1.00	36.3	194.0	42.4	215.0	0.86	0.90
					max	0.86	0.93
					min	0.47	0.85
					average	0.70	0.90
					standard deviation	0.15	0.03

Table 3-55 Comparison of AISC360-10 DM & EC3 Weak Axis Bending Capacities with W10x26-Imperfection "b"

Case Study	Intersection Points						
	AISC360-10 DM Capacity			EC3 Capaciy		AISC DM/EC3 RATIO	
	τb	M (kNm)	P (kN)	M (kNm)	P (kN)	M	P
KL/r=40	0.44	5.9	1441.0	8.1	1535.9	0.73	0.94
KL/r=80	0.97	15.9	990.0	33.1	1053.0	0.48	0.94
KL/r=120	1.00	29.5	497.0	42.4	531.0	0.70	0.94
KL/r=160	1.00	33.6	312.0	42.4	315.3	0.79	0.99
KL/r=200	1.00	36.3	194.0	42.4	204.0	0.86	0.95
					max	0.86	0.99
					min	0.48	0.94
					average	0.71	0.95
					standard deviation	0.14	0.02

Table 3-56 Comparison of AISC360-10 DM & EC3 Weak Axis Bending Capacities with W10x26-Imperfection "c"

Case Study	Intersection Points						
	AISC360-10 DM Capacity			EC3 Capaciy		AISC DM/EC3 RATIO	
	τb	M (kNm)	P (kN)	M (kNm)	P (kN)	M	P
KL/r=40	0.44	5.9	1441.0	9.1	1561.0	0.65	0.92
KL/r=80	0.97	15.9	990.0	34.7	1018.0	0.46	0.97
KL/r=120	1.00	29.5	497.0	42.4	519.0	0.70	0.96
KL/r=160	1.00	33.6	312.0	42.4	353.0	0.79	0.88
KL/r=200	1.00	36.3	194.0	42.4	194.0	0.86	1.00
					max	0.86	1.00
					min	0.46	0.88
					average	0.69	0.95
					standard deviation	0.15	0.05

Table 3-57 Comparison of AISC360-10 DM & EC3 Weak Axis Bending Capacities with W10x26-Imperfection "d"

Case Study	Intersection Points						
	AISC360-10 DM Capacity			EC3 Capaciy		AISC DM/EC3 RATIO	
	τb	M (kNm)	P (kN)	M (kNm)	P (kN)	M	P
KL/r=40	0.44	5.9	1441.0	9.3	1561.0	0.63	0.92
KL/r=80	0.97	15.9	990.0	35.8	1007.0	0.44	0.98
KL/r=120	1.00	29.5	497.0	42.4	503.0	0.70	0.99
KL/r=160	1.00	33.6	312.0	42.4	340.0	0.79	0.92
KL/r=200	1.00	36.3	194.0	42.4	174.0	0.86	1.11
					max	0.86	1.11
					min	0.44	0.92
					average	0.68	0.99
					standard deviation	0.16	0.08

Investigation of W14x605-Strong Axis Bending

W14x605 strong axis bending analysis results are illustrated Table 3-58, Table 3-59, Table 3-60 and Table 3-61.

Table 3-58 Comparison of AISC360-10 DM & EC3 Strong Axis Bending Capacities with W14x605-Imperfection "a"

Case Study	Intersection Points						
	AISC360-10 DM Capacity			EC3 Capaciy		AISC DM/EC3 RATIO	
	τb	M (kNm)	P (kN)	M (kNm)	P (kN)	M	P
KL/r=40	0.45	839.9	34582.0	1075.1	34392.0	0.78	1.01
KL/r=80	0.87	3080.2	22262.0	3104.3	24300.0	0.99	0.92
KL/r=120	0.93	5305.4	11154.0	5524.9	12936.0	0.96	0.86
KL/r=160	1.00	6083.6	6787.0	6613.7	7686.0	0.92	0.88
KL/r=200	1.00	6442.6	4400.0	7239.6	4668.0	0.89	0.94
					max	0.99	1.01
					min	0.78	0.86
					average	0.91	0.92
					standard deviation	0.08	0.06

Table 3-59 Comparison of AISC360-10 DM & EC3 Strong Axis Bending Capacities with W14x605-Imperfection "b"

Case Study	Intersection Points						
	AISC360-10 DM Capacity			EC3 Capaciy		AISC DM/EC3 RATIO	
	τb	M (kNm)	P (kN)	M (kNm)	P (kN)	M	P
KL/r=40	0.45	839.9	34582.0	1099.2	34276.0	0.76	1.01
KL/r=80	0.87	3080.2	22262.0	3304.1	24000.0	0.93	0.93
KL/r=120	0.93	5305.4	11154.0	5587.9	12632.0	0.95	0.88
KL/r=160	1.00	6083.6	6787.0	6652.7	7498.0	0.91	0.91
KL/r=200	1.00	6442.6	4400.0	7175.3	4978.0	0.90	0.88
					max	0.95	1.01
					min	0.76	0.88
					average	0.89	0.92
					standard deviation	0.07	0.05

Table 3-60 Comparison of AISC360-10 DM & EC3 Strong Axis Bending Capacities with W14x605-Imperfection "c"

Case Study	Intersection Points						
	AISC360-10 DM Capacity			EC3 Capaciy		AISC DM/EC3 RATIO	
	τb	M (kNm)	P (kN)	M (kNm)	P (kN)	M	P
KL/r=40	0.45	839.9	34582.0	1129.9	31128.0	0.74	1.11
KL/r=80	0.87	3080.2	22262.0	3386.3	23248.0	0.91	0.96
KL/r=120	0.93	5305.4	11154.0	5608.3	12534.0	0.95	0.89
KL/r=160	1.00	6083.6	6787.0	6694.6	7296.0	0.91	0.93
KL/r=200	1.00	6442.6	4400.0	7121.8	5236.0	0.90	0.84
					max	0.95	1.11
					min	0.74	0.84
					average	0.88	0.95
					standard deviation	0.08	0.10

Table 3-61 Comparison of AISC360-10 DM & EC3 Strong Axis Bending Capacities with W14x605-Imperfection "d"

Case Study	Intersection Points						
	AISC360-10 DM Capacity			EC3 Capaciy		AISC DM/EC3 RATIO	
	τb	M (kNm)	P (kN)	M (kNm)	P (kN)	M	P
KL/r=40	0.45	839.9	34582.0	1161.8	33974.0	0.72	1.02
KL/r=80	0.87	3080.2	22262.0	3557.6	22422.0	0.87	0.99
KL/r=120	0.93	5305.4	11154.0	5621.5	12470.0	0.94	0.89
KL/r=160	1.00	6083.6	6787.0	6647.7	7522.0	0.92	0.90
KL/r=200	1.00	6442.6	4400.0	7179.8	4922.0	0.90	0.89
					max	0.94	1.02
					min	0.72	0.89
					average	0.87	0.94
					standard deviation	0.09	0.06

Investigation of W14x605-Weak Axis Bending

W14x605 weak axis bending analysis results are illustrated Table 3-62, Table 3-63, Table 3-64 and Table 3-65.

Table 3-62 Comparison of AISC360-10 DM & EC3 Weak Axis Bending Capacities with W14x605-Imperfection "a"

Case Study	Intersection Points						
	AISC360-10 DM Capacity			EC3 Capaciy		AISC DM/EC3 RATIO	
	τb	M (kNm)	P (kN)	M (kNm)	P (kN)	M	P
KL/r=40	0.48	400.3	34728.0	640.1	36646.0	0.63	0.95
KL/r=80	0.96	1379.7	23500.0	2557.6	25192.0	0.54	0.93
KL/r=120	1.00	2495.7	12125.0	3569.7	13132.0	0.70	0.92
KL/r=160	1.00	2982.0	6976.0	3688.7	7430.0	0.81	0.94
KL/r=200	1.00	3159.0	4549.0	3688.7	4758.0	0.86	0.96
					max	0.86	0.96
					min	0.54	0.92
					average	0.71	0.94
					standard deviation	0.13	0.01

Table 3-63 Comparison of AISC360-10 DM & EC3 Weak Axis Bending Capacities with W14x605-Imperfection "b"

Case Study	Intersection Points						
	AISC360-10 DM Capacity			EC3 Capaciy		AISC DM/EC3 RATIO	
	τb	M (kNm)	P (kN)	M (kNm)	P (kN)	M	P
KL/r=40	0.48	400.3	34728.0	683.2	36438.0	0.59	0.95
KL/r=80	0.96	1379.7	23500.0	2616.3	24722.0	0.53	0.95
KL/r=120	1.00	2495.7	12125.0	3587.1	12692.0	0.70	0.96
KL/r=160	1.00	2982.0	6976.0	3688.7	7390.0	0.81	0.94
KL/r=200	1.00	3159.0	4549.0	3688.7	4396.0	0.86	1.03
					max	0.86	1.03
					min	0.53	0.94
					average	0.69	0.97
					standard deviation	0.14	0.04

Table 3-64 Comparison of AISC360-10 DM & EC3 Weak Axis Bending Capacities with W14x605-Imperfection "c"

Case Study	Intersection Points						
	AISC360-10 DM Capacity			EC3 Capaciy		AISC DM/EC3 RATIO	
	τb	M (kNm)	P (kN)	M (kNm)	P (kN)	M	P
KL/r=40	0.48	400.3	34728.0	698.9	36362.0	0.57	0.96
KL/r=80	0.96	1379.7	23500.0	2675.2	24238.0	0.52	0.97
KL/r=120	1.00	2495.7	12125.0	3592.3	12552.0	0.69	0.97
KL/r=160	1.00	2982.0	6976.0	3688.7	7082.0	0.81	0.99
KL/r=200	1.00	3159.0	4549.0	3688.7	4376.0	0.86	1.04
					max	0.86	1.04
					min	0.52	0.96
					average	0.69	0.98
					standard deviation	0.15	0.03

Table 3-65 Comparison of AISC360-10 DM & EC3 Weak Axis Bending Capacities with W14x605-Imperfection "d"

Case Study	Intersection Points						
	AISC360-10 DM Capacity			EC3 Capaciy		AISC DM/EC3 RATIO	
	τb	M (kNm)	P (kN)	M (kNm)	P (kN)	M	P
KL/r=40	0.48	400.3	34728.0	675.1	35276.6	0.59	0.98
KL/r=80	0.96	1379.7	23500.0	2746.6	23632.0	0.50	0.99
KL/r=120	1.00	2495.7	12125.0	3599.8	12346.0	0.69	0.98
KL/r=160	1.00	2982.0	6976.0	3688.6	7468.0	0.81	0.93
KL/r=200	1.00	3159.0	4549.0	3657.8	4756.0	0.86	0.96
					max	0.86	0.99
					min	0.50	0.93
					average	0.69	0.97
					standard deviation	0.15	0.02

Investigation of W18x192-Strong Axis Bending

W18x192 strong axis bending analysis results are illustrated Table 3-66, Table 3-67, Table 3-68 and Table 3-69.

Table 3-66 Comparison of AISC360-10 DM & EC3 Strong Axis Bending Capacities with W18x192-Imperfection "a"

Case Study	Intersection Points						
	AISC360-10 DM Capacity			EC3 Capaciy		AISC DM/EC3 RATIO	
	τb	M (kNm)	P (kN)	M (kNm)	P (kN)	M	P
KL/r=40	0.43	304.7	10865.0	366.6	10972.0	0.83	0.99
KL/r=80	0.92	955.0	7368.0	1125.8	7707.0	0.85	0.96
KL/r=120	0.99	1720.4	3738.0	1952.8	4150.0	0.88	0.90
KL/r=160	1.00	2047.5	2131.0	2348.6	2448.0	0.87	0.87
KL/r=200	1.00	2113.0	1497.0	2496.9	1485.0	0.85	1.01
					max	0.88	1.01
					min	0.83	0.87
					average	0.86	0.95
					standard deviation	0.02	0.06

Table 3-67 Comparison of AISC360-10 DM & EC3 Strong Axis Bending Capacities with W18x192-Imperfection "b"

Case Study	Intersection Points						
	AISC360-10 DM Capacity			EC3 Capaciy		AISC DM/EC3 RATIO	
	τb	M (kNm)	P (kN)	M (kNm)	P (kN)	M	P
KL/r=40	0.43	304.7	10865.0	363.8	10984.0	0.84	0.99
KL/r=80	0.92	955.0	7368.0	1136.9	7659.0	0.84	0.96
KL/r=120	0.99	1720.4	3738.0	1958.9	4124.0	0.88	0.91
KL/r=160	1.00	2047.5	2131.0	2349.8	2443.0	0.87	0.87
KL/r=200	1.00	2113.0	1497.0	2496.9	1750.0	0.85	0.86
					max	0.88	0.99
					min	0.84	0.86
					average	0.85	0.92
					standard deviation	0.02	0.06

Table 3-68 Comparison of AISC360-10 DM & EC3 Strong Axis Bending Capacities with W18x192-Imperfection "c"

Case Study	Intersection Points						
	AISC360-10 DM Capacity			EC3 Capaciy		AISC DM/EC3 RATIO	
	τb	M (kNm)	P (kN)	M (kNm)	P (kN)	M	P
KL/r=40	0.43	304.7	10865.0	382.8	10902.0	0.80	1.00
KL/r=80	0.92	955.0	7368.0	1168.8	7522.0	0.82	0.98
KL/r=120	0.99	1720.4	3738.0	1967.3	4088.0	0.87	0.91
KL/r=160	1.00	2047.5	2131.0	2364.9	2378.0	0.87	0.90
KL/r=200	1.00	2113.0	1497.0	2496.9	1449.0	0.85	1.03
					max	0.87	1.03
					min	0.80	0.90
					average	0.84	0.96
					standard deviation	0.03	0.06

Table 3-69 Comparison of AISC360-10 DM & EC3 Strong Axis Bending Capacities with W18x192-Imperfection "d"

Case Study	Intersection Points						
	AISC360-10 DM Capacity			EC3 Capaciy		AISC DM/EC3 RATIO	
	τb	M (kNm)	P (kN)	M (kNm)	P (kN)	M	P
KL/r=40	0.43	304.7	10865.0	394.7	10851.0	0.77	1.00
KL/r=80	0.92	955.0	7368.0	1229.5	7261.0	0.78	1.01
KL/r=120	0.99	1720.4	3738.0	1995.6	3990.0	0.86	0.94
KL/r=160	1.00	2047.5	2131.0	2377.0	2326.0	0.86	0.92
KL/r=200	1.00	2113.0	1497.0	2496.9	1407.0	0.85	1.06
					max	0.86	1.06
					min	0.77	0.92
					average	0.82	0.99
					standard deviation	0.05	0.06

Investigation of W18x192-Weak Axis Bending

W18x192 weak axis bending analysis results are illustrated Table 3-70, Table 3-71, Table 3-72 and Table 3-73.

Table 3-70 Comparison of AISC360-10 DM & EC3 Weak Axis Bending Capacities with W18x192-Imperfection "a"

Case Study	Intersection Points						
	AISC360-10 DM Capacity			EC3 Capaciy		AISC DM/EC3 RATIO	
	τb	M (kNm)	P (kN)	M (kNm)	P (kN)	M	P
KL/r=40	0.43	96.6	10630.0	130.7	11634.0	0.74	0.91
KL/r=80	0.92	270.5	7170.0	511.3	7989.0	0.53	0.90
KL/r=120	1.00	463.3	3736.0	671.0	3999.0	0.69	0.93
KL/r=160	1.00	551.5	2128.0	672.2	2293.0	0.82	0.93
KL/r=200	1.00	586.9	1353.0	672.2	1509.0	0.87	0.90
					max	0.87	0.93
					min	0.53	0.90
					average	0.73	0.91
					standard deviation	0.13	0.02

Table 3-71 Comparison of AISC360-10 DM & EC3 Weak Axis Bending Capacities with W18x192-Imperfection "b"

Case Study	Intersection Points						
	AISC360-10 DM Capacity			EC3 Capaciy		AISC DM/EC3 RATIO	
	τb	M (kNm)	P (kN)	M (kNm)	P (kN)	M	P
KL/r=40	0.43	96.6	10630.0	141.1	11556.0	0.68	0.92
KL/r=80	0.92	270.5	7170.0	524.2	7810.0	0.52	0.92
KL/r=120	1.00	463.3	3736.0	671.1	3993.0	0.69	0.94
KL/r=160	1.00	551.5	2128.0	672.2	2250.0	0.82	0.95
KL/r=200	1.00	586.9	1353.0	672.2	1460.0	0.87	0.93
					max	0.87	0.95
					min	0.52	0.92
					average	0.72	0.93
					standard deviation	0.14	0.01

Table 3-72 Comparison of AISC360-10 DM & EC3 Weak Axis Bending Capacities with W18x192-Imperfection "c"

Case Study	Intersection Points						
	AISC360-10 DM Capacity			EC3 Capaciy		AISC DM/EC3 RATIO	
	τb	M (kNm)	P (kN)	M (kNm)	P (kN)	M	P
KL/r=40	0.43	96.6	10630.0	141.3	11555.0	0.68	0.92
KL/r=80	0.92	270.5	7170.0	531.5	7705.0	0.51	0.93
KL/r=120	1.00	463.3	3736.0	671.8	3852.0	0.69	0.97
KL/r=160	1.00	551.5	2128.0	672.2	2268.0	0.82	0.94
KL/r=200	1.00	586.9	1353.0	672.2	1419.0	0.87	0.95
					max	0.87	0.97
					min	0.51	0.92
					average	0.72	0.94
					standard deviation	0.14	0.02

Table 3-73 Comparison of AISC360-10 DM & EC3 Weak Axis Bending Capacities with W18x192-Imperfection "d"

Case Study	Intersection Points						
	AISC360-10 DM Capacity			EC3 Capaciy		AISC DM/EC3 RATIO	
	τb	M (kNm)	P (kN)	M (kNm)	P (kN)	M	P
KL/r=40	0.43	96.6	10630.0	143.7	11537.0	0.67	0.92
KL/r=80	0.92	270.5	7170.0	556.1	7332.0	0.49	0.98
KL/r=120	1.00	463.3	3736.0	672.1	3731.0	0.69	1.00
KL/r=160	1.00	551.5	2128.0	672.2	2206.0	0.82	0.96
KL/r=200	1.00	586.9	1353.0	672.2	1367.0	0.87	0.99
					max	0.87	1.00
					min	0.49	0.92
					average	0.71	0.97
					standard deviation	0.15	0.03

Discussion for Effect of EC3 Imperfections for Different Cross Sections

Above tables show the comparison of AISC360 DM and EC3 capacities with different imperfection values. As it has been mentioned in Section 3.4, 3.5, 3.6 and 3.7, EC3 initial bow imperfection values are determined depending on flange thickness and $\frac{h}{b}$ ratio of the section.Analysis that were performed in Section 3.8, are illustrated with maximum, minimum, average and standard deviation values in order to show the behaviour of each cross section with other $\frac{e_0}{L}$ values.

Starting with W10x60 strong axis and weak bending cases, the most consistent results were obtained with imperfection *b*, which is $\frac{e_0}{L} = \frac{1}{200}$. Table 3-43 and Table 3-47 show that, maximum, minimum and average P-M ratios are the most favorable

results comparing to other tables. According to Table 1-2, suggested imperfection value for W10x60 strong axis bending is imperfection *b.* For this reason, results are favorable with suggested imperfection value. On the other hand, there is no major difference between weak axis bending capacities obtained with other imperfections.

For W10x26 strong axis and weak bending cases, the most consistent results were obtained with imperfection *b*, which is $\frac{e_0}{L} = \frac{1}{200}$. Table 3-43 and Table 3-47 show that, maximum, minimum and average P-M ratios are the most favorable results comparing to other tables. In addition to this, selected imperfection value for strong axis bending that provide criteria mentioned above is *b.* For this reason, results are suitable with suggested imperfection value. On the other hand, there is no major difference between weak axis bending capacities obtained with other imperfections.

For W14x605 imperfection value that must be used for strong axis bending is *d*. Results show that, the most consistent capacity ratios were obtained from imperfection a, *b and c*, which are $\frac{e_0}{L} = \frac{1}{300}$, $\frac{e_0}{L} = \frac{1}{250}$ and $\frac{e_0}{L} = \frac{1}{200}$. Standard deviations of Table 3-58, Table 3-59 and Table 3-61 are more uniform comparing to results shown in Table 3-60. For weak axis bending, analysis were performed with the initial bow imperfection of *d*. Statistical parameters show that, the most reasonable results were obtained with imperfection *d* which is equal to $\frac{1}{150}$.

Finally, there is no major difference between W18x192 strong axis and weak bending analysis results. Maximum, minimum and average values are close to each other. Therefore, any imperfection value can be used to come at the capacities offered by AISC360.

General Evaluation of EC3 Bow Imperfections

In this part, each imperfection value isevaluated by taking into consideration all sections with all slenderness ratios. For the initial bow imperfection values of *a, b, c* and *d*, maximum, minimum, average and standard deviation values were determined to make a comparison between axial and flexural capacities.

Strong Axis Bending

Table 3-74, Table 3-75, Table 3-76 and Table 3-77 show strong axis bending moment and axial compression capacity values that were obtained from EC3 imperfections of *a*, *b*, *c* and *d* respectively. Furthermore, an overall comprasion of strong axis bending of EC3 *a*, *b*, *c* and *d* imperfections with W10x60, W10x26, W14x605 and W18x192 cross sections is presented in Table 3-78.

Table 3-74 Comparison of AISC360-10 DM & EC3 Strong Axis Bending Capacities-Imperfection "a"

Case Study	Column Profile	Intersection Points						
		AISC360-10 DM Capacity			EC3 Capaciy		AISC DM/EC3 RATIO	
		τb	M (kNm)	P (kN)	M (kNm)	P (kN)	M	P
KL/r=40	W10x60	0.39	60.9	3326.0	62.6	3411.0	0.97	0.98
KL/r=40	W10x26	0.40	24.4	1442.0	25.6	1496.0	0.95	0.96
KL/r=40	W14x605	0.45	839.9	34582.0	1075.1	34392.0	0.78	1.01
KL/r=40	W18x192	0.43	304.7	10865.0	366.6	10972.0	0.83	0.99
KL/r=80	W10x60	0.95	157.4	2335.0	194.9	2328.0	0.81	1.00
KL/r=80	W10x26	0.91	67.0	979.0	83.3	1042.0	0.80	0.94
KL/r=80	W14x605	0.87	3080.2	22262.0	3104.3	24300.0	0.99	0.92
KL/r=80	W18x192	0.92	955.0	7368.0	1125.8	7707.0	0.85	0.96
KL/r=120	W10x60	1.00	289.6	1185.0	319.7	1280.0	0.91	0.93
KL/r=120	W10x26	1.00	121.4	507.0	141.4	567.0	0.86	0.89
KL/r=120	W14x605	0.93	5305.4	11154.0	5524.9	12936.0	0.96	0.86
KL/r=120	W18x192	0.99	1720.4	3738.0	1952.8	4150.0	0.88	0.90
KL/r=160	W10x60	1.00	344.7	671.0	381.0	772.0	0.90	0.87
KL/r=160	W10x26	1.00	145.8	283.0	170.6	330.0	0.85	0.86
KL/r=160	W14x605	1.00	6083.6	6787.0	6613.7	7686.0	0.92	0.88
KL/r=160	W18x192	1.00	2047.5	2131.0	2348.6	2448.0	0.87	0.87
KL/r=200	W10x60	1.00	359.4	457.0	416.5	517.5	0.86	0.88
KL/r=200	W10x26	1.00	153.5	186.0	176.8	210.0	0.87	0.89
KL/r=200	W14x605	1.00	6442.6	4400.0	7239.6	4668.0	0.89	0.94
KL/r=200	W18x192	1.00	2113.0	1497.0	2496.9	1485.0	0.85	1.01
						max	0.99	1.01
						min	0.78	0.86
						average	0.88	0.93
						standard deviation	0.06	0.05

Table 3-75 Comparison of AISC360-10 DM & EC3 Strong Axis Bending Capacities-Imperfection "b"

Case Study	Column Profile	Intersection Points						
		AISC360-10 DM Capacity			EC3 Capaciy		AISC DM/EC3 RATIO	
		τb	M (kNm)	P (kN)	M (kNm)	P (kN)	M	P
KL/r=40	W10x60	0.39	60.9	3326.0	61.0	3455.0	1.00	0.96
KL/r=40	W10x26	0.40	24.4	1442.0	26.1	1492.0	0.93	0.97
KL/r=40	W14x605	0.45	839.9	34582.0	1099.2	34276.0	0.76	1.01
KL/r=40	W18x192	0.43	304.7	10865.0	363.8	10984.0	0.84	0.99
KL/r=80	W10x60	0.95	157.4	2335.0	198.0	2350.0	0.79	0.99
KL/r=80	W10x26	0.91	67.0	979.0	84.3	1034.0	0.80	0.95
KL/r=80	W14x605	0.87	3080.2	22262.0	3304.1	24000.0	0.93	0.93
KL/r=80	W18x192	0.92	955.0	7368.0	1136.9	7659.0	0.84	0.96
KL/r=120	W10x60	1.00	289.6	1185.0	317.6	1336.0	0.91	0.89
KL/r=120	W10x26	1.00	121.4	507.0	142.7	556.0	0.85	0.91
KL/r=120	W14x605	0.93	5305.4	11154.0	5587.9	12632.0	0.95	0.88
KL/r=120	W18x192	0.99	1720.4	3738.0	1958.9	4124.0	0.88	0.91
KL/r=160	W10x60	1.00	344.7	671.0	382.1	763.0	0.90	0.88
KL/r=160	W10x26	1.00	145.8	283.0	170.5	331.0	0.86	0.85
KL/r=160	W14x605	1.00	6083.6	6787.0	6652.7	7498.0	0.91	0.91
KL/r=160	W18x192	1.00	2047.5	2131.0	2349.8	2443.0	0.87	0.87
KL/r=200	W10x60	1.00	359.4	457.0	411.7	518.0	0.87	0.88
KL/r=200	W10x26	1.00	153.5	186.0	176.8	222.2	0.87	0.84
KL/r=200	W14x605	1.00	6442.6	4400.0	7175.3	4978.0	0.90	0.88
KL/r=200	W18x192	1.00	2113.0	1497.0	2496.9	1750.0	0.85	0.86
						max	1.00	1.01
						min	0.76	0.84
						average	0.88	0.92
						standard deviation	0.06	0.05

Table 3-76 Comparison of AISC360-10 DM & EC3 Strong Axis Bending Capacities-Imperfection "c"

Case Study	Column Profile	Intersection Points						
		AISC360-10 DM Capacity			EC3 Capaciy		AISC DM/EC3 RATIO	
		τb	M (kNm)	P (kN)	M (kNm)	P (kN)	M	P
KL/r=40	W10x60	0.39	60.9	3326.0	63.3	3405.0	0.96	0.98
KL/r=40	W10x26	0.40	24.4	1442.0	26.9	1486.0	0.91	0.97
KL/r=40	W14x605	0.45	839.9	34582.0	1129.9	31128.0	0.74	1.11
KL/r=40	W18x192	0.43	304.7	10865.0	382.8	10902.0	0.80	1.00
KL/r=80	W10x60	0.95	157.4	2335.0	206.3	2220.0	0.76	1.05
KL/r=80	W10x26	0.91	67.0	979.0	86.3	1018.0	0.78	0.96
KL/r=80	W14x605	0.87	3080.2	22262.0	3386.3	23248.0	0.91	0.96
KL/r=80	W18x192	0.92	955.0	7368.0	1168.8	7522.0	0.82	0.98
KL/r=120	W10x60	1.00	289.6	1185.0	323.9	1245.0	0.89	0.95
KL/r=120	W10x26	1.00	121.4	507.0	145.4	535.0	0.84	0.95
KL/r=120	W14x605	0.93	5305.4	11154.0	5608.3	12534.0	0.95	0.89
KL/r=120	W18x192	0.99	1720.4	3738.0	1967.3	4088.0	0.87	0.91
KL/r=160	W10x60	1.00	344.7	671.0	385.1	738.0	0.90	0.91
KL/r=160	W10x26	1.00	145.8	283.0	172.0	319.0	0.85	0.89
KL/r=160	W14x605	1.00	6083.6	6787.0	6694.6	7296.0	0.91	0.93
KL/r=160	W18x192	1.00	2047.5	2131.0	2364.9	2378.0	0.87	0.90
KL/r=200	W10x60	1.00	359.4	457.0	417.4	470.0	0.86	0.97
KL/r=200	W10x26	1.00	153.5	186.0	176.8	220.0	0.87	0.85
KL/r=200	W14x605	1.00	6442.6	4400.0	7121.8	5236.0	0.90	0.84
KL/r=200	W18x192	1.00	2113.0	1497.0	2496.9	1449.0	0.85	1.03
						max	0.96	1.11
						min	0.74	0.84
						average	0.86	0.95
						standard deviation	0.06	0.07

Table 3-77 Comparison of AISC360-10 DM & EC3 Strong Axis Bending Capacities-Imperfection "d"

Case Study	Column Profile	Intersection Points						
		AISC360-10 DM Capacity			EC3 Capaciy		AISC DM/EC3 RATIO	
		τ_b	M (kNm)	P (kN)	M (kNm)	P (kN)	M	P
KL/r=40	W10x60	0.39	60.9	3326.0	67.0	3375.0	0.91	0.99
KL/r=40	W10x26	0.40	24.4	1442.0	28.2	1476.0	0.87	0.98
KL/r=40	W14x605	0.45	839.9	34582.0	1161.8	33974.0	0.72	1.02
KL/r=40	W18x192	0.43	304.7	10865.0	394.7	10851.0	0.77	1.00
KL/r=80	W10x60	0.95	157.4	2335.0	212.2	2171.0	0.74	1.08
KL/r=80	W10x26	0.91	67.0	979.0	89.9	989.0	0.75	0.99
KL/r=80	W14x605	0.87	3080.2	22262.0	3557.6	22422.0	0.87	0.99
KL/r=80	W18x192	0.92	955.0	7368.0	1229.5	7261.0	0.78	1.01
KL/r=120	W10x60	1.00	289.6	1185.0	328.9	1204.0	0.88	0.98
KL/r=120	W10x26	1.00	121.4	507.0	146.0	530.0	0.83	0.96
KL/r=120	W14x605	0.93	5305.4	11154.0	5621.5	12470.0	0.94	0.89
KL/r=120	W18x192	0.99	1720.4	3738.0	1995.6	3990.0	0.86	0.94
KL/r=160	W10x60	1.00	344.7	671.0	388.0	714.0	0.89	0.94
KL/r=160	W10x26	1.00	145.8	283.0	172.5	315.0	0.85	0.90
KL/r=160	W14x605	1.00	6083.6	6787.0	6647.7	7522.0	0.92	0.90
KL/r=160	W18x192	1.00	2047.5	2131.0	2377.0	2326.0	0.86	0.92
KL/r=200	W10x60	1.00	359.4	457.0	415.8	484.0	0.86	0.94
KL/r=200	W10x26	1.00	153.5	186.0	176.8	219.9	0.87	0.85
KL/r=200	W14x605	1.00	6442.6	4400.0	7179.8	4922.0	0.90	0.89
KL/r=200	W18x192	1.00	2113.0	1497.0	2496.9	1407.0	0.85	1.06
						max	0.94	1.08
						min	0.72	0.85
						average	0.85	0.96
						standard deviation	0.06	0.06

Table 3-78 Comparison of AISC360-10 DM & EC3 Strong Axis Bending Capacities-Imperfection "a, b, c, d"

Case Study	Column Profile	Intersection Points							
		EC3 Imperfection	AISC360-10 DM Capacity			EC3 Capaciy		AISC DM/EC3 RATIO	
			τ_b	M (kNm)	P (kN)	M (kNm)	P (kN)	M	P
KL/r=40	W10x60	a	0.39	60.9	3326.0	62.6	3411.0	0.97	0.98
KL/r=40	W10x26	a	0.40	24.4	1442.0	25.6	1496.0	0.95	0.96
KL/r=40	W14x605	a	0.45	839.9	34582.0	1075.1	34392.0	0.78	1.01
KL/r=40	W18x192	a	0.43	304.7	10865.0	366.6	10972.0	0.83	0.99
KL/r=80	W10x60	a	0.95	157.4	2335.0	194.9	2328.0	0.81	1.00
KL/r=80	W10x26	a	0.91	67.0	979.0	83.3	1042.0	0.80	0.94
KL/r=80	W14x605	a	0.87	3080.2	22262.0	3104.3	24300.0	0.99	0.92
KL/r=80	W18x192	a	0.92	955.0	7368.0	1125.8	7707.0	0.85	0.96
KL/r=120	W10x60	a	1.00	289.6	1185.0	319.7	1280.0	0.91	0.93
KL/r=120	W10x26	a	1.00	121.4	507.0	141.4	567.0	0.86	0.89
KL/r=120	W14x605	a	0.93	5305.4	11154.0	5524.9	12936.0	0.96	0.86
KL/r=120	W18x192	a	0.99	1720.4	3738.0	1952.8	4150.0	0.88	0.90
KL/r=160	W10x60	a	1.00	344.7	671.0	381.0	772.0	0.90	0.87
KL/r=160	W10x26	a	1.00	145.8	283.0	170.6	330.0	0.85	0.86
KL/r=160	W14x605	a	1.00	6083.6	6787.0	6613.7	7686.0	0.92	0.88
KL/r=160	W18x192	a	1.00	2047.5	2131.0	2348.6	2448.0	0.87	0.87
KL/r=200	W10x60	a	1.00	359.4	457.0	416.5	517.5	0.86	0.88
KL/r=200	W10x26	a	1.00	153.5	186.0	176.8	210.0	0.87	0.89
KL/r=200	W14x605	a	1.00	6442.6	4400.0	7239.6	4668.0	0.89	0.94
KL/r=200	W18x192	a	1.00	2113.0	1497.0	2496.9	1485.0	0.85	1.01
KL/r=40	W10x60	b	0.39	60.9	3326.0	61.0	3455.0	1.00	0.96
KL/r=40	W10x26	b	0.40	24.4	1442.0	26.1	1492.0	0.93	0.97
KL/r=40	W14x605	b	0.45	839.9	34582.0	1099.2	34276.0	0.76	1.01
KL/r=40	W18x192	b	0.43	304.7	10865.0	363.8	10984.0	0.84	0.99
KL/r=80	W10x60	b	0.95	157.4	2335.0	198.0	2350.0	0.79	0.99
KL/r=80	W10x26	b	0.91	67.0	979.0	84.3	1034.0	0.80	0.95
KL/r=80	W14x605	b	0.87	3080.2	22262.0	3304.1	24000.0	0.93	0.93
KL/r=80	W18x192	b	0.92	955.0	7368.0	1136.9	7659.0	0.84	0.96
KL/r=120	W10x60	b	1.00	289.6	1185.0	317.6	1336.0	0.91	0.89
KL/r=120	W10x26	b	1.00	121.4	507.0	142.7	556.0	0.85	0.91
KL/r=120	W14x605	b	0.93	5305.4	11154.0	5587.9	12632.0	0.95	0.88
KL/r=120	W18x192	b	0.99	1720.4	3738.0	1958.9	4124.0	0.88	0.91
KL/r=160	W10x60	b	1.00	344.7	671.0	382.1	763.0	0.90	0.88
KL/r=160	W10x26	b	1.00	145.8	283.0	170.5	331.0	0.86	0.85
KL/r=160	W14x605	b	1.00	6083.6	6787.0	6652.7	7498.0	0.91	0.91
KL/r=160	W18x192	b	1.00	2047.5	2131.0	2349.8	2443.0	0.87	0.87
KL/r=200	W10x60	b	1.00	359.4	457.0	411.7	518.0	0.87	0.88
KL/r=200	W10x26	b	1.00	153.5	186.0	176.8	222.2	0.87	0.84
KL/r=200	W14x605	b	1.00	6442.6	4400.0	7175.3	4978.0	0.90	0.88
KL/r=200	W18x192	b	1.00	2113.0	1497.0	2496.9	1750.0	0.85	0.86

KL/r=40	W10x60	c	0.39	60.9	3326.0	63.3	3405.0	0.96	0.98
KL/r=40	W10x26	c	0.40	24.4	1442.0	26.9	1486.0	0.91	0.97
KL/r=40	W14x605	c	0.45	839.9	34582.0	1129.9	31128.0	0.74	1.11
KL/r=40	W18x192	c	0.43	304.7	10865.0	382.8	10902.0	0.80	1.00
KL/r=80	W10x60	c	0.95	157.4	2335.0	206.3	2220.0	0.76	1.05
KL/r=80	W10x26	c	0.91	67.0	979.0	86.3	1018.0	0.78	0.96
KL/r=80	W14x605	c	0.87	3080.2	22262.0	3386.3	23248.0	0.91	0.96
KL/r=80	W18x192	c	0.92	955.0	7368.0	1168.8	7522.0	0.82	0.98
KL/r=120	W10x60	c	1.00	289.6	1185.0	323.9	1245.0	0.89	0.95
KL/r=120	W10x26	c	1.00	121.4	507.0	145.4	535.0	0.84	0.95
KL/r=120	W14x605	c	0.93	5305.4	11154.0	5608.3	12534.0	0.95	0.89
KL/r=120	W18x192	c	0.99	1720.4	3738.0	1967.3	4088.0	0.87	0.91
KL/r=160	W10x60	c	1.00	344.7	671.0	385.1	738.0	0.90	0.91
KL/r=160	W10x26	c	1.00	145.8	283.0	172.0	319.0	0.85	0.89
KL/r=160	W14x605	c	1.00	6083.6	6787.0	6694.6	7296.0	0.91	0.93
KL/r=160	W18x192	c	1.00	2047.5	2131.0	2364.9	2378.0	0.87	0.90
KL/r=200	W10x60	c	1.00	359.4	457.0	417.4	470.0	0.86	0.97
KL/r=200	W10x26	c	1.00	153.5	186.0	176.8	220.0	0.87	0.85
KL/r=200	W14x605	c	1.00	6442.6	4400.0	7121.8	5236.0	0.90	0.84
KL/r=200	W18x192	c	1.00	2113.0	1497.0	2496.9	1449.0	0.85	1.03
KL/r=40	W10x60	d	0.39	60.9	3326.0	67.0	3375.0	0.91	0.99
KL/r=40	W10x26	d	0.40	24.4	1442.0	28.2	1476.0	0.87	0.98
KL/r=40	W14x605	d	0.45	839.9	34582.0	1161.8	33974.0	0.72	1.02
KL/r=40	W18x192	d	0.43	304.7	10865.0	394.7	10851.0	0.77	1.00
KL/r=80	W10x60	d	0.95	157.4	2335.0	212.2	2171.0	0.74	1.08
KL/r=80	W10x26	d	0.91	67.0	979.0	89.9	989.0	0.75	0.99
KL/r=80	W14x605	d	0.87	3080.2	22262.0	3557.6	22422.0	0.87	0.99
KL/r=80	W18x192	d	0.92	955.0	7368.0	1229.5	7261.0	0.78	1.01
KL/r=120	W10x60	d	1.00	289.6	1185.0	328.9	1204.0	0.88	0.98
KL/r=120	W10x26	d	1.00	121.4	507.0	146.0	530.0	0.83	0.96
KL/r=120	W14x605	d	0.93	5305.4	11154.0	5621.5	12470.0	0.94	0.89
KL/r=120	W18x192	d	0.99	1720.4	3738.0	1995.6	3990.0	0.86	0.94
KL/r=160	W10x60	d	1.00	344.7	671.0	388.0	714.0	0.89	0.94
KL/r=160	W10x26	d	1.00	145.8	283.0	172.5	315.0	0.85	0.90
KL/r=160	W14x605	d	1.00	6083.6	6787.0	6647.7	7522.0	0.92	0.90
KL/r=160	W18x192	d	1.00	2047.5	2131.0	2377.0	2326.0	0.86	0.92
KL/r=200	W10x60	d	1.00	359.4	457.0	415.8	484.0	0.86	0.94
KL/r=200	W10x26	d	1.00	153.5	186.0	176.8	219.9	0.87	0.85
KL/r=200	W14x605	d	1.00	6442.6	4400.0	7179.8	4922.0	0.90	0.89
KL/r=200	W18x192	d	1.00	2113.0	1497.0	2496.9	1407.0	0.85	1.06
							max	1.00	1.11
							min	0.72	0.84
							average	0.87	0.94
							standard deviation	0.06	0.06

Weak Axis Bending

Weak axis bending moment and axial compression capacity values were shown in Table 3-79, Table 3-80, Table 3-81 and Table 3-82. Moreover, an overall comprasion of weak axis bending of EC3 *a*, *b*, *c* and *d* imperfections with W10x60, W10x26, W14x605 and W18x192 cross sections is presented in Table 3-83.

Table 3-79 Comparison of AISC360-10 DM & EC3 Capacities-Imperfection "a"

Case Study	Column Profile	Intersection Points						
		AISC360-10 DM Capacity			EC3 Capaciy		AISC DM/EC3 RATIO	
		τb	M (kNm)	P (kN)	M (kNm)	P (kN)	M	P
KL/r=40	W10x60	0.47	24.9	3389.0	34.2	3653.0	0.73	0.93
KL/r=40	W10x26	0.44	5.9	1441.0	8.6	1569.0	0.69	0.92
KL/r=40	W14x605	0.48	400.3	34728.0	640.1	36646.0	0.63	0.95
KL/r=40	W18x192	0.43	96.6	10630.0	130.7	11634.0	0.74	0.91
KL/r=80	W10x60	0.90	84.1	2175.0	144.7	2458.0	0.58	0.88
KL/r=80	W10x26	0.97	15.9	990.0	34.0	1079.0	0.47	0.92
KL/r=80	W14x605	0.96	1379.7	23500.0	2557.6	25192.0	0.54	0.93
KL/r=80	W18x192	0.92	270.5	7170.0	511.3	7989.0	0.53	0.90
KL/r=120	W10x60	1.00	133.3	1211.0	195.0	1234.0	0.68	0.98
KL/r=120	W10x26	1.00	29.5	497.0	42.4	535.0	0.70	0.93
KL/r=120	W14x605	1.00	2495.7	12125.0	3569.7	13132.0	0.70	0.92
KL/r=120	W18x192	1.00	463.3	3736.0	671.0	3999.0	0.69	0.93
KL/r=160	W10x60	1.00	161.3	677.0	197.7	716.0	0.82	0.95
KL/r=160	W10x26	1.00	33.6	312.0	42.4	369.0	0.79	0.85
KL/r=160	W14x605	1.00	2982.0	6976.0	3688.7	7430.0	0.81	0.94
KL/r=160	W18x192	1.00	551.5	2128.0	672.2	2293.0	0.82	0.93
KL/r=200	W10x60	1.00	170.8	439.0	197.7	472.0	0.86	0.93
KL/r=200	W10x26	1.00	36.3	194.0	42.4	215.0	0.86	0.90
KL/r=200	W14x605	1.00	3159.0	4549.0	3688.7	4758.0	0.86	0.96
KL/r=200	W18x192	1.00	586.9	1353.0	672.2	1509.0	0.87	0.90
						max	0.87	0.98
						min	0.47	0.85
						average	0.72	0.92
						standard deviation	0.12	0.03

Table 3-80 Comparison of AISC360-10 DM & EC3 Capacities-Imperfection "b"

Case Study	Column Profile	Intersection Points						
		AISC360-10 DM Capacity			EC3 Capaciy		AISC DM/EC3 RATIO	
		τb	M (kNm)	P (kN)	M (kNm)	P (kN)	M	P
KL/r=40	W10x60	0.47	24.9	3389.0	35.5	3642.0	0.70	0.93
KL/r=40	W10x26	0.44	5.9	1441.0	8.1	1535.9	0.73	0.94
KL/r=40	W14x605	0.48	400.3	34728.0	683.2	36438.0	0.59	0.95
KL/r=40	W18x192	0.43	96.6	10630.0	141.1	11556.0	0.68	0.92
KL/r=80	W10x60	0.90	84.1	2175.0	147.4	2417.0	0.57	0.90
KL/r=80	W10x26	0.97	15.9	990.0	33.1	1053.0	0.48	0.94
KL/r=80	W14x605	0.96	1379.7	23500.0	2616.3	24722.0	0.53	0.95
KL/r=80	W18x192	0.92	270.5	7170.0	524.2	7810.0	0.52	0.92
KL/r=120	W10x60	1.00	133.3	1211.0	195.5	1201.0	0.68	1.01
KL/r=120	W10x26	1.00	29.5	497.0	42.4	531.0	0.70	0.94
KL/r=120	W14x605	1.00	2495.7	12125.0	3587.1	12692.0	0.70	0.96
KL/r=120	W18x192	1.00	463.3	3736.0	671.1	3993.0	0.69	0.94
KL/r=160	W10x60	1.00	161.3	677.0	197.7	700.0	0.82	0.97
KL/r=160	W10x26	1.00	33.6	312.0	42.4	315.3	0.79	0.99
KL/r=160	W14x605	1.00	2982.0	6976.0	3688.7	7390.0	0.81	0.94
KL/r=160	W18x192	1.00	551.5	2128.0	672.2	2250.0	0.82	0.95
KL/r=200	W10x60	1.00	170.8	439.0	197.7	459.0	0.86	0.96
KL/r=200	W10x26	1.00	36.3	194.0	42.4	204.0	0.86	0.95
KL/r=200	W14x605	1.00	3159.0	4549.0	3688.7	4396.0	0.86	1.03
KL/r=200	W18x192	1.00	586.9	1353.0	672.2	1460.0	0.87	0.93
						max	0.87	1.03
						min	0.48	0.90
						average	0.71	0.95
						standard deviation	0.12	0.03

Table 3-81 Comparison of AISC360-10 DM & EC3 Capacities-Imperfection "c"

Case Study	Column Profile	Intersection Points						
		AISC360-10 DM Capacity			EC3 Capaciy		AISC DM/EC3 RATIO	
		τ_b	M (kNm)	P (kN)	M (kNm)	P (kN)	M	P
KL/r=40	W10x60	0.47	24.9	3389.0	38.6	3612.0	0.65	0.94
KL/r=40	W10x26	0.44	5.9	1441.0	9.1	1561.0	0.65	0.92
KL/r=40	W14x605	0.48	400.3	34728.0	698.9	36362.0	0.57	0.96
KL/r=40	W18x192	0.43	96.6	10630.0	141.3	11555.0	0.68	0.92
KL/r=80	W10x60	0.90	84.1	2175.0	148.4	2375.0	0.57	0.92
KL/r=80	W10x26	0.97	15.9	990.0	34.7	1018.0	0.46	0.97
KL/r=80	W14x605	0.96	1379.7	23500.0	2675.2	24238.0	0.52	0.97
KL/r=80	W18x192	0.92	270.5	7170.0	531.5	7705.0	0.51	0.93
KL/r=120	W10x60	1.00	133.3	1211.0	192.4	1258.0	0.69	0.96
KL/r=120	W10x26	1.00	29.5	497.0	42.4	519.0	0.70	0.96
KL/r=120	W14x605	1.00	2495.7	12125.0	3592.3	12552.0	0.69	0.97
KL/r=120	W18x192	1.00	463.3	3736.0	671.8	3852.0	0.69	0.97
KL/r=160	W10x60	1.00	161.3	677.0	196.2	724.0	0.82	0.94
KL/r=160	W10x26	1.00	33.6	312.0	42.4	353.0	0.79	0.88
KL/r=160	W14x605	1.00	2982.0	6976.0	3688.7	7082.0	0.81	0.99
KL/r=160	W18x192	1.00	551.5	2128.0	672.2	2268.0	0.82	0.94
KL/r=200	W10x60	1.00	170.8	439.0	197.1	465.0	0.87	0.94
KL/r=200	W10x26	1.00	36.3	194.0	42.4	194.0	0.86	1.00
KL/r=200	W14x605	1.00	3159.0	4549.0	3688.7	4376.0	0.86	1.04
KL/r=200	W18x192	1.00	586.9	1353.0	672.2	1419.0	0.87	0.95
						max	0.87	1.04
						min	0.46	0.88
						average	0.70	0.95
						standard deviation	0.13	0.03

Table 3-82 Comparison of AISC360-10 DM & EC3 Capacities-Imperfection "d"

Case Study	Column Profile	Intersection Points						
		AISC360-10 DM Capacity			EC3 Capaciy		AISC DM/EC3 RATIO	
		τ_b	M (kNm)	P (kN)	M (kNm)	P (kN)	M	P
KL/r=40	W10x60	0.47	24.9	3389.0	38.8	3614.0	0.64	0.94
KL/r=40	W10x26	0.44	5.9	1441.0	9.3	1561.0	0.63	0.92
KL/r=40	W14x605	0.48	400.3	34728.0	675.1	35276.6	0.59	0.98
KL/r=40	W18x192	0.43	96.6	10630.0	143.7	11537.0	0.67	0.92
KL/r=80	W10x60	0.90	84.1	2175.0	153.4	2340.0	0.55	0.93
KL/r=80	W10x26	0.97	15.9	990.0	35.8	1007.0	0.44	0.98
KL/r=80	W14x605	0.96	1379.7	23500.0	2746.6	23632.0	0.50	0.99
KL/r=80	W18x192	0.92	270.5	7170.0	556.1	7332.0	0.49	0.98
KL/r=120	W10x60	1.00	133.3	1211.0	195.7	1185.0	0.68	1.02
KL/r=120	W10x26	1.00	29.5	497.0	42.4	503.0	0.70	0.99
KL/r=120	W14x605	1.00	2495.7	12125.0	3599.8	12346.0	0.69	0.98
KL/r=120	W18x192	1.00	463.3	3736.0	672.1	3731.0	0.69	1.00
KL/r=160	W10x60	1.00	161.3	677.0	197.7	682.0	0.82	0.99
KL/r=160	W10x26	1.00	33.6	312.0	42.4	340.0	0.79	0.92
KL/r=160	W14x605	1.00	2982.0	6976.0	3688.6	7468.0	0.81	0.93
KL/r=160	W18x192	1.00	551.5	2128.0	672.2	2206.0	0.82	0.96
KL/r=200	W10x60	1.00	170.8	439.0	197.7	445.0	0.86	0.99
KL/r=200	W10x26	1.00	36.3	194.0	42.4	174.0	0.86	1.11
KL/r=200	W14x605	1.00	3159.0	4549.0	3657.8	4756.0	0.86	0.96
KL/r=200	W18x192	1.00	586.9	1353.0	672.2	1367.0	0.87	0.99
						max	0.87	1.11
						min	0.44	0.92
						average	0.70	0.98
						standard deviation	0.13	0.04

Table 3-83 Comparison of AISC360-10 DM & EC3 Capacities-Imperfection "a, b, c, d"

Case Study	Column Profile	Intersection Points							
		EC3 Imperfection	AISC360-10 DM Capacity			EC3 Capaciy		AISC DM/EC3 RATIO	
			τb	M (kNm)	P (kN)	M (kNm)	P (kN)	M	P
KL/r=40	W10x60	a	0.47	24.9	3389.0	34.2	3653.0	0.73	0.93
KL/r=40	W10x26	a	0.44	5.9	1441.0	8.6	1569.0	0.69	0.92
KL/r=40	W14x605	a	0.48	400.3	34728.0	640.1	36646.0	0.63	0.95
KL/r=40	W18x192	a	0.43	96.6	10630.0	130.7	11634.0	0.74	0.91
KL/r=80	W10x60	a	0.90	84.1	2175.0	144.7	2458.0	0.58	0.88
KL/r=80	W10x26	a	0.97	15.9	990.0	34.0	1079.0	0.47	0.92
KL/r=80	W14x605	a	0.96	1379.7	23500.0	2557.6	25192.0	0.54	0.93
KL/r=80	W18x192	a	0.92	270.5	7170.0	511.3	7989.0	0.53	0.90
KL/r=120	W10x60	a	1.00	133.3	1211.0	195.0	1234.0	0.68	0.98
KL/r=120	W10x26	a	1.00	29.5	497.0	42.4	535.0	0.70	0.93
KL/r=120	W14x605	a	1.00	2495.7	12125.0	3569.7	13132.0	0.70	0.92
KL/r=120	W18x192	a	1.00	463.3	3736.0	671.0	3999.0	0.69	0.93
KL/r=160	W10x60	a	1.00	161.3	677.0	197.7	716.0	0.82	0.95
KL/r=160	W10x26	a	1.00	33.6	312.0	42.4	369.0	0.79	0.85
KL/r=160	W14x605	a	1.00	2982.0	6976.0	3688.7	7430.0	0.81	0.94
KL/r=160	W18x192	a	1.00	551.5	2128.0	672.2	2293.0	0.82	0.93
KL/r=200	W10x60	a	1.00	170.8	439.0	197.7	472.0	0.86	0.93
KL/r=200	W10x26	a	1.00	36.3	194.0	42.4	215.0	0.86	0.90
KL/r=200	W14x605	a	1.00	3159.0	4549.0	3688.7	4758.0	0.86	0.96
KL/r=200	W18x192	a	1.00	586.9	1353.0	672.2	1509.0	0.87	0.90
KL/r=40	W10x60	b	0.47	24.9	3389.0	35.5	3642.0	0.70	0.93
KL/r=40	W10x26	b	0.44	5.9	1441.0	8.1	1535.9	0.73	0.94
KL/r=40	W14x605	b	0.48	400.3	34728.0	683.2	36438.0	0.59	0.95
KL/r=40	W18x192	b	0.43	96.6	10630.0	141.1	11556.0	0.68	0.92
KL/r=80	W10x60	b	0.90	84.1	2175.0	147.4	2417.0	0.57	0.90
KL/r=80	W10x26	b	0.97	15.9	990.0	33.1	1053.0	0.48	0.94
KL/r=80	W14x605	b	0.96	1379.7	23500.0	2616.3	24722.0	0.53	0.95
KL/r=80	W18x192	b	0.92	270.5	7170.0	524.2	7810.0	0.52	0.92
KL/r=120	W10x60	b	1.00	133.3	1211.0	195.5	1201.0	0.68	1.01
KL/r=120	W10x26	b	1.00	29.5	497.0	42.4	531.0	0.70	0.94
KL/r=120	W14x605	b	1.00	2495.7	12125.0	3587.1	12692.0	0.70	0.96
KL/r=120	W18x192	b	1.00	463.3	3736.0	671.1	3993.0	0.69	0.94
KL/r=160	W10x60	b	1.00	161.3	677.0	197.7	700.0	0.82	0.97
KL/r=160	W10x26	b	1.00	33.6	312.0	42.4	315.3	0.79	0.99
KL/r=160	W14x605	b	1.00	2982.0	6976.0	3688.7	7390.0	0.81	0.94
KL/r=160	W18x192	b	1.00	551.5	2128.0	672.2	2250.0	0.82	0.95
KL/r=200	W10x60	b	1.00	170.8	439.0	197.7	459.0	0.86	0.96
KL/r=200	W10x26	b	1.00	36.3	194.0	42.4	204.0	0.86	0.95
KL/r=200	W14x605	b	1.00	3159.0	4549.0	3688.7	4396.0	0.86	1.03
KL/r=200	W18x192	b	1.00	586.9	1353.0	672.2	1460.0	0.87	0.93

KL/r=40	W10x60	c	0.47	24.9	3389.0	38.6	3612.0	0.65	0.94
KL/r=40	W10x26	c	0.44	5.9	1441.0	9.1	1561.0	0.65	0.92
KL/r=40	W14x605	c	0.48	400.3	34728.0	698.9	36362.0	0.57	0.96
KL/r=40	W18x192	c	0.43	96.6	10630.0	141.3	11555.0	0.68	0.92
KL/r=80	W10x60	c	0.90	84.1	2175.0	148.4	2375.0	0.57	0.92
KL/r=80	W10x26	c	0.97	15.9	990.0	34.7	1018.0	0.46	0.97
KL/r=80	W14x605	c	0.96	1379.7	23500.0	2675.2	24238.0	0.52	0.97
KL/r=80	W18x192	c	0.92	270.5	7170.0	531.5	7705.0	0.51	0.93
KL/r=120	W10x60	c	1.00	133.3	1211.0	192.4	1258.0	0.69	0.96
KL/r=120	W10x26	c	1.00	29.5	497.0	42.4	519.0	0.70	0.96
KL/r=120	W14x605	c	1.00	2495.7	12125.0	3592.3	12552.0	0.69	0.97
KL/r=120	W18x192	c	1.00	463.3	3736.0	671.8	3852.0	0.69	0.97
KL/r=160	W10x60	c	1.00	161.3	677.0	196.2	724.0	0.82	0.94
KL/r=160	W10x26	c	1.00	33.6	312.0	42.4	353.0	0.79	0.88
KL/r=160	W14x605	c	1.00	2982.0	6976.0	3688.7	7082.0	0.81	0.99
KL/r=160	W18x192	c	1.00	551.5	2128.0	672.2	2268.0	0.82	0.94
KL/r=200	W10x60	c	1.00	170.8	439.0	197.1	465.0	0.87	0.94
KL/r=200	W10x26	c	1.00	36.3	194.0	42.4	194.0	0.86	1.00
KL/r=200	W14x605	c	1.00	3159.0	4549.0	3688.7	4376.0	0.86	1.04
KL/r=200	W18x192	c	1.00	586.9	1353.0	672.2	1419.0	0.87	0.95
KL/r=40	W10x60	d	0.47	24.9	3389.0	38.8	3614.0	0.64	0.94
KL/r=40	W10x26	d	0.44	5.9	1441.0	9.3	1561.0	0.63	0.92
KL/r=40	W14x605	d	0.48	400.3	34728.0	675.1	35276.6	0.59	0.98
KL/r=40	W18x192	d	0.43	96.6	10630.0	143.7	11537.0	0.67	0.92
KL/r=80	W10x60	d	0.90	84.1	2175.0	153.4	2340.0	0.55	0.93
KL/r=80	W10x26	d	0.97	15.9	990.0	35.8	1007.0	0.44	0.98
KL/r=80	W14x605	d	0.96	1379.7	23500.0	2746.6	23632.0	0.50	0.99
KL/r=80	W18x192	d	0.92	270.5	7170.0	556.1	7332.0	0.49	0.98
KL/r=120	W10x60	d	1.00	133.3	1211.0	195.7	1185.0	0.68	1.02
KL/r=120	W10x26	d	1.00	29.5	497.0	42.4	503.0	0.70	0.99
KL/r=120	W14x605	d	1.00	2495.7	12125.0	3599.8	12346.0	0.69	0.98
KL/r=120	W18x192	d	1.00	463.3	3736.0	672.1	3731.0	0.69	1.00
KL/r=160	W10x60	d	1.00	161.3	677.0	197.7	682.0	0.82	0.99
KL/r=160	W10x26	d	1.00	33.6	312.0	42.4	340.0	0.79	0.92
KL/r=160	W14x605	d	1.00	2982.0	6976.0	3688.6	7468.0	0.81	0.93
KL/r=160	W18x192	d	1.00	551.5	2128.0	672.2	2206.0	0.82	0.96
KL/r=200	W10x60	d	1.00	170.8	439.0	197.7	445.0	0.86	0.99
KL/r=200	W10x26	d	1.00	36.3	194.0	42.4	174.0	0.86	1.11
KL/r=200	W14x605	d	1.00	3159.0	4549.0	3657.8	4756.0	0.86	0.96
KL/r=200	W18x192	d	1.00	586.9	1353.0	672.2	1367.0	0.87	0.99
							max	0.87	1.11
							min	0.44	0.85
							average	0.71	0.95
							standard deviation	0.13	0.04

According to above tables, there is a minor difference between flexural moment and axial compression capacities for strong axis bending results. Average axial capacity ratios show that, axial compression capacity approaches to one when initial bow imperfection from *a* to *d*. On the other hand, there is no major difference between flexural moment capacities for different imperfection values. For major axis bending imperfection curve *b* provide the best estimates where the maximum difference in axial load capacities is close to one.

Contrary to major axis bending analysis results, axial compression ratios move away from 1 when initial bow imperfection from *a* to *d* for weak axis bending. Moreover, minor axis bending capacities are not as consistent as major axis bending capacities.

Standard deviations for minor axis bending moment capacities are always greater than those obtained for major axis bending moment capacities. For minor axis bending imperfection curve *b* can as well be used used to estimate the capacities.

CHAPTER 4

COMPARISON OF STABILITY APPROACHES OF AISC360-10 AND EC3 SPECIFICATIONS FOR 2D PLANE FRAMES

To extend the study of individual members, stability provisions of AISC360 and EC3 specifications were applied to two dimensional plane frames in this chapter. Five different columns that are part of two plane frames were investigated to make comparison between each method and specification. For individual member, effective length factor has been assumed as 2. In this chapter, effective length factor of plane frame column was assumed as 3. With the consideration of this factor, five cases were created with slenderness ratios of frame columns KL/r = 40, 80, 120, 160, 200 respectively. Similar to analysis carried out for individual members, two dimensional plane frames were analysed by taking into account nonlinear second order effects. As explained in Chapter 3, each EC3 analysis was performed by taking into consideration sway-bow loading. Also, AISC360 provisions mentioned in Chapter 1 were included in these frames both for ELM and DM analysis. Base reactions of axial compression (P) and strong axis bending moment (M) values are tabulated for each method in the following parts.

4.1 Case Studies

As can be seen in Figure 4-1, plane frame system consists of beam and column members. Considering the effective length factor as K=3 beam and column lengths are determined in accordance with the alignment chart given for sidesway permitted system in AISC360. Capacity curve of ELM was formed using K=3. On the other hand, capacity curve of DM was formed using K=1.

Application of Notional Loads for AISC360 and EC3

For analysis related with ELM and DM, notional loads are applied as shown in Figure 4-1.

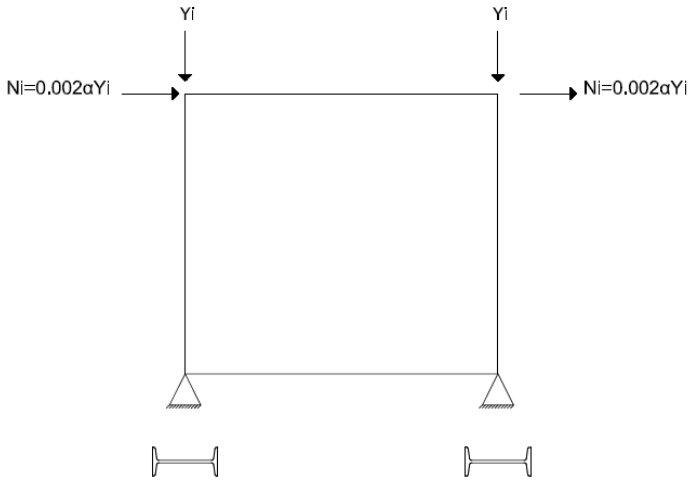

Figure 4-1 Loading of Plane Frame with AISC360 provisions

For EC3 analysis, sway and bow imperfections are included in frame system as illustrated in Figure 4-2 and 4-3.

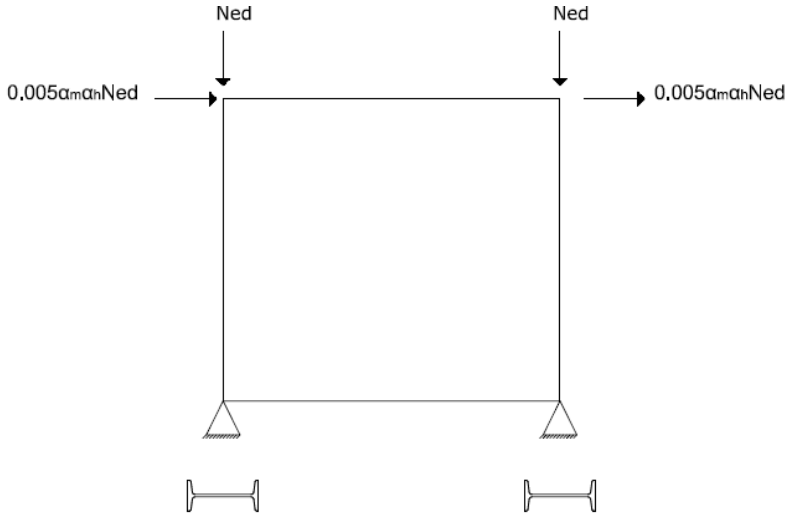

Figure 4-2 Sway Imperfection Loading for Plane Frame (EC3 Direction)

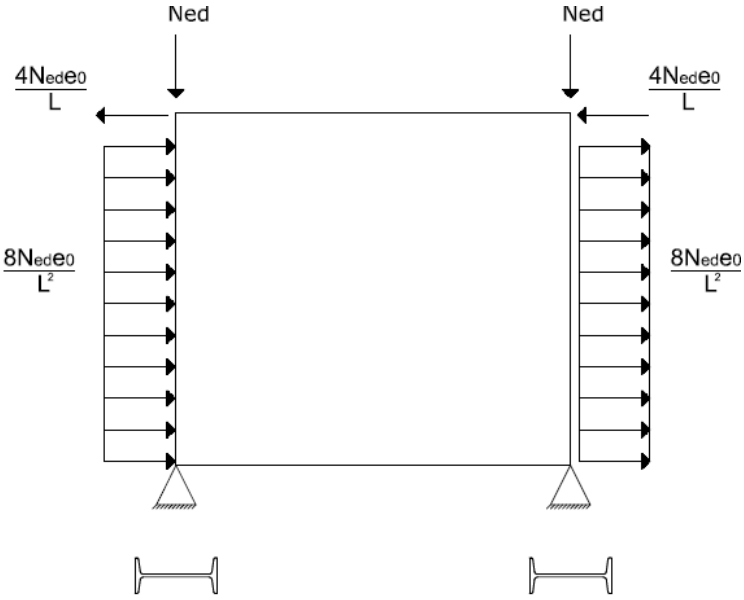

Figure 4-3 Bow Imperfection Loading for Plane Frame (EC3 Direction)

For each case study, properties of plane frame members are shown in Table 4-1. This table consists of column profile type, column height, beam profile and beam length.

Table 4-1 2D Plane Frame Properties with W10x60

Case Study	Column Profile	Column Height	Beam Profile	Beam Length
KL/r = 40	W10x60	1.491 m	HEB160	2.45 m
KL/r = 80	W10x60	2.981 m	HEA140	2.45 m
KL/r = 120	W10x60	4.472 m	HEB120	2.45 m
KL/r = 160	W10x60	5.963 m	IPE140	2.45 m
KL/r = 200	W10x60	7.453 m	HEB100	2.45 m

Due to the direction of horizontal loads, it is clear that right support has more critical P-M capacities than the other support. Therefore, P-M reactions were exported from right support as shown in Figure 4-4.

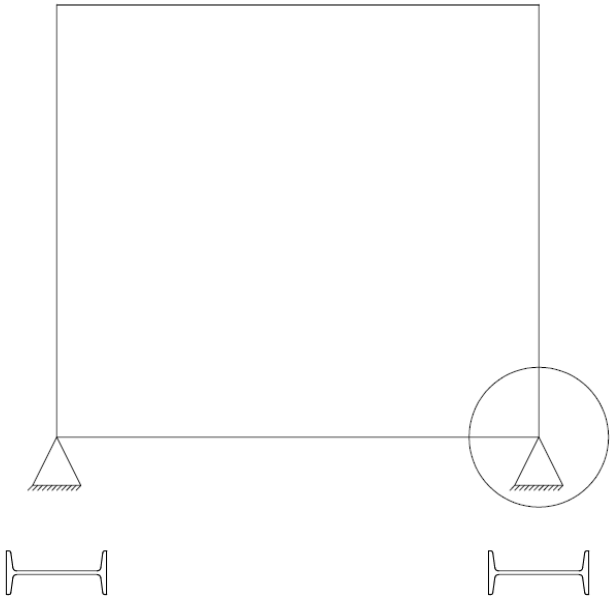

Figure 4-4 Exported P-M Values

Loading values are determined depending on the parameters stated in AISC360 and EC3 specifications. Applied gravity loads, notional loads and modified stiffness parameters are presented in Table 4-2.

Table 4-2 Strong Axis Bending Loading Parameters for AISC360 and EC3

Case Study	AISC Loading Parameters					EC Loading Parameters			
	Applied Axial Force P (kN)	Applied Notional Load Ni (kN)	Modified Stiffness Parameters			Applied Axial Force Ned (kN)	Sway Imperfection Load (kN)	Bow Imperfection Loads	
			τ_b	EI*	EA*			$\frac{4N_{ed}e_0}{L}$ (kN)	$\frac{8N_{ed}e_0}{L^2}$ ($\frac{kN}{m}$)
KL/r = 40	3750	7.5	0.17	0.14	0.80EA	3750	16.24	60.00	80.50
KL/r = 80	2800	5.6	0.82	0.66	0.80EA	2800	12.12	44.80	30.05
KL/r = 120	1800	3.6	1.00	0.80	0.80EA	1800	7.37	28.80	12.88
KL/r = 160	1200	2.4	1.00	0.80	0.80EA	1200	4.26	19.20	6.44
KL/r = 200	800	1.6	1.00	0.80	0.80EA	800	2.54	12.80	3.43

Similar to figures given in Chapter 3, capacity curves of frame columns are plotted with respect to axial compression P_u (kN) and strong axis base moment M_u (kNm). Graphs include closed form solution, ELM, DM and EC3 capacity curves with related analysis results. P-M capacity curves with related loading curves are illustrated in Table 4-5, 4-6, 4-7, 4-8 and 4-9 respectively.

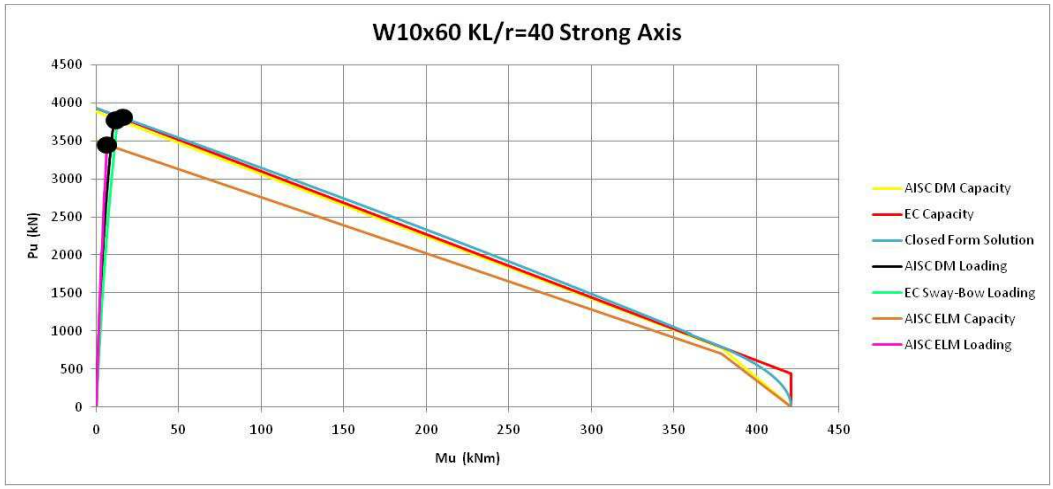

Figure 4-5 Strong Axis Interaction Diagram for $\frac{KL}{r} = 40$ W10x60 Column

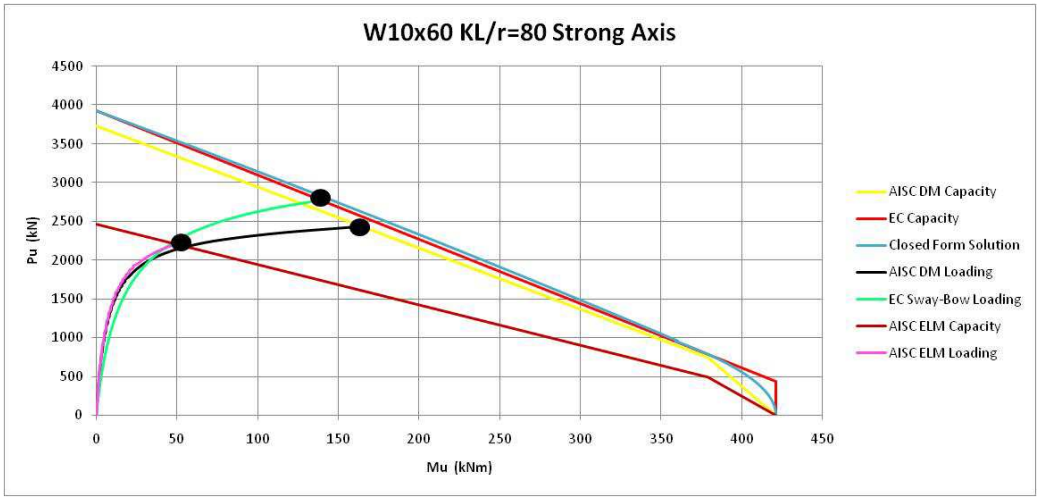

Figure 4-6 Strong Axis Interaction Diagram for $\frac{KL}{r} = 80$ W10x60 Column

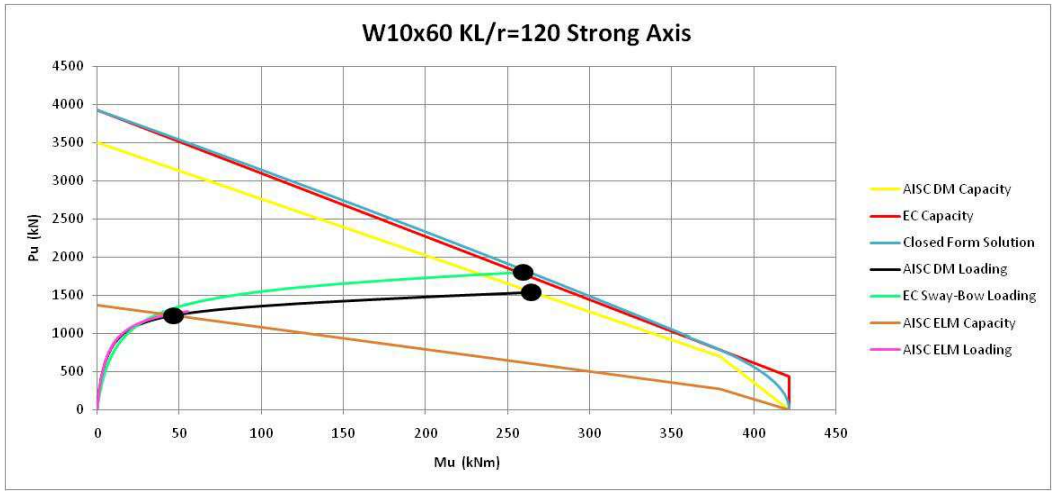

Figure 4-7 Strong Axis Interaction Diagram for $\frac{KL}{r} = 120$ W10x60 Column

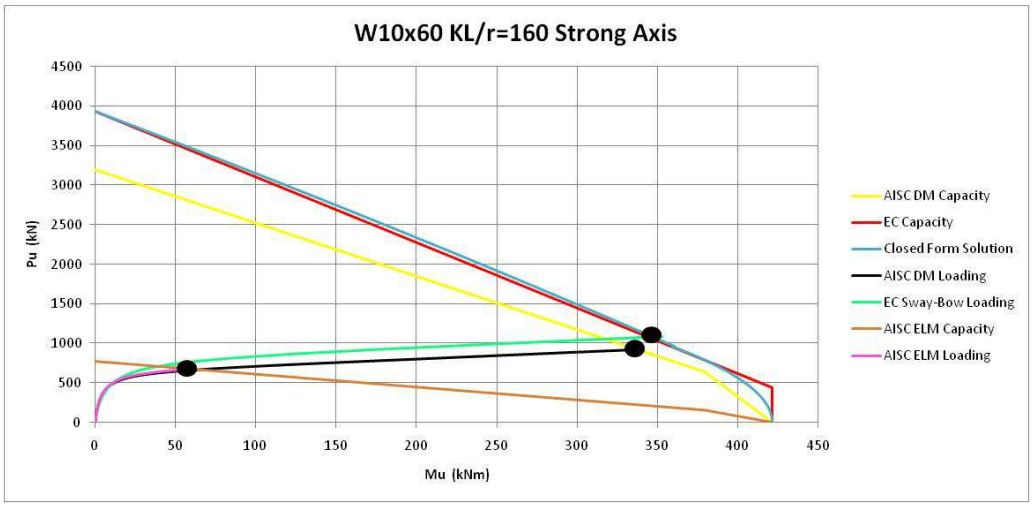

Figure 4-8 Strong Axis Interaction Diagram for $\frac{KL}{r} = 160$ W10x60 Column

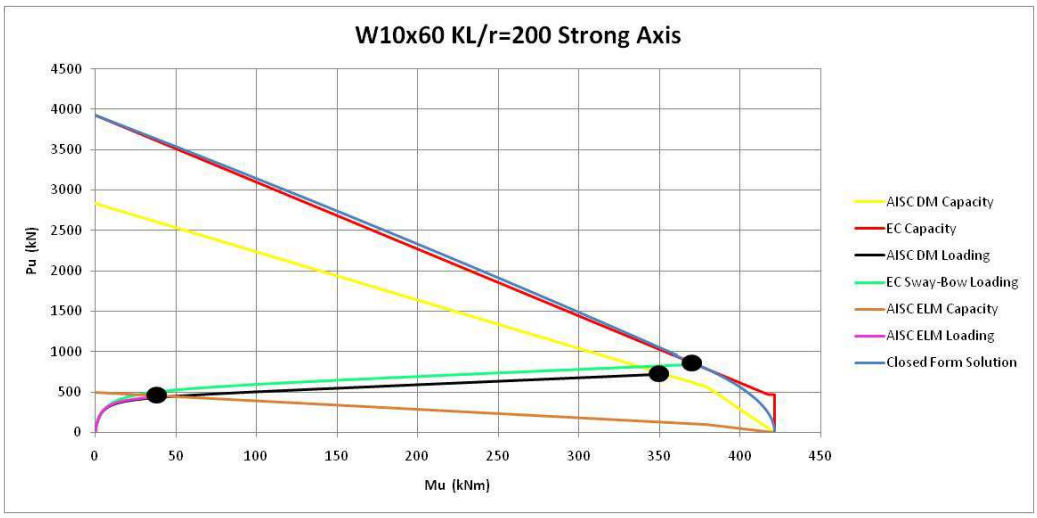

Figure 4-9 Strong Axis Interaction Diagram for $\frac{KL}{r} = 200$ W10x60 Column

Axial compression (P) and strong axis bending moment (M) capacities for each case and method are presented in following tables.

Table 4-3 Comparison of AISC360-10 DM & EC3 Strong Axis Analysis Results

Case Study	Intersection Points						
	AISC DM Capacity			EC3 Capacity		AISC DM/EC3 RATIO	
	τb	M (kNm)	P (kN)	M (kNm)	P (kN)	M	P
KL/r=40	0.14	14.6	3760.0	18.9	3773.0	0.77	1.00
KL/r=80	0.82	166.0	2424.0	139.5	2774.0	1.19	0.87
KL/r=120	1.00	266.1	1533.0	259.0	1783.0	1.03	0.86
KL/r=160	1.00	338.4	913.0	343.0	1087.0	0.99	0.84
KL/r=200	1.00	352.1	730.0	374.1	829.0	0.94	0.88

Table 4-4 Comparison of AISC360-10 DM & ELM Strong Axis Analysis Results

Case Study	Intersection Points						
	AISC DM Capacity			AISC ELM Capacity		AISC DM/ELM RATIO	
	τb	M (kNm)	P (kN)	M (kNm)	P (kN)	M	P
KL/r=40	0.14	14.6	3760.0	9.9	3423.0	1.47	1.10
KL/r=80	0.82	166.0	2424.0	55.4	2174.0	3.00	1.11
KL/r=120	1.00	266.1	1533.0	47.5	1233.0	5.60	1.24
KL/r=160	1.00	338.4	913.0	59.0	675.0	5.74	1.35
KL/r=200	1.00	352.1	730.0	41.7	450.0	8.45	1.62

Table 4-5 Comparison of EC3 & AISC360-10 ELM Strong Axis Analysis Results

Case Study	Intersection Points					
	EC3 Capacity		AISC ELM Capacity		EC3/AISC ELM RATIO	
	M (kNm)	P (kN)	M (kNm)	P (kN)	M	P
KL/r=40	18.9	3773.0	9.9	3423.0	1.91	1.10
KL/r=80	139.5	2774.0	55.4	2174.0	2.52	1.28
KL/r=120	259.0	1783.0	47.5	1233.0	5.45	1.45
KL/r=160	343.0	1087.0	59.0	675.0	5.82	1.61
KL/r=200	374.1	829.0	41.7	450.0	8.98	1.84

In this chapter, W10x60 columns that are part of 2D plane frames were studied. Naturally, slenderness is an important parameter for members carrying axial compression force. Similar to the study carried out for individual member, five different analysis for each method were performed to show how axial compression capacity changes with increasing slenderness. Table 4-3 shows the comparison of AISC360-10 DM and EC3 results. For KL/r=40 case, column member has the shortest length among other columns. Therefore, this case is not suitable for determining bending moment capacity. Except this case, there is a consistency between bending moment capacities. On the other hand, there is 10% difference

between axial compression capacities for KL/r=40, 80, 120, 160 and 200 cases. Comparison of EC3 and AISC360-10 ELM results are shown in Table 4-4. Results show that there is no consistency between moment capacities because ELM always give smaller moment capacity comparing to other methods. As can be seen from P ratios, there is no consistency between axial compression capacities. As mentioned in section 1.5.4, in order to use ELM for analysis, the ratio of storey drifts obtained from second order to first order analysis should not be greater than 1.5. For the KL/r=120, 160 and 200 cases, storey drift ratios are 1.586, 1.829 and 1.867 respectively. Due to exceeding the storey drift ratio limitation, KL/r=120, 160 and 200 cases are not suitable to be investigated by ELM. Finally, comparison of ELM and DM results were illustrated in Table 4-5. There is a large difference between moment capacities. Bending moment ratios increase with KL/r proportionally. As mentioned in EC3 and ELM comparions, compression capacity ratio of last three cases are considerably high. Except these cases, axial load capacities are compatible with each other.

4.2 Effect of K Factor on Axial Compression Capacity

In order to present the effect of using large effective length factor on ELM results, an additional case was studied by considering K=2.5. Comparing to individual member analysis results, there is a difference between DM and ELM axial compression strengths for plane frame columns. However, a relatively large effective length factor of 3 (compared to 1.0) results in underestimating the axial compression resistance of the beam-column member and the net effect is a conservative interaction check that exceeds to 1.0. This illustrates that the effective length approach may produce conservative results, but these results are based on a comparison of internal forces and resistance terms that are not necessarily representative of the actual limit state behavior of the structure (Surovek A. E., Ziemian R. D., 2005). Figure 4-10 shows capacity curves of ELM, DM and EC3 methods.

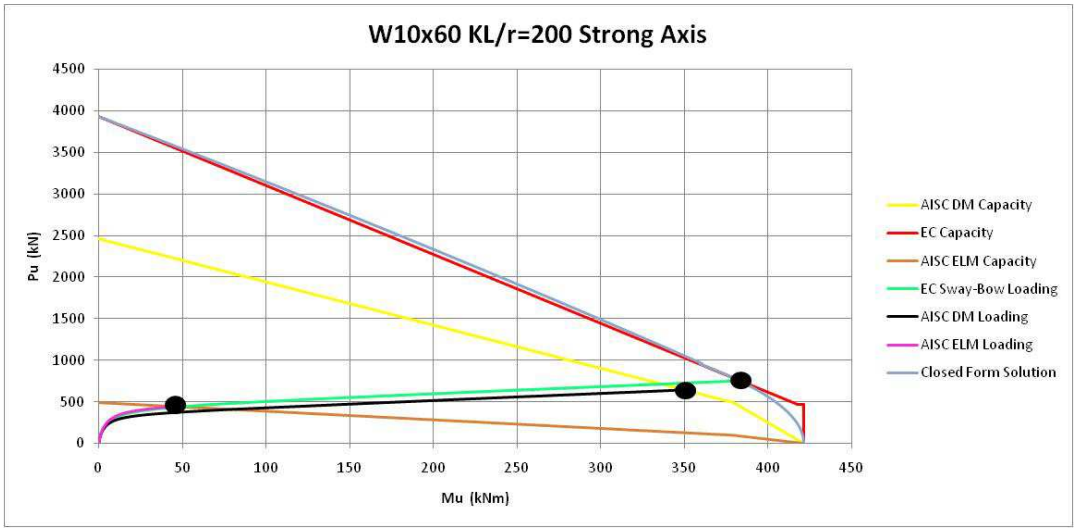

Figure 4-10 Strong Axis Interaction Diagram for $\frac{KL}{r} = 200$ Column (K=2.5)

P-M results for KL/r=200 case are shown in Table 4-6, 4-7 and 4-8.

Table 4-6 Comparison of AISC360-10 DM & EC3 Strong Axis Analysis Results for $\frac{KL}{r} = 200$ Case for K=2.5

Case Study	Intersection Points						
	AISC DM Capacity			EC3 Capacity		AISC DM/EC3 RATIO	
	τb	M (kNm)	P (kN)	M (kNm)	P (kN)	M	P
KL/r=200	1.00	353.98	623	386.67	725	0.92	0.86

Table 4-7 Comparison of AISC360-10 DM & ELM Strong Axis Bending Capacities for $\frac{KL}{r} = 200$ Case for K=2.5

Case Study	Intersection Points						
	AISC DM Capacity			AISC ELM Capacity		AISC DM/ELM RATIO	
	τb	M (kNm)	P (kN)	M (kNm)	P (kN)	M	P
KL/r=200	1.00	353.98	623	47.43	444	7.46	1.40

Table 4-8 Comparison of EC3 & AISC360-10 ELM Strong Axis Bending Capacities for $\frac{KL}{r} = 200$ Case for K=2.5

Case Study	Intersection Points					
	EC3 Capacity		AISC ELM Capacity		EC3/AISC ELM RATIO	
	M (kNm)	P (kN)	M (kNm)	P (kN)	M	P
KL/r=200	386.67	725	47.43	444	8.15	1.63

Table 4-7 illustrates the capacity values of AISC DM and ELM for KL/r=200. Comparing to Table 4-5 KL/r=200 case, the difference between the axial load capacity of DM and ELM decreased by 22%. This result shows that, using relatively high effective length factors do not give accurate results in terms of axial compression capacity.

CHAPTER 5

CONCLUSIONS

5.1 Summary and Concluding Comments

The goal of this thesis is to compare stability provisions of AISC360 and EC3 specifications for members under compression.

Effective Length Method is one of the most commonly used method for determining axial load capacity of a member. Support conditions and length of the member are crucial parameters for ELM. In addition to these parameters, AISC360 offers destabilizing effects on structures namely geometrical imperfections. To represent these geometrical imperfections, notional load is applied at each storey of structure in lateral direction. As mentioned in Chapter 1, the magnitude of notional load is 0.002 times total gravity load at each storey. This value corresponds to maximum permitted out of plumb ratio which is 1/500 times frame length. These parameters strongly affect axial compression capacity of a member. Nominal axial compression force P_n, which is a function of critical stress, effective length factor and Euler buckling stress, determines axial compression capacity of a member. For axial load and strong or weak axis bending capacity of a member is determined with Equations 1-6 and 1-7.

Another method AISC360 indicates is the Direct Analysis Method. This method is more straightforward compared to Effective Length Method. Design for stability by the Direct Analysis Method involves a second-order analysis, use of reduced stiffness in the analysis, consideration of initial imperfections (either by direct modeling of the imperfections or by application of notional loads in the analysis) under certain circumstances, and strength check of components using an effective length factor, K, of unity for members subject to compression. (Nair et al, 2011) DM eliminates the calculation procedure of effective length factor. For all members with any kind of support conditions, effective length factor is considered as K=1. Similar

to ELM, DM includes geometrical imperfection to contribute unstable condition with notional loads. Moreover, there are modifications on flexural stiffness and axial stiffness of the member. It is suggested that all steel member properties contributing to the elastic stiffness be multiplied by 0.8 with the exception of member flexural rigidities, which should be multiplied by $0.8\tau_b$. (Griffis and White, 2013). For frames with slender members, where the governing limit state is elastic instability, the 0.8 stiffness adjustment provides roughly an equivalent margin of safety for frames as implied by current design provisions for slender columns. For frames with intermediate or stocky columns, the $0.8\tau_b$ factor reduces the flexural stiffness to account for inelastic softening prior to the members reaching their design strength. The τ_b factor is similar to the inelastic stiffness reduction factor implied in the AISC column curve to account for loss of stiffness under high compression loads, such that $P_u>0.5P_y$, and the 0.8 factor accounts for additional softening under combined axial compression and bending. (Deirlein, 2004). Using the effective length factor K=1, axial load bending moment capacity of a member is determined with Equation 1-6 and 1-7.

Similar to AISC360, EC3 offers to apply some destabilizing effects to the system. These effects are stated as imperfections related with member production, erection process and uncertainties in the structural system. Initial sway and initial bow imperfections stand for these destabilizing effects in the structure. As explained in 1.6.3 and 1.6.4, each of them has different parameters and application methodology to the system. With the application of sway and bow imperfections, EC3 permits to omit buckling check of the compression member. While the major axis bending capacity of a member is determined with Equation 1-24, minor axis bending capacity is determined with Equations 1-25 and 1-26.

In Chapter 2, two different benchmark problems given in AISC360 were studied to verify SAP2000. Benchmark cases were studied to provide a guideline for modeling members. According to given loads by AISC360, target span and target base moments were compared with SAP2000 analysis results for each problem. In absence of axial load cases, target results and SAP2000 analysis results coincide. As can be seen in Table 2-2 and Table 2-3, error percentage is decreasing when the

element is divided into more than one element. Therefore, elements were divided into five elements to obtain small errors when determining axial load and bending moment capacities.

In Chapter 3, individual fixed base cantilever members with W10x60, W10x26, W14x605 and W18x192 sections were investigated. Effective length member of fixed base columns was considered as K=2. With the assumption of this factor, each member length was determined with related radius of gyration with the slenderness ratio of members which are KL/r=40, 80, 120, 160 and 200. Each section was studied according to ELM, DM and EC3 provisions for strong axis and weak axis bending. Strong and weak axis bending buckling curve of each section was determined by using Table 1-2 which is given by EC3. Each method was compared with each other with related buckling curve value. Moreover, to observe the changing of axial compression and bending moment capacities with different imperfections, these members were studied according to "a, b, c, d" imperfections respectively. Furthermore, each EC3 imperfection was compared with ELM and DM results. Totally one hundred sixty members were investigated and some statistical conclusions were obtained. As explained in Chapter 3, there is a consistency between axial load capacities for each method, generally. The results show that, there is no major difference of axial load and bending moment capacities for different imperfections given by EC3. Moreover, minor differences exist in DM and EC3 bending moment capacities. On the other hand, ELM always give smaller moment capacities compared to DM and EC3 capacities.

Column members that are part of two dimensional plane frames under strong axis bending were studied in Chapter 4. Column member of plane frames is W10x60 and KL/r are identical with the study of individual members. Similar procedures mentioned in Chapter 3 were applied to study of 2D plane frames. Structural systems were created by taking consideration the effective length factor as K=3. With the application of provisions given in AISC360 and EC3 specifications, five plane frames that have different height of W10x60 column were analyzed for each method. Similar to Chapter 3, compression and bending analysis results are compatible for DM and EC3 cases. Individual member results show that, favorable axial

compression capacities have been obtained for DM and ELM when effective length factor is K=2. For the first two cases of Table 4-5, there is a considerable difference between axial compression capacities of DM and ELM. This can be explained as using relatively high effective length factor results is difference between axial load capacities. For this reason, compression capacity ratios of EC3/ELM and DM/ELM are greater than results obtained for individual members. The effect of using relatively high K value was investigated in Section 4.2. In this section, analysis of the KL/r=200 case was repeated by taking into account effective length factor as K=2.5. Results show that, difference between axial load capacities of Direct Analysis Method and Effective Length Method decreased by 22%.

In conclusion, AISC360 and EC3 specifications have different point of view about stability concept. Analysis carried out for ELM, DM and EC3 show that, there is a minor difference between axial load capacities. Results show that, favorable axial compression capacities were obtained for ELM, DM and EC3 methods. However, ELM gives lower moment capacities when compared to DM and EC3 analysis. For this reason, comparison of moment capacity ratios of ELM with other methods are considerably high. Furthermore, studies conducted for different EC3 imperfections show that there is no major difference on P-M capacities when using different bow imperfection instead of the offered value.

5.2 Recommendations for Future Studies

The investigated topics in this thesis requires to be expanded for composite columns with different geometrical sections. For instance, a comparative study can be conducted for composite columns with circular section for provisions given in AISC360 and EC3 specifications.

In addition to two dimensional analysis of individual member and plane frame, this study needs to be extended for three dimensional analysis of these systems. Furthermore, a study of 3D frame with vertical bracing systems can be carried out to compare stability provisions of these specifications.

Finally, this study requires to be expanded with the considerations of superposition of notional loads with other types of lateral loads such as earthquake and wind loads.

REFERENCES

ANSI/AISC 360-10 An American National Standard (2010). *Specification for Structural Steel Buildings*

Bruneau, M.,Uang, C., &Sabelli, R. (2011). *Ductile design of steel structures*. New York: McGraw-Hill.

Deierlein, G. (2004). Direct Analysis Method for Stability Design of Steel-Framed Buildings. *Structural Engineer*.

Eurocode 3 (1993) : EN Design of steel structures - Part 1-1: General rules and rules for buildings

Griffis, L. G., & White, D. W. (2013). *Stability Design of Steel Buildings*

Lu, Y. (2011). *Effects of member overstrength and initial residual stresses on the behaviour of 2D steel structure:*(Unpublished master's thesis).

Maleck, A. E., and White, D. W. (2003). "Direct analysis approach for the assessment of frame stability: verification studies." *Proceedings Annual Technical Sessions*, Structural Stability Research Council, Rolla, MO. 18

Nair, R. S., Malley, J. O., & Hooper, J. D. (2011). Design of Steel Buildings for Earthquake and Stability by Application of ASCE 7 and AISC 360. *Engineering Journal/Third Quarter*, 199-204.

Nelson, D. A. (2012). *Stability analysis of pipe racks for industrial facilities* (Unpublished master's thesis).

Surovek, A. E., & Ziemian, R. D. (2005). The Direct Analysis Method : Bridging the Gap from Linear Elastic Analysis to Advanced Analysis in Steel Frame Design. *Structures Congress 2005*

Topkaya, C.,& Şahin, S. (2011). A Comparative Study of AISC-360 and EC3 Strength Limit States. *International Journal of Steel Structures Int J Steel Struct*.

Yuan, Z. (2004). *Advanced Analysis of Steel Frame Structures Subjected to Lateral Torsional Buckling Effects* (Unpublished master's thesis).

Yong, D. J.,López, A., &Serna, M. A. (2011). Beam-Column Resistance Of Steel Members: A Comparative Study Of AISC LRFD and EC3 Approaches. *Int. J. Str. Stab. Dyn. International Journal of Structural Stability and Dynamics,11*(02), 345-361.

Ziemian, R. D. (2010). *Guide to stability design criteria for metal structures*. Hoboken, NJ: John Wiley & Sons.